Weak gravitational lensing

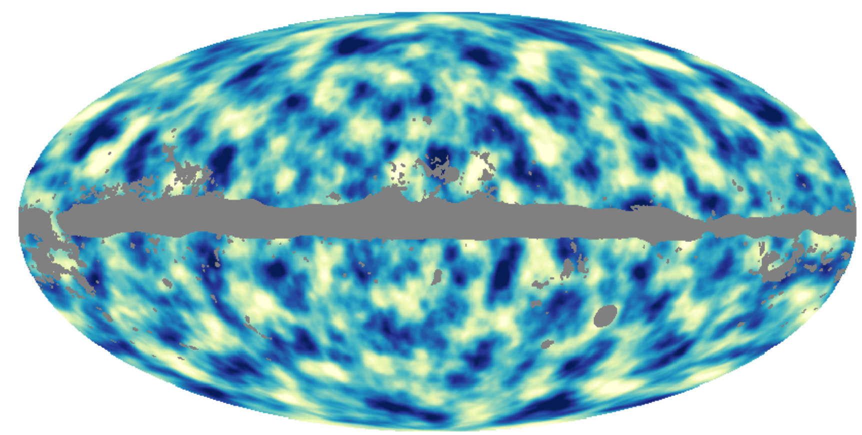

A. Benoit-Lévy

University College London

46ème Ecole de GIF - La Cosmologie après PLANCK

Outline

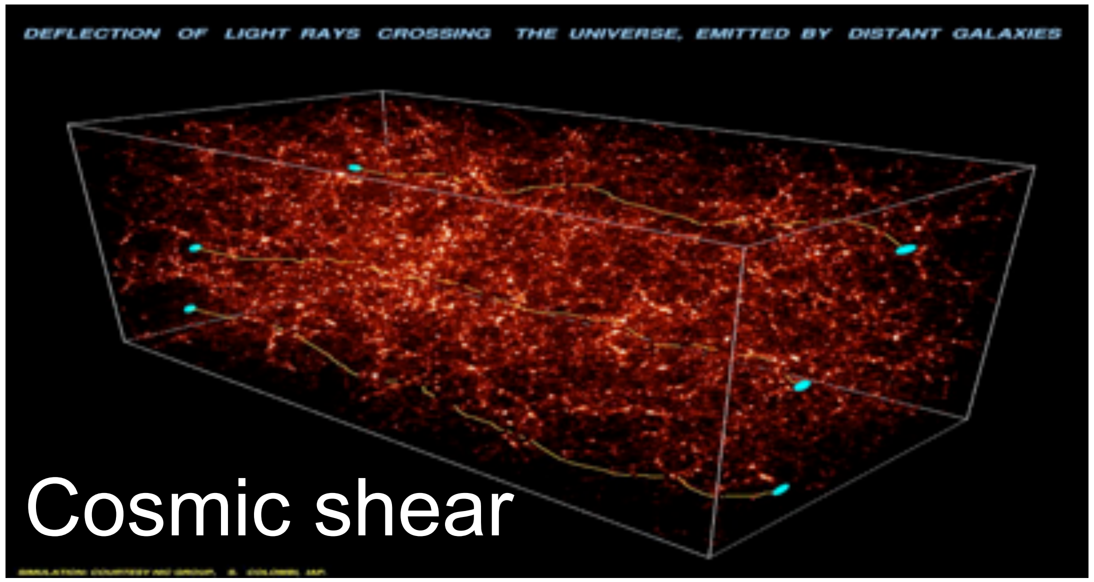

1. the lens equation
2. potential, convergence and shear
3. the lensing Jacobian
4. ellipticities estimation
5. cosmic shear

1. differences with cosmic shear
2. the lensing potential
3. impact on CMB power spectra
4. lensing reconstruction
5. Planck and beyond

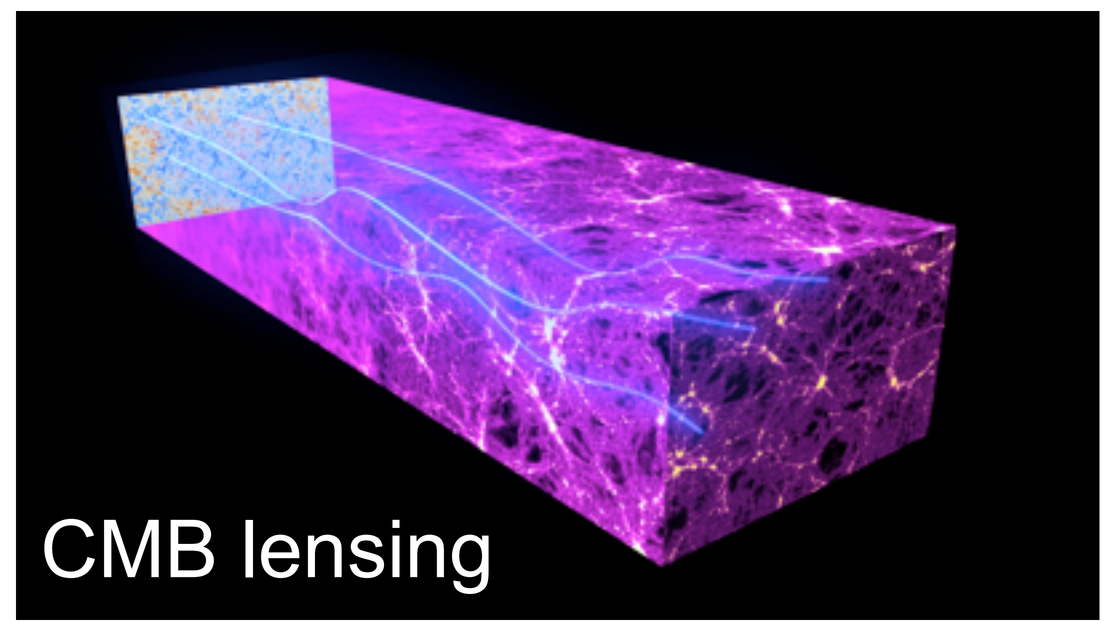

Deflection of photons path in an inhomogeneous Universe

Brief historical overview

1801

Soldner computes the deflection angle of a light ray passing near the sun

ON THE DEVIATION OF A LIGHT RAY FROM ITS MOTION ALONG A STRAIGHT LINE THROUGH THE ATTRACTION OF A CELESTIAL BODY WHICH IT PASSES CLOSE BY

Herr Joh. Soldner

Berlin, March 1801[22]

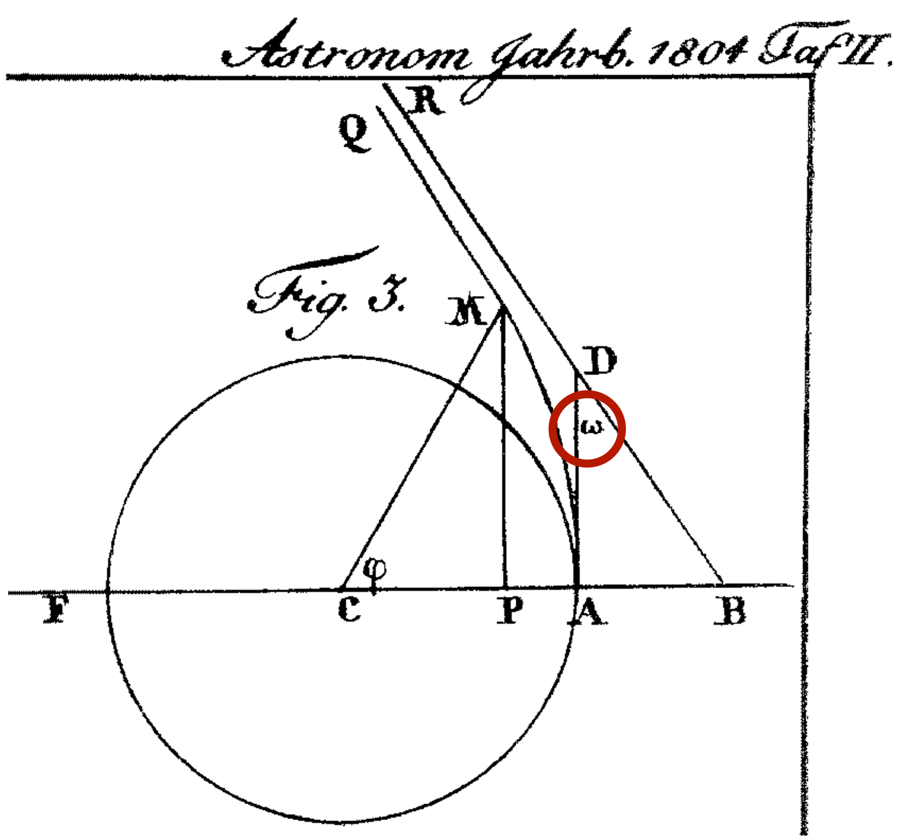

If one substitutes in the formula for $\tan\omega$ the acceleration of gravity on the surface of the sun, and one takes the radius of that body for unity, then one finds $\omega = 0''.84$. If one could observe the fixed stars very close to the sun, then one would have to take this very much into account. But since this is not known to happen, the perturbation caused by the sun can also be neglected. For light rays which come from Venus, a star which Vidal [now]

Therefore it is clear that nothing makes it necessary, at least in the present state of practical astronomy, that one should take into account the perturbation of light rays by attracting celestial bodies.

At any rate, I do not believe that there is any need on my part to apologize for having published the present essay just because the result is that all perturbations are unobservable. For it would still be just as important for us to know what is presented by theory, though it has no noticeable influence on praxis, as we are interested in what has in retrospect real influence on it. Our insights would by both be equally enlarged. One also demon-

Brief historical overview

1911
Einstein re-calcultes the same value by considering the equivalence principle (still Newtonian)

$$\alpha = \frac{1}{c^2} \int_{\vartheta = -\frac{\pi}{2}}^{\vartheta = +\frac{\pi}{2}} \frac{k\,M}{r^2} \cos\vartheta \cdot ds = \frac{2\,k\,M}{c^2\,\Delta},$$

wobei k die Gravitationskonstante, M die Masse des Himmelskörpers, Δ den Abstand des Lichtstrahles vom Mittelpunkt des Himmelskörpers bedeutet. *Ein an der Sonne vorbeigehender Lichtstrahl erlitte demnach eine Ablenkung vom Betrage* $4 \cdot 10^{-6}$ $= 0{,}83$ *Bogensekunden.* Um diesen Betrag er-

Brief historical overview

1911

Einstein re-calcultes the same value by considering the equivalence principle (still Newtonian)

$$\alpha = \frac{1}{c^2} \int_{\vartheta = -\frac{\pi}{2}}^{\vartheta = +\frac{\pi}{2}} \frac{k M}{r^2} \cos \vartheta \cdot ds = \frac{2 k M}{c^2 \Delta},$$

wobei k die Gravitationskonstante, M die Masse des Himmelskörpers, Δ den Abstand des Lichtstrahles vom Mittelpunkt des Himmelskörpers bedeutet. *Ein an der Sonne vorbeigehender Lichtstrahl erlitte demnach eine Ablenkung vom Betrage* $4 \cdot 10^{-6} = 0{,}83$ *Bogensekunden.* Um diesen Betrag er-

1915

GR value is computed to be exactly twice the Newtonian value: 1.7’’

$$\hat{\alpha} = \frac{4GM}{c^2 \xi} = 1''\!.75 \left(\frac{M}{M_\odot}\right) \left(\frac{\xi}{R_\odot}\right)^{-1} .$$

Brief historical overview

1919

Eddington measures the displacement of position of stars during a Sun eclipse to be consistent wth GR prediction

Dyson and others. *Phil. Trans., A, vol. 220, Plate 1.*

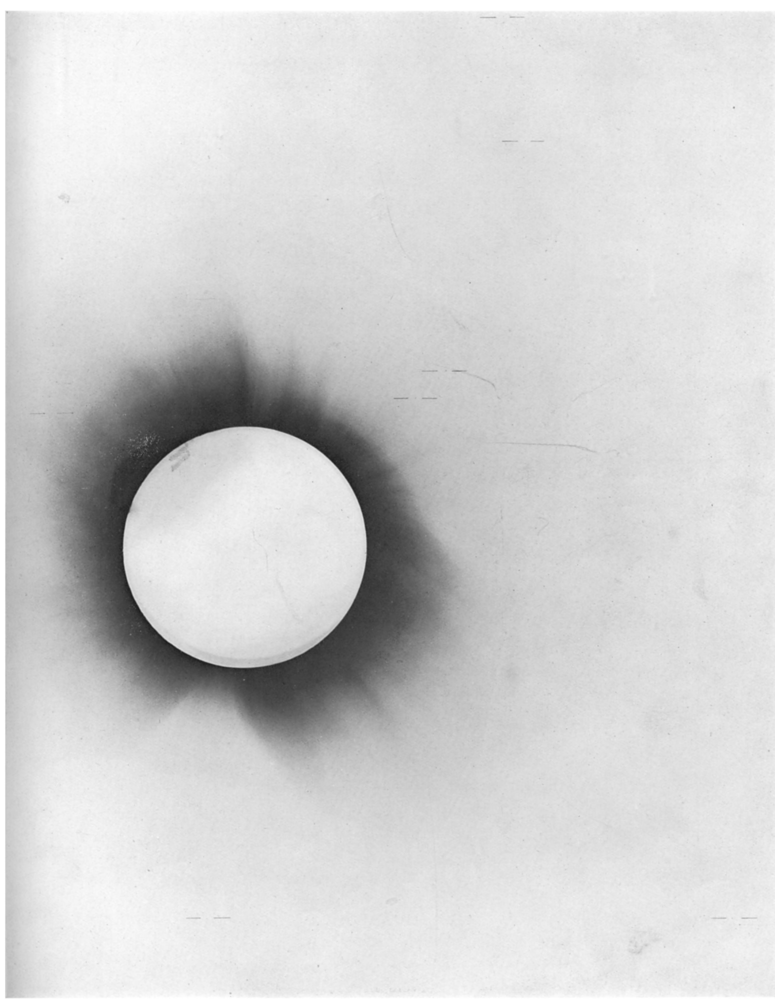

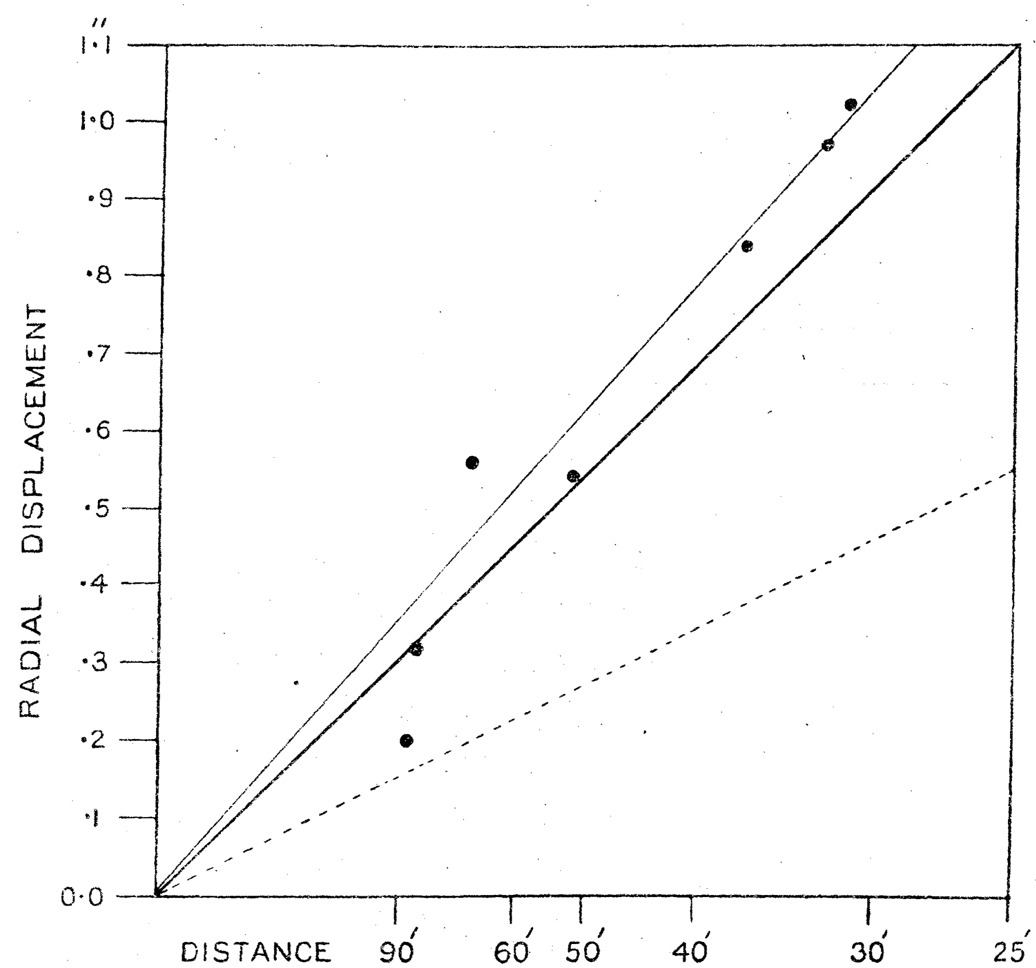

Diagram 2.

GR prediction

Newtonian prediction

(error bars are mentioned in the text of the article)

Cosmic shear

Objective of this lecture

linking the observations to theory

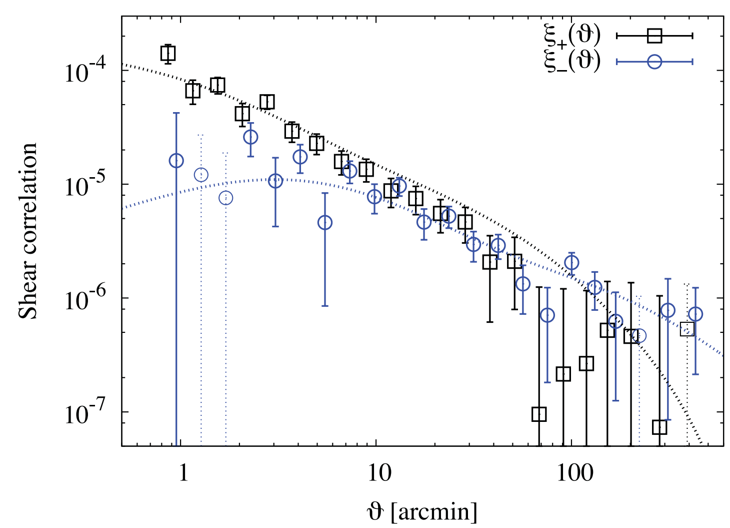

Figure 6. The measured shear correlation functions ξ_+ (black squares) and ξ_- (blue circles), combined from all four Wide patches. The error bars correspond to the total covariance diagonal. Negative values are shown as thin points with dotted error bars. The lines are the theoretical prediction using the *WMAP7* best-fitting cosmology and the non-linear model described in Section 4.3. The data points and error bars are listed in Table B1.

Kilbinger *et al*, 2013 (CFHTLens)

Cosmic shear

Objective of this lecture

linking the observations to theory
to get constraints on cosmological parameters

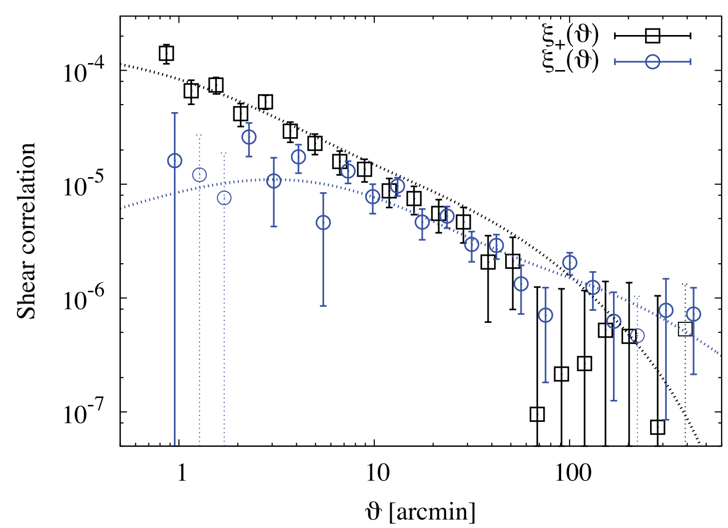

Figure 6. The measured shear correlation functions ξ_+ (black squares) and ξ_- (blue circles), combined from all four Wide patches. The error bars correspond to the total covariance diagonal. Negative values are shown as thin points with dotted error bars. The lines are the theoretical prediction using the *WMAP7* best-fitting cosmology and the non-linear model described in Section 4.3. The data points and error bars are listed in Table B1.

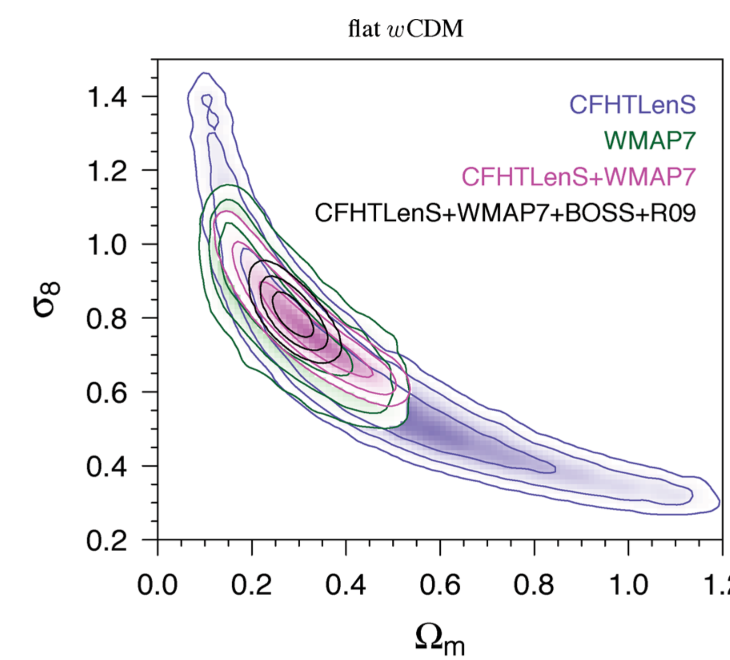

Kilbinger *et al*, 2013 (CFHTLens)

The lens equation

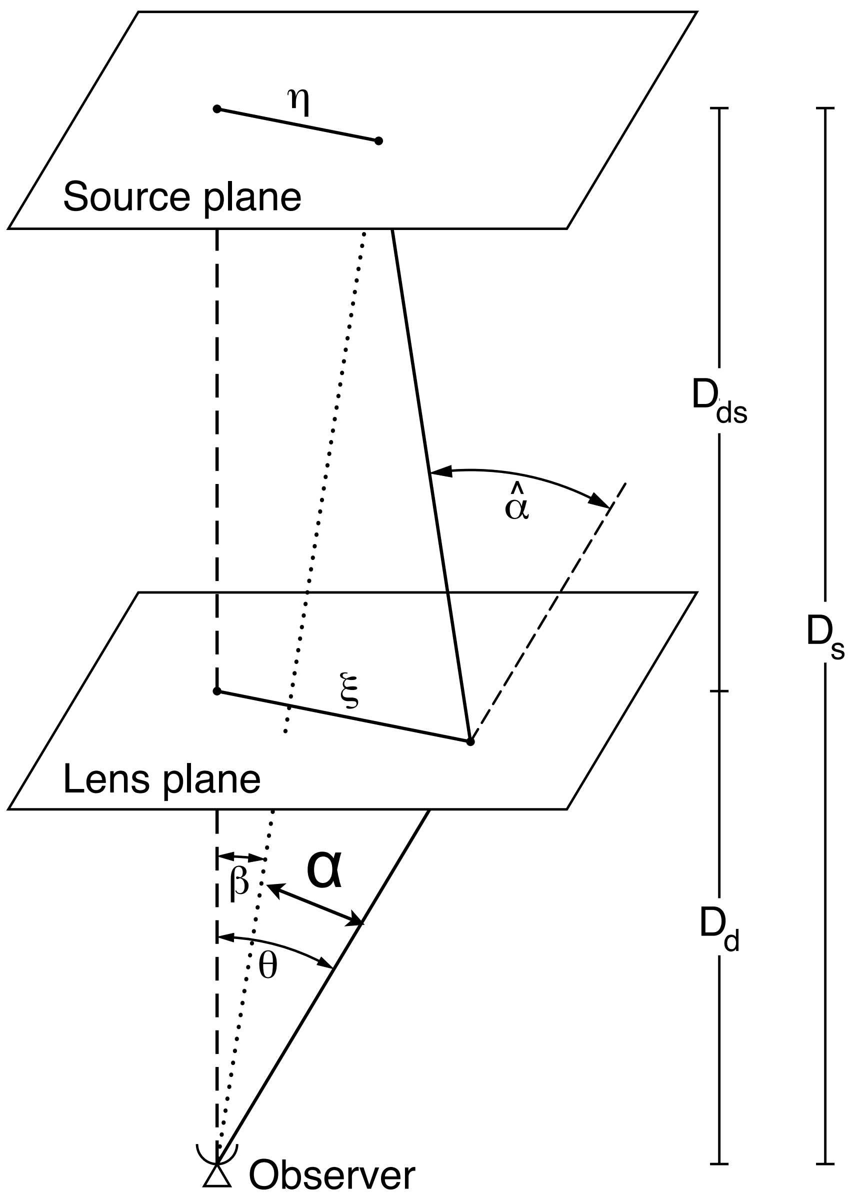

Fig. 12. Sketch of a typical gravitational lens system.

Most of the formula and figures come from

Bartelmann & Schneider, 2001

Schneider, 33 Saas-Fee School, 2004

The lens equation

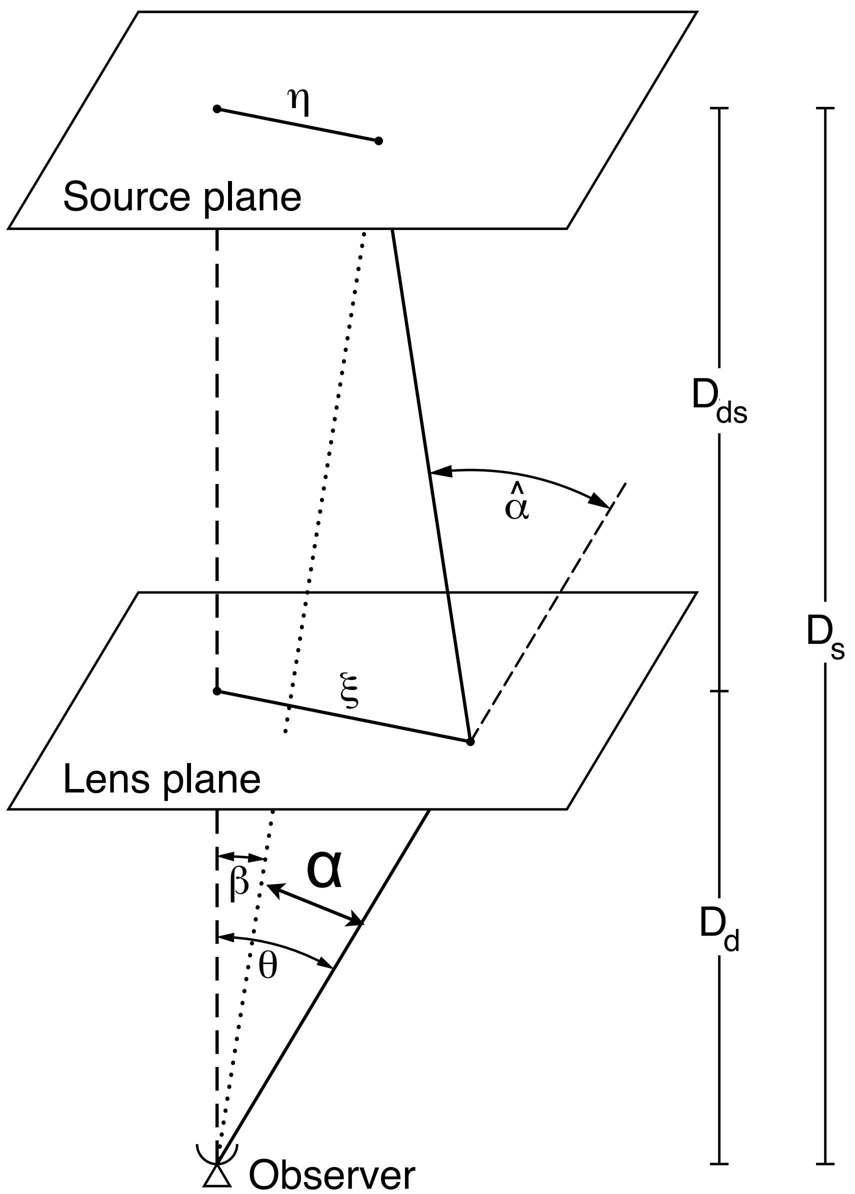

Fig. 12. Sketch of a typical gravitational lens system.

In the absence of lensing, the source would be seen at position β. Due to lensing, it is seen at position θ. All angles are small, so we have

$$\boldsymbol{\eta} = \frac{D_\mathrm{s}}{D_\mathrm{d}}\boldsymbol{\xi} - D_\mathrm{ds}\hat{\boldsymbol{\alpha}}(\boldsymbol{\xi}) \ .$$

we obtain the lens equation

$$\boldsymbol{\beta} = \boldsymbol{\theta} - \frac{D_\mathrm{ds}}{D_\mathrm{s}}\,\hat{\boldsymbol{\alpha}}(D_\mathrm{d}\boldsymbol{\theta}) \equiv \boldsymbol{\theta} - \boldsymbol{\alpha}(\boldsymbol{\theta}) \ ,$$

Scaled deflection angle

Most of the formula and figures come from

Bartelmann & Schneider, 2001

Schneider, 33rd Saas-Fee School, 2004

The lens equation

Double Einstein ring

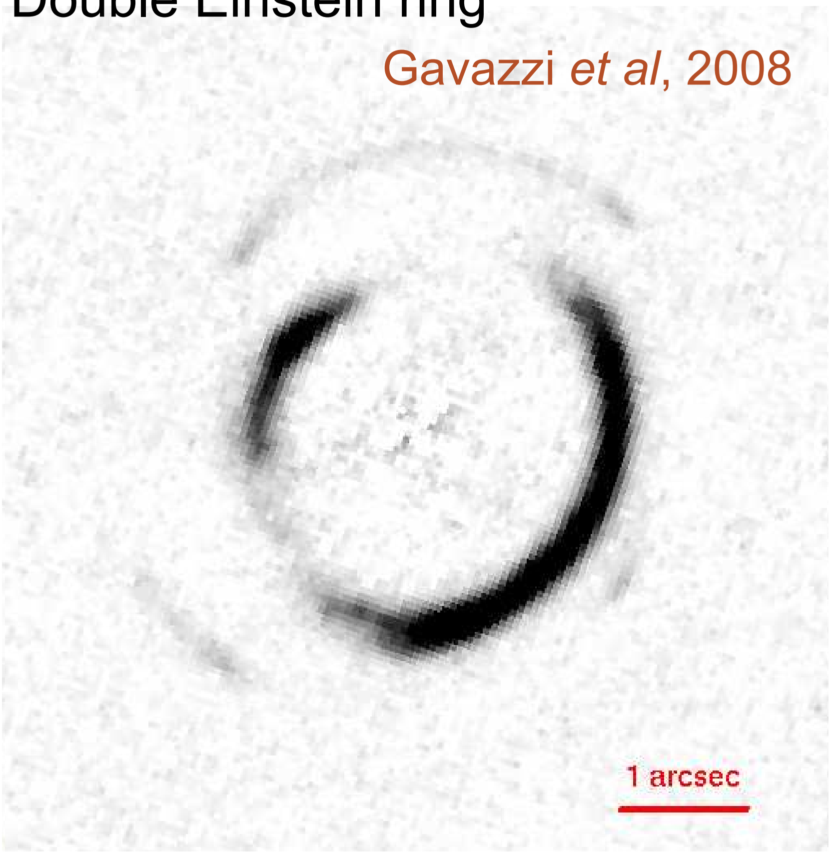

Here the lens is at redshift 0.61 and the1st radius is 1.43''. The 2nd is 2.07''

From GR we know that

$$\hat{\alpha} = \frac{4GM}{c^2\,\xi}\ .$$

If β=0, the source, lens, and observer are aligned and the image is a ring, an Einstein ring. We can then calculated the mass inside the lens

$$\theta_E^2 = \frac{4GM_{<\theta_E}}{c^2}\frac{D_{ds}}{D_s D_d}$$

The lens equation

Defining the surface mass density for the lens plane

$$\Sigma(\boldsymbol{\xi}) \equiv \int \mathrm{d}r_3\, \rho(\xi_1, \xi_2, r_3) \ ,$$

If we consider a circular symmetric lens with constant surface density. The mass contained in a radius *r* is $\Sigma \pi r^2$

We can use the deflection angle to define a critical density such that when $\Sigma = \Sigma_{\mathrm{crit}}$ we have an Eistein ring.

$$\Sigma_{\mathrm{cr}} = \frac{c^2}{4\pi G} \frac{\mathrm{D_s}}{\mathrm{D_d}\,\mathrm{D_{ds}}} .$$

The lens equation

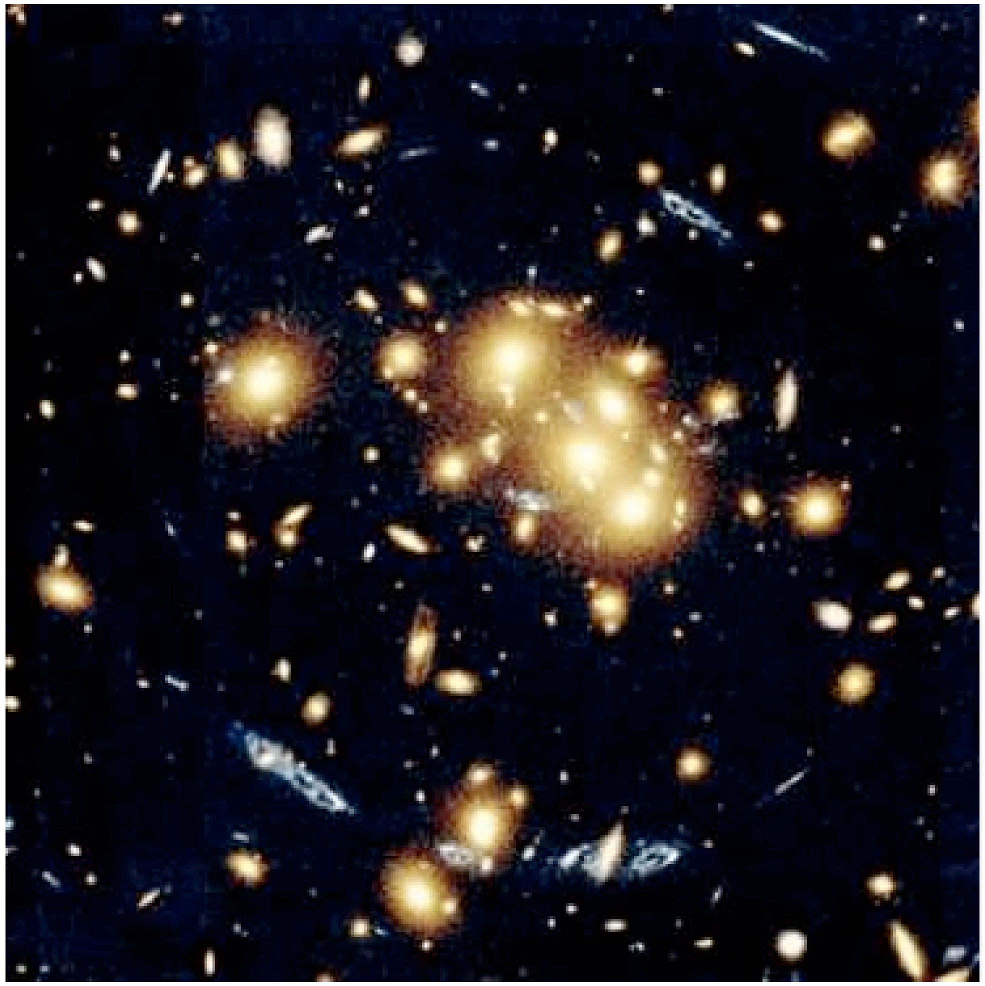

Hubble space telescope image of strong gravitational lensing by the galaxy cluster 0024+1654 (NASA HST archive).

In practice, lenses are more complicated but it is useful to the define the dimensionless surface mass density or *convergence*

$$\kappa(\boldsymbol{\theta}) = \frac{\Sigma(\mathrm{D_d}\,\boldsymbol{\theta})}{\Sigma_{\mathrm{cr}}}.$$

the value of κ marks the limit between strong and weak lensing.

In the following we will consider the weak lensing case, κ <<1.

Deflection for a mass distribution

Let's consider a mass distribution

We assume:

- Weak field, $\alpha << 1$
- Mass distribution split into cells of volume dV
- $dm=\rho(r)\, dV$
- Consider a light ray propagating along the 3rd axis with position (ξ, r_3) near a mass element dm at position (ξ', r_3')
- Use the Born approximation: near the deflector the light ray can be approximated as a straight line with impact parameter $(\xi-\xi')$
- Total deflection is the sum of individual deflections

Deflection for a mass distribution

$$\hat{\boldsymbol{\alpha}}(\boldsymbol{\xi}) = \frac{4G}{c^2} \sum \mathrm{d}m(\xi'_1, \xi'_2, r'_3) \frac{\boldsymbol{\xi} - \boldsymbol{\xi}'}{|\boldsymbol{\xi} - \boldsymbol{\xi}'|^2}$$
$$= \frac{4G}{c^2} \int \mathrm{d}^2\xi' \int \mathrm{d}r'_3 \, \rho(\xi'_1, \xi'_2, r'_3) \frac{\boldsymbol{\xi} - \boldsymbol{\xi}'}{|\boldsymbol{\xi} - \boldsymbol{\xi}'|^2} \, ,$$

Defining the surface mass density for the lens plane

$$\Sigma(\boldsymbol{\xi}) \equiv \int \mathrm{d}r_3 \, \rho(\xi_1, \xi_2, r_3) \, ,$$

We find the deflection angle

$$\hat{\boldsymbol{\alpha}}(\boldsymbol{\xi}) = \frac{4G}{c^2} \int \mathrm{d}^2\xi' \, \Sigma(\boldsymbol{\xi}') \frac{\boldsymbol{\xi} - \boldsymbol{\xi}'}{|\boldsymbol{\xi} - \boldsymbol{\xi}'|^2} \, ,$$

Deflection for a mass distribution

$$\boldsymbol{\beta} = \boldsymbol{\theta} - \frac{D_{\mathrm{ds}}}{D_{\mathrm{s}}} \hat{\boldsymbol{\alpha}}(D_{\mathrm{d}}\boldsymbol{\theta}) \equiv \boldsymbol{\theta} - \boldsymbol{\alpha}(\boldsymbol{\theta}) \ ,$$

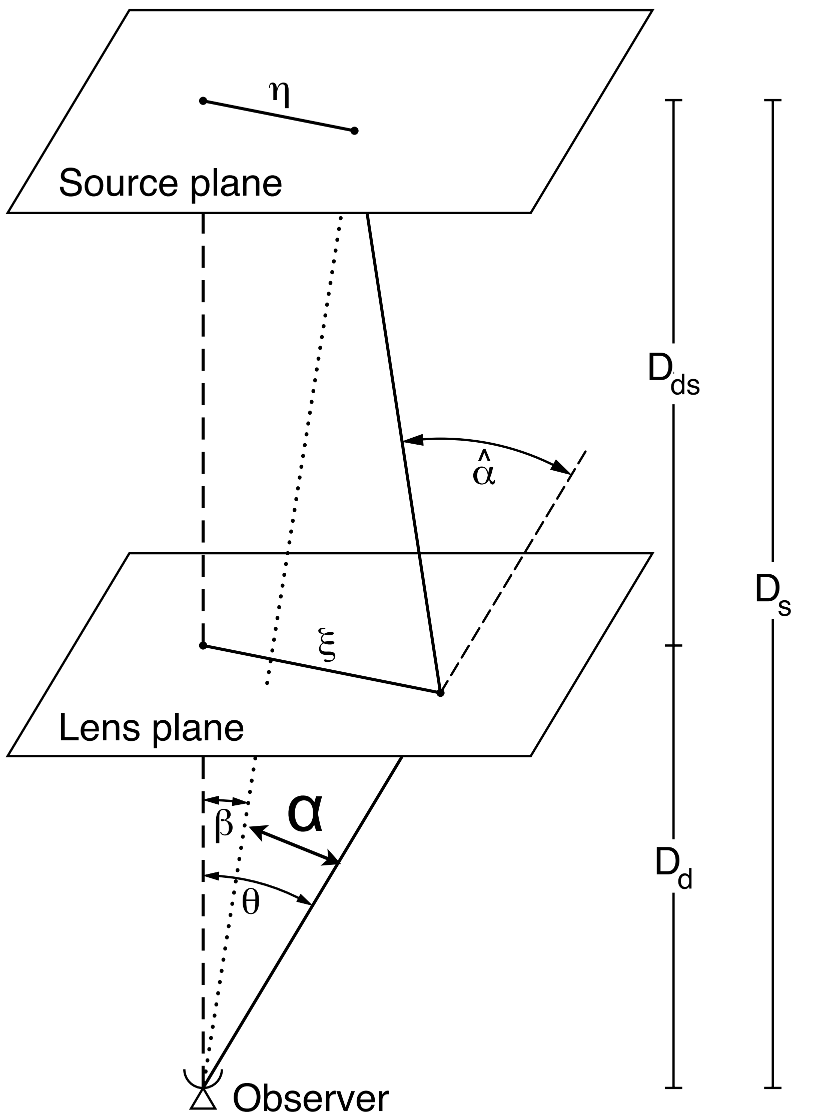

Fig. 12. Sketch of a typical gravitational lens system.

$$\boldsymbol{\alpha}(\boldsymbol{\theta}) = \frac{1}{\pi} \int_{\mathbb{R}^2} \mathrm{d}^2\theta' \, \kappa(\boldsymbol{\theta}') \, \frac{\boldsymbol{\theta} - \boldsymbol{\theta}'}{|\boldsymbol{\theta} - \boldsymbol{\theta}'|^2} \ ,$$

Defining a potential

$$\psi(\boldsymbol{\theta}) = \frac{1}{\pi} \int_{\mathbb{R}^2} \mathrm{d}^2\theta' \, \kappa(\boldsymbol{\theta}') \, \ln|\boldsymbol{\theta} - \boldsymbol{\theta}'|$$

$$\boldsymbol{\alpha} = \nabla\psi \ ,$$

The deflection angle is the gradient of the lensing potential

convergence, shear and Jacobian

The distorsions induced by lensing are discribed by the *Jacobian matrix*

$$\mathscr{A}(\boldsymbol{\theta}) = \frac{\partial \boldsymbol{\beta}}{\partial \boldsymbol{\theta}} = \left(\delta_{ij} - \frac{\partial^2 \psi(\boldsymbol{\theta})}{\partial \theta_i \partial \theta_j}\right) = \begin{pmatrix} 1-\kappa-\gamma_1 & -\gamma_2 \\ -\gamma_2 & 1-\kappa+\gamma_1 \end{pmatrix},$$

Decomposition as trace and trace-free

where the complex *shear* is defined as

$$\gamma \equiv \gamma_1 + \mathrm{i}\gamma_2 = |\gamma|\mathrm{e}^{2\mathrm{i}\varphi}, \qquad \gamma_1 = \tfrac{1}{2}(\psi_{,11} - \psi_{,22}), \quad \gamma_2 = \psi_{,12}$$

Shear is a spin-2 field. Rings a bell?

convergence, shear and Jacobian

Let's re-write the Jacobian as

$$\mathcal{A}(\boldsymbol{\theta}) = (1-\kappa)\begin{pmatrix} 1-g_1 & -g_2 \\ -g_2 & 1+g_1 \end{pmatrix}$$

where the *reduced shear* is defined as

$$g \equiv \frac{\gamma}{1-\kappa} = \frac{|\gamma|}{1-\kappa}\,\mathrm{e}^{2\mathrm{i}\varphi}$$

The Jacobian describes the mapping between the source and image planes

The convergence will only change the size of the object,
and the shear will distort the images

Action of the Jacobian matrix

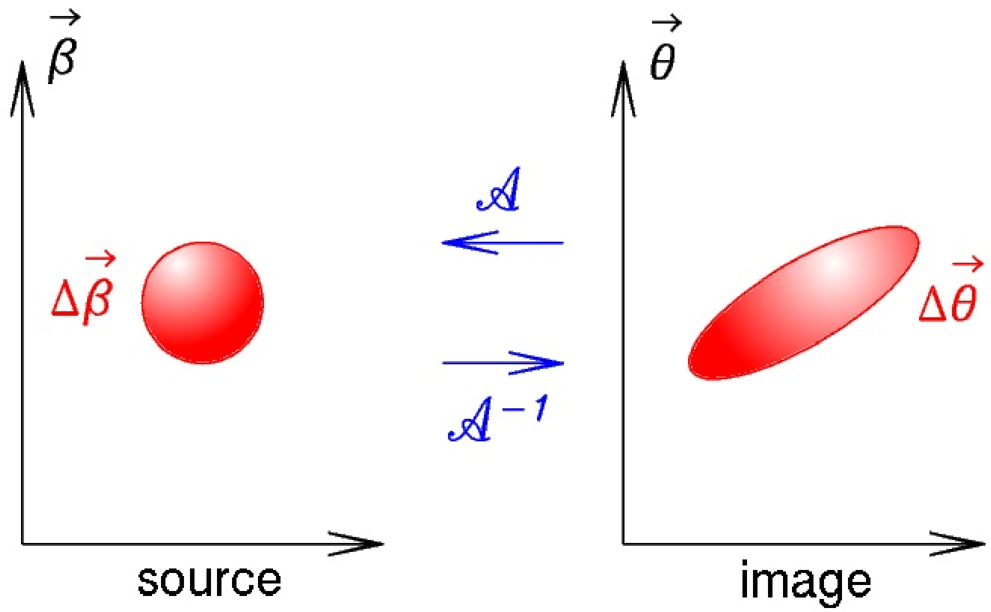

A circle will be mapped into an ellipse with axes

$$|(1-\kappa)(1+|g|)|^{-1} \qquad |(1-\kappa)(1-|g|)|^{-1}$$

If galaxies were intrinsically round, we would easily deduce the reduced shear

Action of the Jacobian matrix

$$\mathcal{A}(\boldsymbol{\theta}) = (1-\kappa)\begin{pmatrix} 1-g_1 & -g_2 \\ -g_2 & 1+g_1 \end{pmatrix}$$

Isotropic stretch

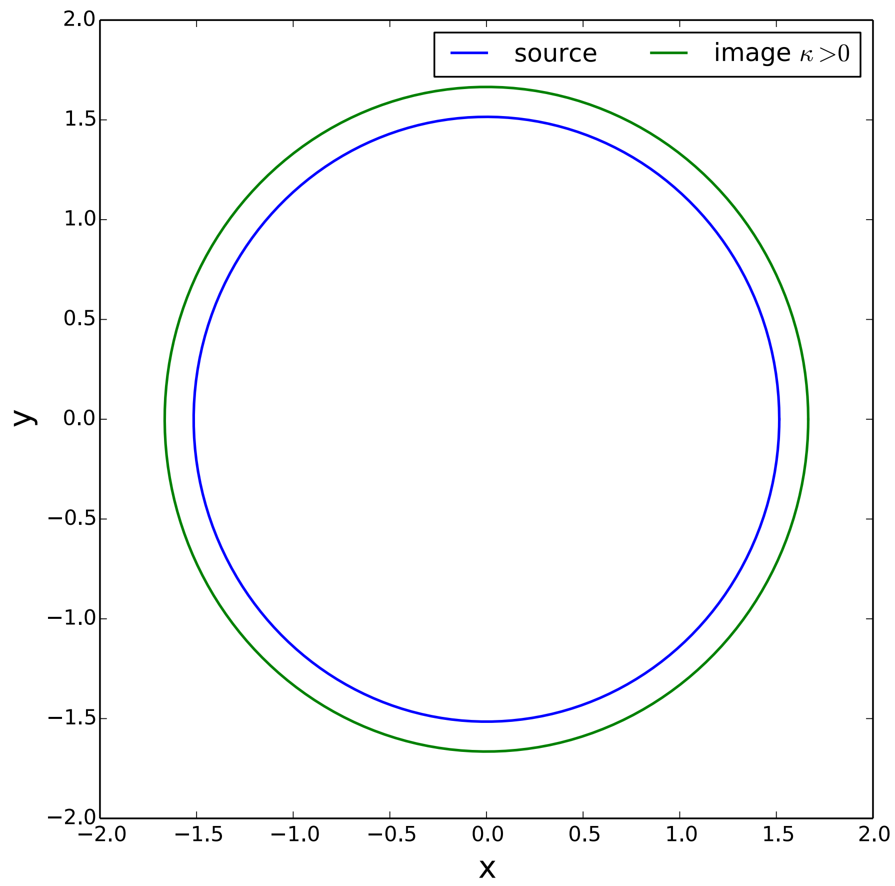

Action of the Jacobian matrix

$$\mathcal{A}(\boldsymbol{\theta}) = (1-\kappa)\begin{pmatrix} 1-g_1 & -g_2 \\ -g_2 & 1+g_1 \end{pmatrix}$$

anisotropic elongation

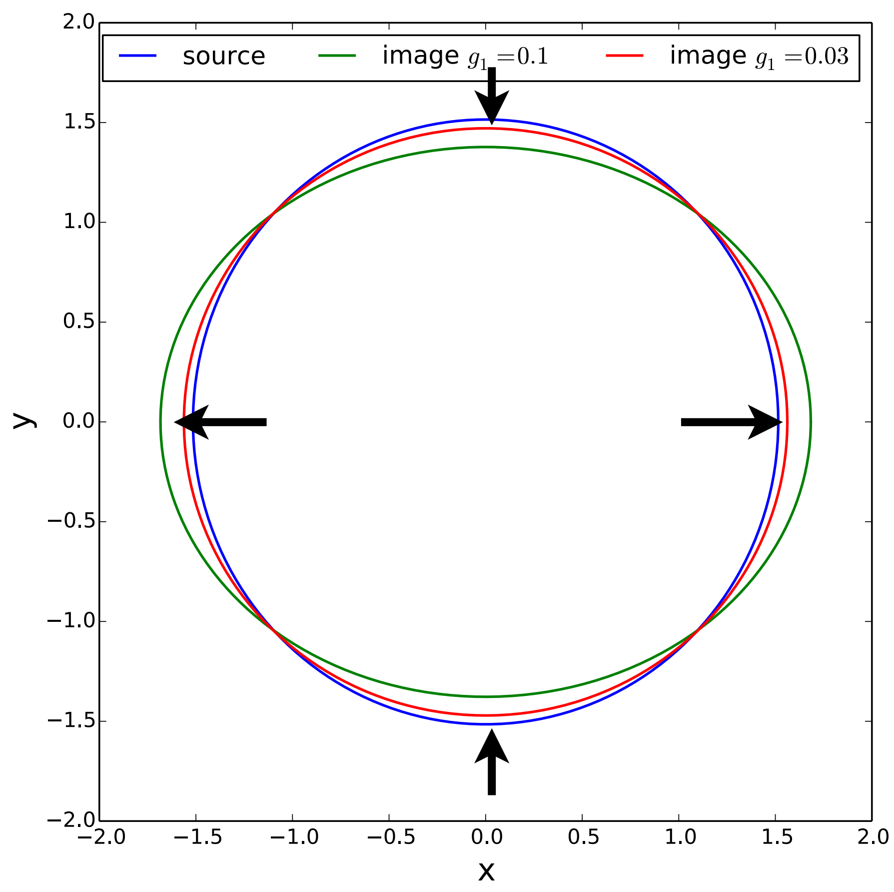

g_1 >0

stretches an image along the *x-axis* and compresses along the *y*-axis

Action of the Jacobian matrix

$$\mathcal{A}(\boldsymbol{\theta}) = (1-\kappa)\begin{pmatrix} 1-g_1 & -g_2 \\ -g_2 & 1+g_1 \end{pmatrix}$$

anisotropic elongation

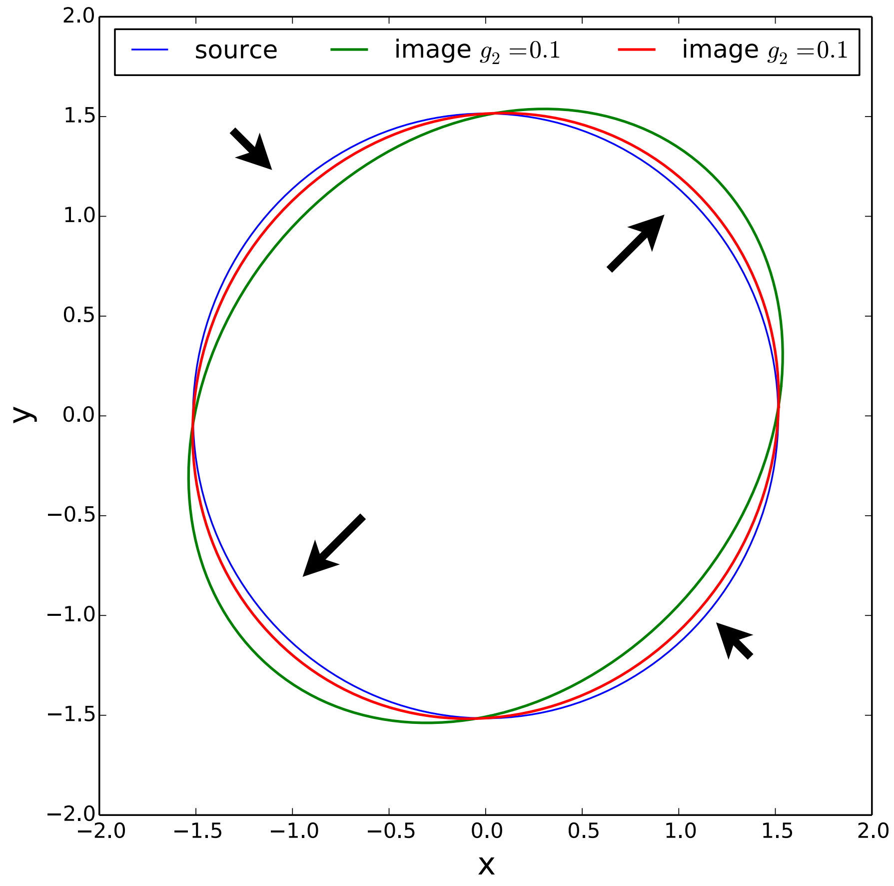

$g_2 > 0$

stretches an image along the *y*=*x* direction and compresses along the *y*=-*x* direction

Ellipticities estimation

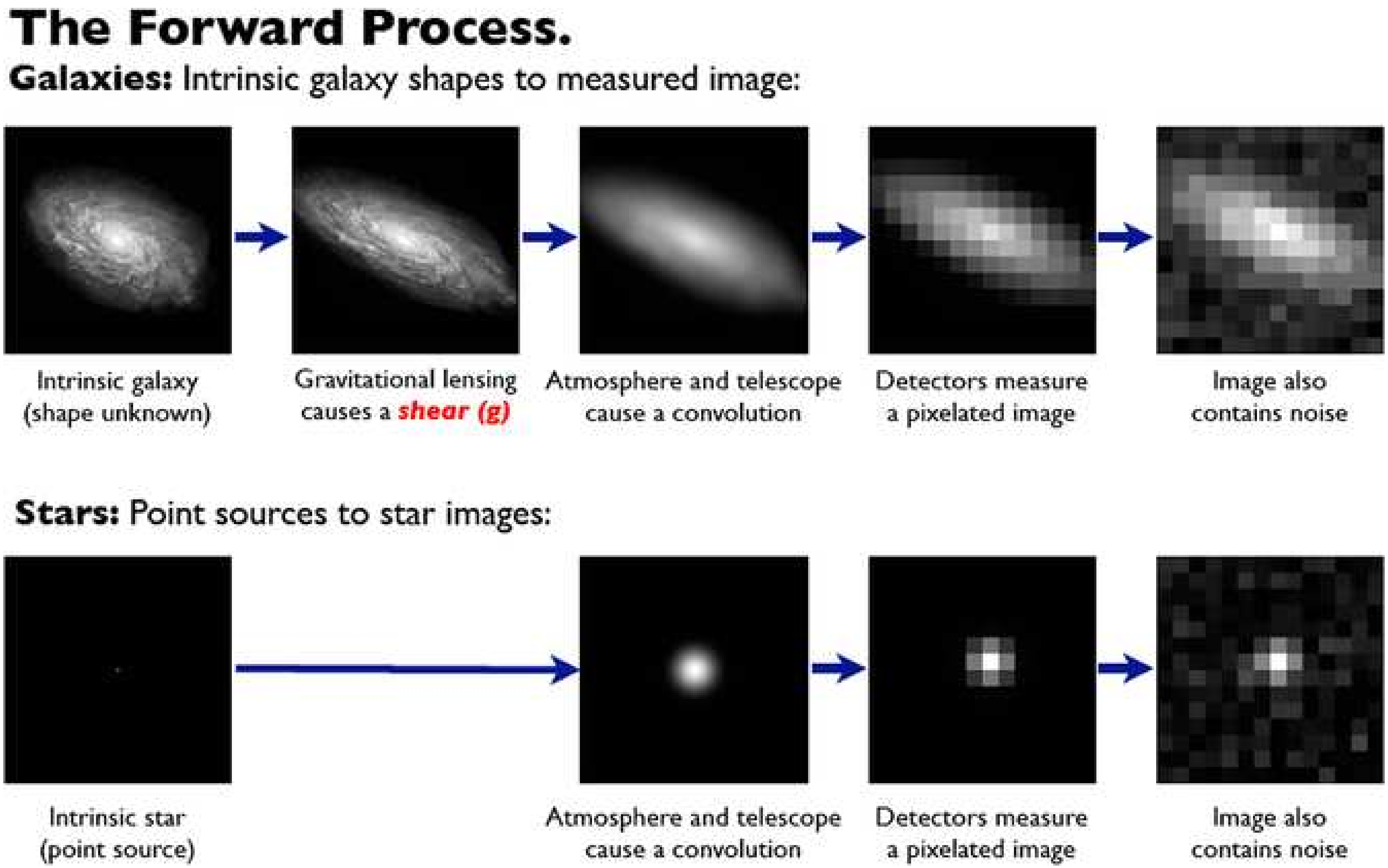

HANDBOOK FOR THE GREAT08 CHALLENGE: AN IMAGE ANALYSIS COMPETITION FOR COSMOLOGICAL LENSING

Ellipticities estimation

Estimating the ellipticities of the observed galaxies with the quadrupole moments

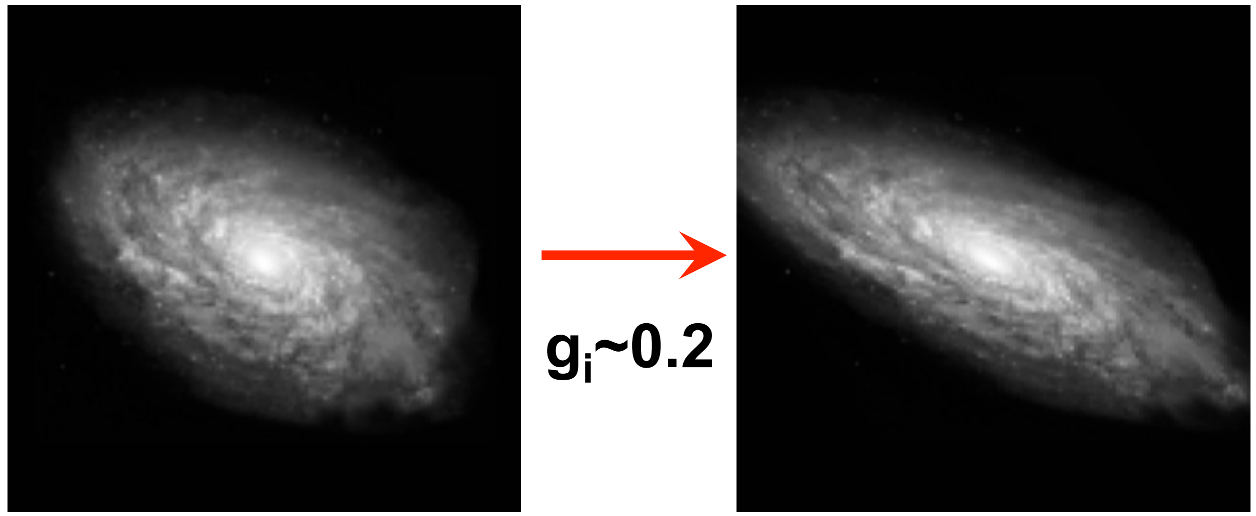

The object is defined on the image by its brightness

Its center is found with the first moments

$$\bar{x} = \frac{\int I(x,y)x \, dx \, dy}{\int I(x,y) \, dx \, dy}, \qquad \bar{y} = \frac{\int I(x,y)y \, dx \, dy}{\int I(x,y) \, dx \, dy},$$

Quadrupole moments

$$\mathcal{Q}_{yy} = \frac{\int I(x,y)(y-\bar{y})^2 \, dx \, dy}{\int I(x,y) \, dx \, dy}. \qquad \mathcal{Q}_{xx} = \frac{\int I(x,y)(x-\bar{x})^2 \, dx \, dy}{\int I(x,y) \, dx \, dy},$$

$$\mathcal{Q}_{xy} = \frac{\int I(x,y)(x-\bar{x})(y-\bar{y}) \, dx \, dy}{\int I(x,y) \, dx \, dy},$$

Ellipticities estimation

Define an ellipticity

$$\epsilon \equiv \epsilon_1 + i\epsilon_2 = \frac{\mathcal{Q}_{xx} - \mathcal{Q}_{yy} + 2i\mathcal{Q}_{xy}}{\mathcal{Q}_{xx} + \mathcal{Q}_{yy} + 2(\mathcal{Q}_{xx}\mathcal{Q}_{yy} - \mathcal{Q}_{xy}^2)^{1/2}},$$

Bonnet & Mellier 1995

$$\mathcal{Q}^{\mathrm{u}} = \mathcal{A}\mathcal{Q}^{\mathrm{l}}\mathcal{A}^T,$$

$$\epsilon^{\mathrm{l}} = \frac{\epsilon^{\mathrm{u}} + g}{1 + g^*\epsilon^{\mathrm{u}}}$$

Ellipticities estimation

Assuming that the unlensed ellipticities average to zero, $0 = \mathrm{E}\left(\epsilon^{(\mathrm{s})}\right)$ we have

$$\mathrm{E}(\epsilon) = \begin{cases} g & \text{if } |g| \leq 1 \\ 1/g^* & \text{if } |g| > 1 \ . \end{cases}$$

Seitz & Schneider 1997

Averaged galaxy ellipticities provide a unbiased estimate of the reduced shear

Ellipticities estimation

Assuming that the unlensed ellipticities average to zero, $0 = \mathrm{E}\left(\epsilon^{(\mathrm{s})}\right)$ we have

$$\mathrm{E}(\epsilon) = \begin{cases} g & \text{if } |g| \leq 1 \\ 1/g^* & \text{if } |g| > 1 \,. \end{cases}$$

Seitz & Schneider 1997

Averaged galaxy ellipticities provide a unbiased estimate of the reduced shear

Two mains difficulties for current and future weak lensing experiments

Shape measurements

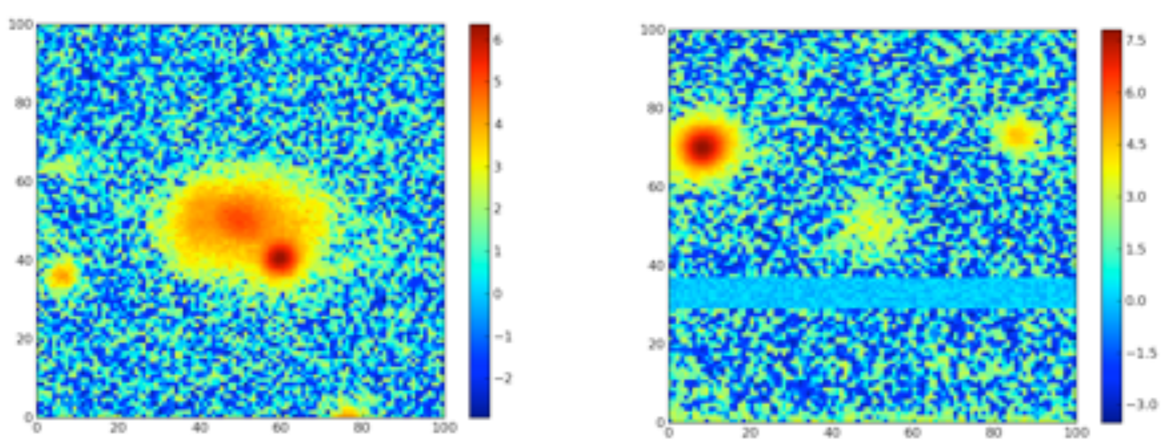

Examples from the Dark Energy Survey

Intrinsic ellipticities do not necessarily average to zero

Intrisic alignments!!

Cosmic shear

In a cosmological context, the deflection angle becomes for a source at distance *w*

$$\boldsymbol{\alpha}(\boldsymbol{\theta}, w) = \frac{f_K(w)\boldsymbol{\theta} - \boldsymbol{x}(\boldsymbol{\theta}, w)}{f_K(w)} = \frac{2}{c^2}\int_0^w \mathrm{d}w' \frac{f_K(w - w')}{f_K(w)} \nabla_\perp \Phi[f_K(w')\boldsymbol{\theta}, w']$$

Cosmic shear

In a cosmological context, the deflection angle becomes for a source at distance *w*

$$\boldsymbol{\alpha}(\boldsymbol{\theta}, w) = \frac{f_K(w)\boldsymbol{\theta} - \boldsymbol{x}(\boldsymbol{\theta}, w)}{f_K(w)} = \frac{2}{c^2}\int_0^w \mathrm{d}w' \frac{f_K(w - w')}{f_K(w)} \nabla_\perp \Phi[f_K(w')\boldsymbol{\theta}, w']$$

Then the lensing potential becomes

$$\psi(\boldsymbol{\theta}, w) := \frac{2}{c^2}\int_0^w \mathrm{d}w' \, \frac{f_K(w - w')}{f_K(w) \, f_K(w')} \, \Phi\left(f_K(w')\boldsymbol{\theta}, w'\right)$$

and the Jacobian matrix is defined the same as in the thin-lens case $\mathcal{A}_{ij} = \delta_{ij} - \psi_{,ij}$;

and the 3-D matter distribution can be treated as an equivalent lens plane with potential ψ, convergence $\kappa = \nabla^2\psi/2$, and shear $(\psi_{,11} - \psi_{,22})/2 + \mathrm{i}\psi_{,12}$.

Cosmic shear

Last step, integrate on all sources

For a redshift distribution of sources with $p_z(z)\,\mathrm{d}z = p_w(w)\,\mathrm{d}w$, the effective surface mass density becomes

$$\begin{aligned}\kappa(\boldsymbol{\theta}) &= \int \mathrm{d}w\; p_w(w)\,\kappa(\boldsymbol{\theta}, w) \\ &= \frac{3H_0^2\Omega_\mathrm{m}}{2c^2} \int_0^{w_\mathrm{h}} \mathrm{d}w\; g(w)\, f_K(w)\, \frac{\delta\left(f_K(w)\boldsymbol{\theta}, w\right)}{a(w)}\;, \end{aligned} \tag{93}$$

with

$$g(w) = \int_w^{w_\mathrm{h}} \mathrm{d}w'\; p_w(w')\,\frac{f_K(w'-w)}{f_K(w')}\;, \tag{94}$$

Then use Limber approximation to obtain the power spectrum of the convergence

$$P_\kappa(\ell) = \frac{9H_0^4\Omega_\mathrm{m}^2}{4c^4} \int_0^{w_\mathrm{h}} \mathrm{d}w\; \frac{g^2(w)}{a^2(w)}\, P_\delta\left(\frac{\ell}{f_K(w)}, w\right)\;.$$

Current status of cosmic shear

In practice people consider real-space based observables that are related to the convergence power spectrum

$$\xi_\pm(\theta) = \langle \gamma_t \gamma_t \rangle (\theta) \pm \langle \gamma_\times \gamma_\times \rangle (\theta) \ , \quad \xi_\times(\theta) = \langle \gamma_t \gamma_\times \rangle (\theta) \ .$$

$$\xi_+(\theta) = \int_0^\infty \frac{\mathrm{d}\ell \, \ell}{2\pi} \mathrm{J}_0(\ell\theta) \, P_\kappa(\ell) \ ; \quad \xi_-(\theta) = \int_0^\infty \frac{\mathrm{d}\ell \, \ell}{2\pi} \mathrm{J}_4(\ell\theta) \, P_\kappa(\ell) \ ,$$

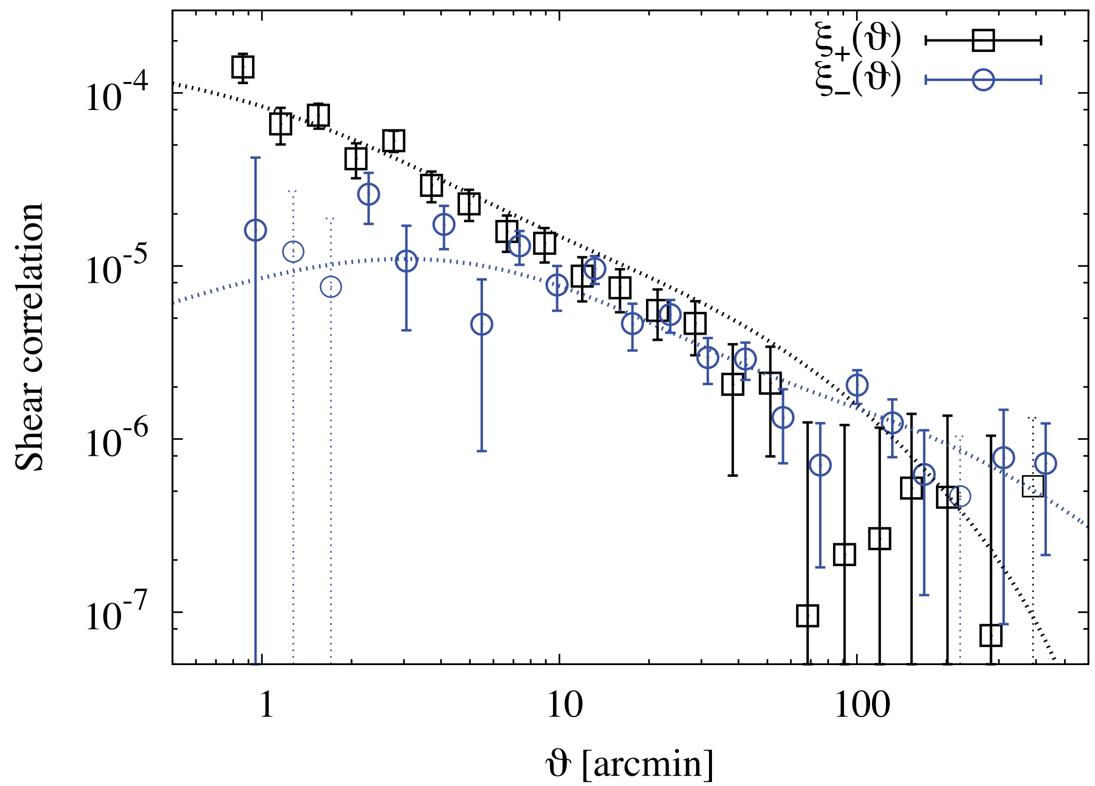

Figure 6. The measured shear correlation functions ξ_+ (black squares) and ξ_- (blue circles), combined from all four Wide patches. The error bars correspond to the total covariance diagonal. Negative values are shown as thin points with dotted error bars. The lines are the theoretical prediction using the *WMAP7* best-fitting cosmology and the non-linear model described in Section 4.3. The data points and error bars are listed in Table B1.

Kilbinger *et al*, 2013 (CFHTLens)

Current status of cosmic shear

The shear dispersion. Consider a circular aperture of radius θ; the mean shear in this aperture is $\bar{\gamma}$. Averaging over many such apertures, one defines the shear dispersion $\left\langle |\bar{\gamma}|^2 \right\rangle (\theta)$. It is related to the power spectrum through

$$\left\langle |\bar{\gamma}|^2 \right\rangle (\theta) = \frac{1}{2\pi} \int \mathrm{d}\ell \, \ell \, P_\kappa(\ell) \, W_{\mathrm{TH}}(\ell\theta) \, , \quad \text{where} \;\; W_{\mathrm{TH}}(\eta) = \frac{4 \mathrm{J}_1^2(\eta)}{\eta^2} \qquad (106)$$

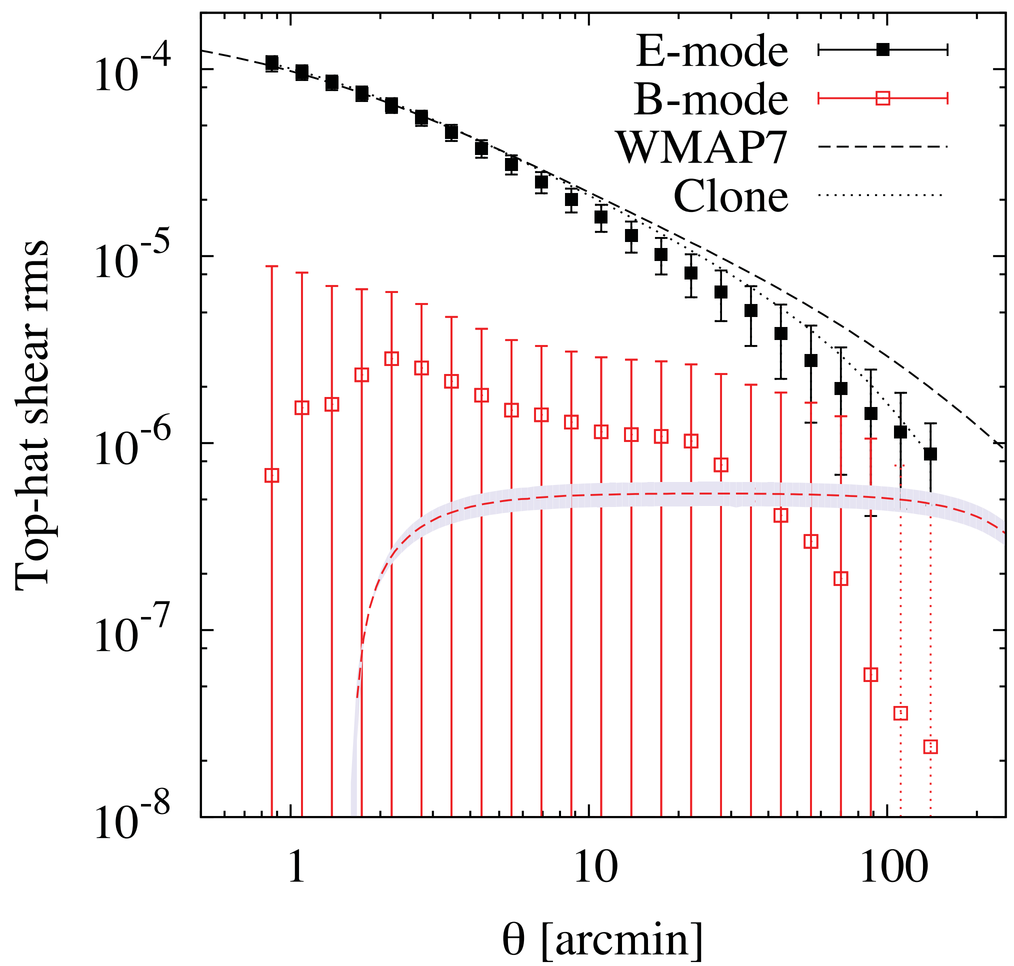

Kilbinger *et al*, 2013 (CFHTLens)

Current status of cosmic shear

Weak lensing constraints on parameters

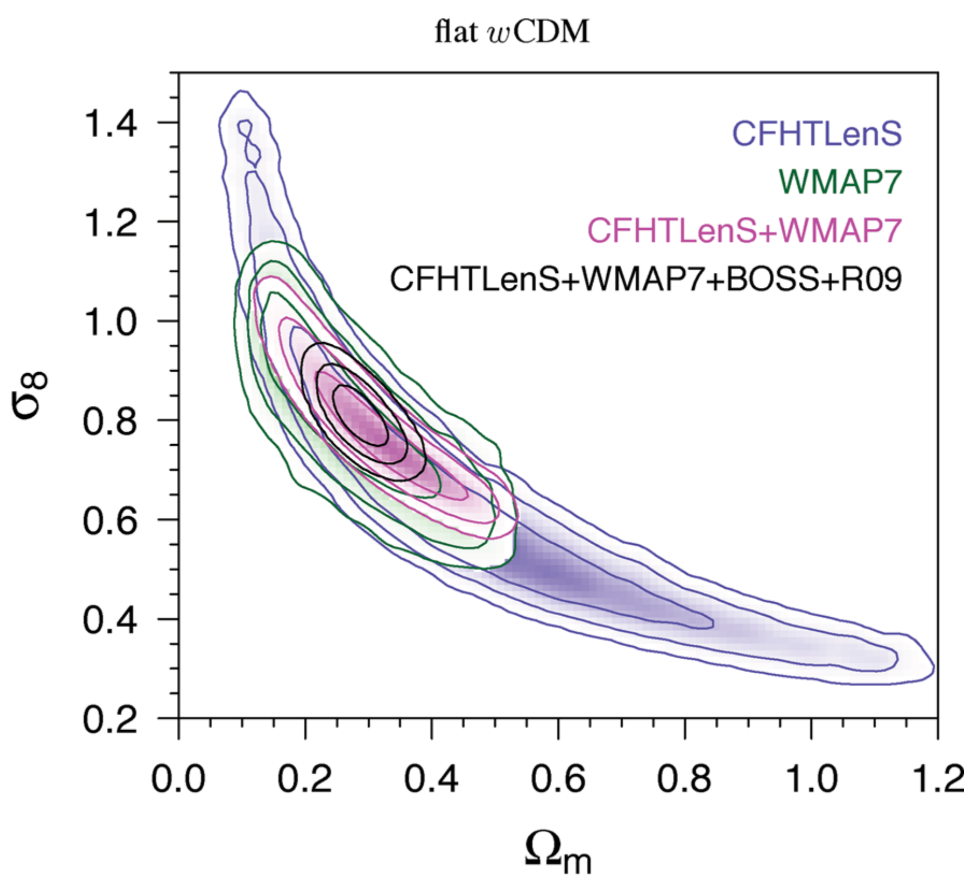

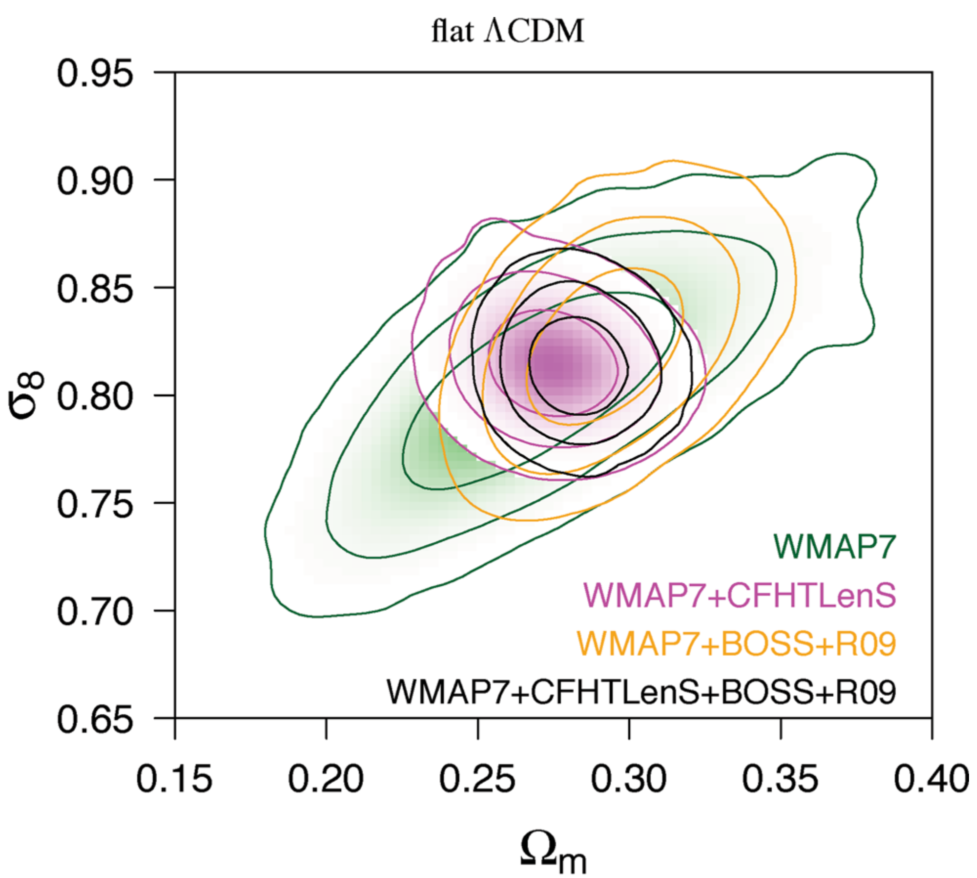

Kilbinger *et al*, 2013 (CFHTLens)

CFHTLens survey size is about 150 sq.deg.

The Dark Energy Survey

4m Blanco telescope at CTIO

Multiband survey

- 5000 deg^2 grizY to 24th mag = 25 times CFHTLens
- 15 deg^2 for type Ia supernovae
- 5 years
- 300 millions photometric redshifts
- will provide visible data to Euclid.

Other surveys

- Vista Hemisphere Survey (JHK)
- South Pole Telescope

DES footprint

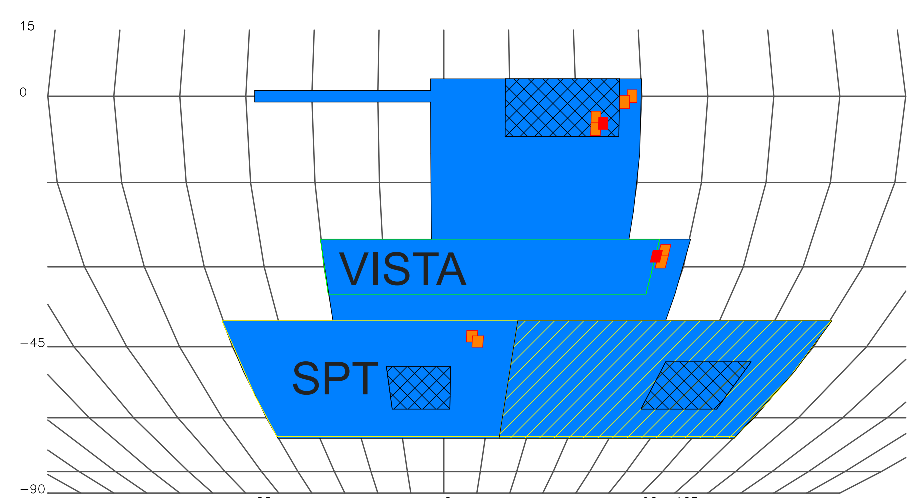

Survey actual coverage

- Early data: ~250 deg^2 at full depth. Early science results to expect within the year
- 1st year data: Oct13 - Fev 14. ~2000 sq deg^2. Data processing ongoing
- 2nd year data taking has started

Stay tuned for DES cosmic shear results!

References

General reviews on weak lensing

M. Bartelmann, P. Schneider / Physics Reports 340 (2001) 291–472

Peter Schneider, Proceeding of the 33rd Saas-Fee Advanced Course, 2003
astro-ph/0509252

Great08

HANDBOOK FOR THE GREAT08 CHALLENGE: AN IMAGE ANALYSIS COMPETITION FOR COSMOLOGICAL LENSING

arxiv: 0802.1214

Latest CFHTLens results

www.cfhtlens.org

CMB Lensing

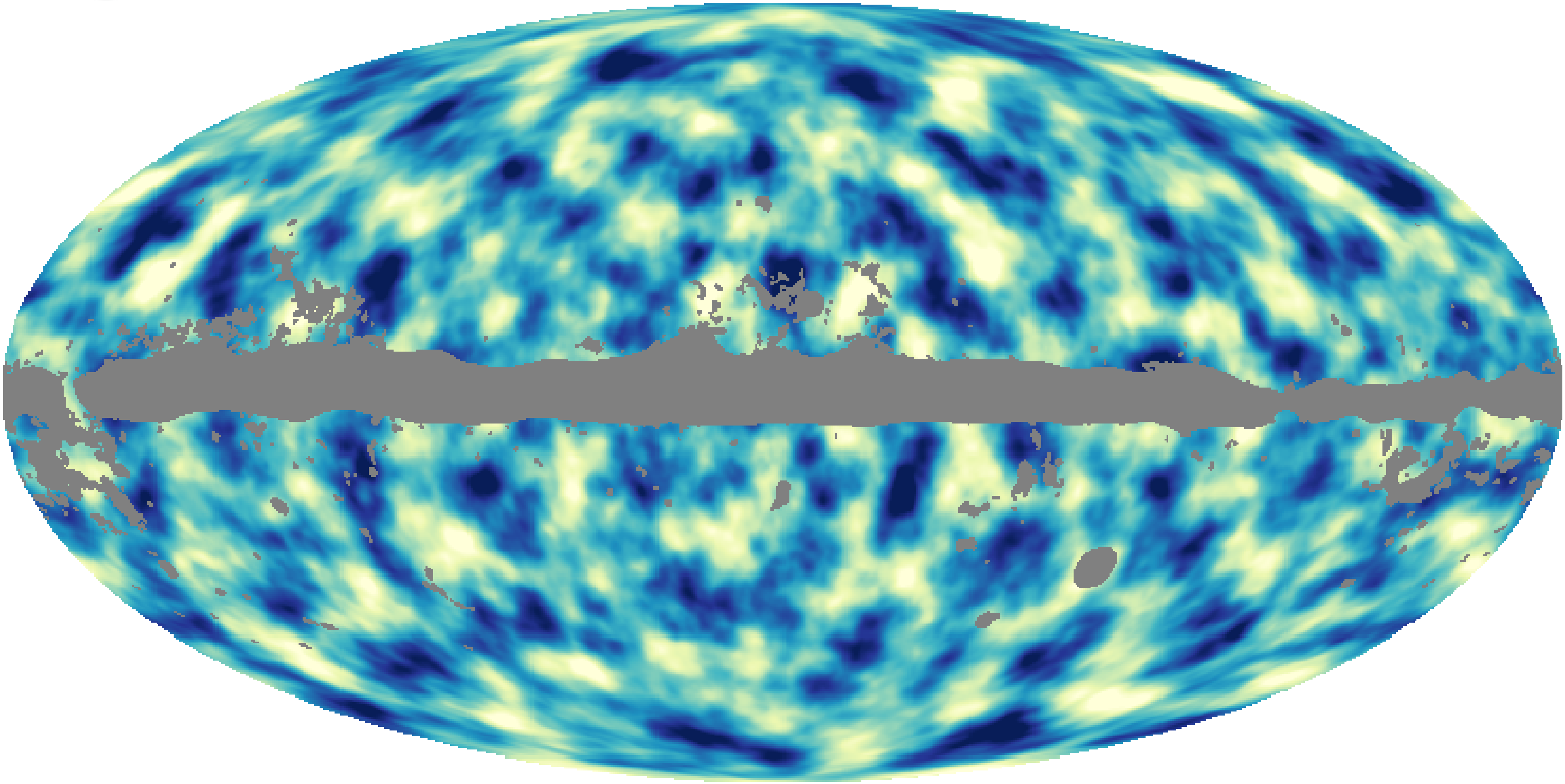

The lensing map traces the matter distribution up to the last scattering surface

CMB Lensing

Astron. Astrophys. 184, 1–6 (1987)

ASTRONOMY
AND
ASTROPHYSICS

Gravitational lensing effect on the fluctuations of the cosmic background radiation

A. Blanchard[1,2] **and J. Schneider**[1]

[1] Groupe d'astrophysique Relativiste, Observatoire de Paris, Section de Meudon, Place J. Janssen, F-92195 Meudon Principal Cedex, France
[2] Université de Paris VII, 2, Place Jussieu, F-75251 Paris Cedex 05, France

Received November 4, 1986; accepted March 13, 1987

Effect investigated in 1987, first detected in 2007, and has now become a standard cosmological probe

What is different from galaxy weak lensing?

CMB Lensing vs Cosmis shear

distant galaxies

located over a range of redshift

Intrinsic properties

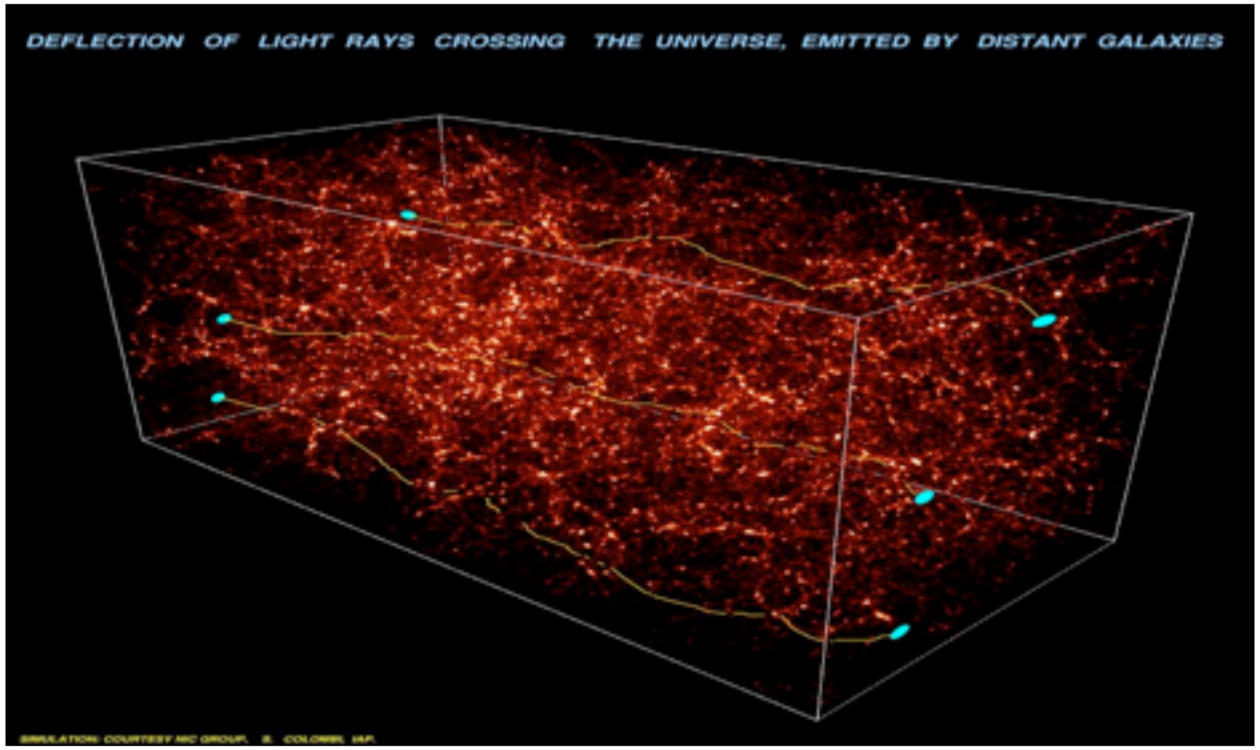

shape measurements

last scattering surface

random field

redshift known

statistical properties well know

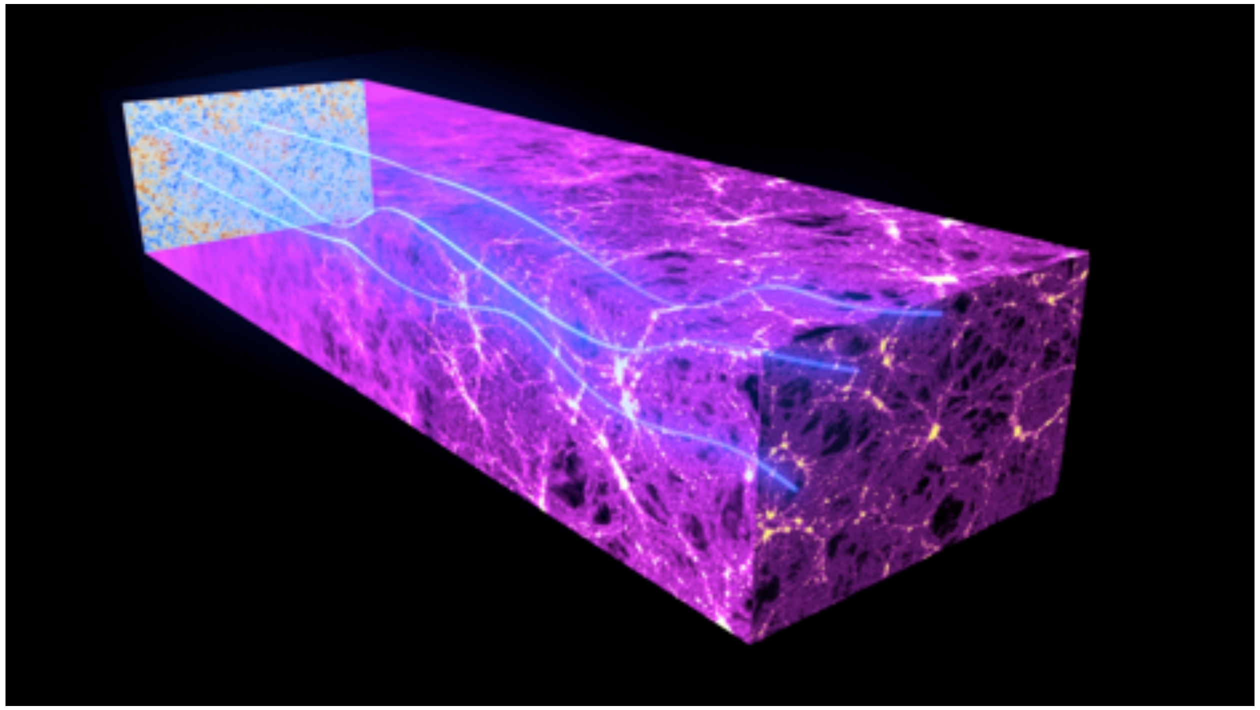

CMB T+P anisotropies

CMB Lensing

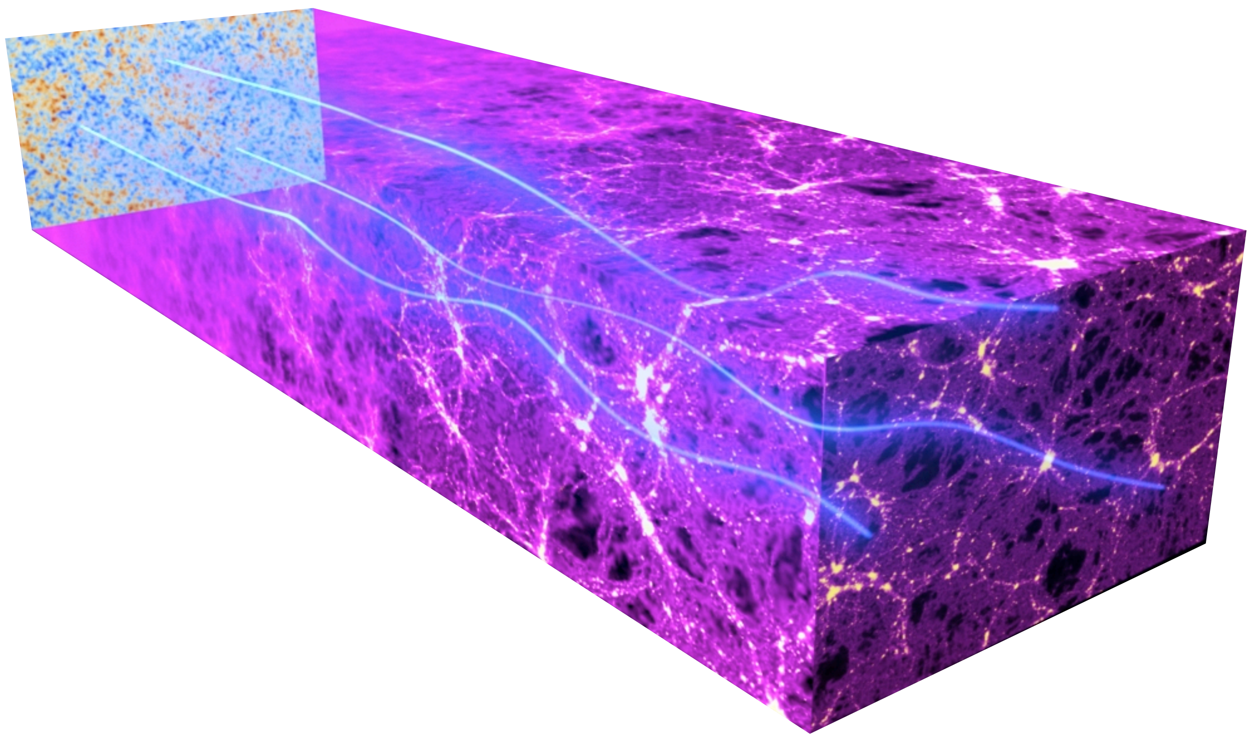

Typical deflection δβ sourced by potential Ψ

$\Psi \sim 2\ 10^{-5}$ $\delta\beta \sim 10^{-4}$

Photons encounter ~ 50 potential wells

r.m.s deflection
$50^{1/2} * 10^{-4} \sim 2$ arcmin

$$\Theta[\hat{\mathbf{n}}] = \tilde{\Theta}[\hat{\mathbf{n}} + \nabla\phi(\hat{\mathbf{n}})]$$

$$\phi(\hat{\boldsymbol{n}}) = -2\int_0^{\chi_*} d\chi \frac{f_K(\chi_* - \chi)}{f_K(\chi_*)f_K(\chi)} \Psi(\chi\hat{\boldsymbol{n}}; \eta_0 - \chi).$$

Lensing potential power spectrum

$$\phi(\hat{\boldsymbol{n}}) = -2\int_0^{\chi_*} d\chi \frac{f_K(\chi_* - \chi)}{f_K(\chi_*)f_K(\chi)} \Psi(\chi\hat{\boldsymbol{n}}; \eta_0 - \chi).$$

Contribution of LSS at different redshifts to the lensing potential power spectrum

Absolute spectrum

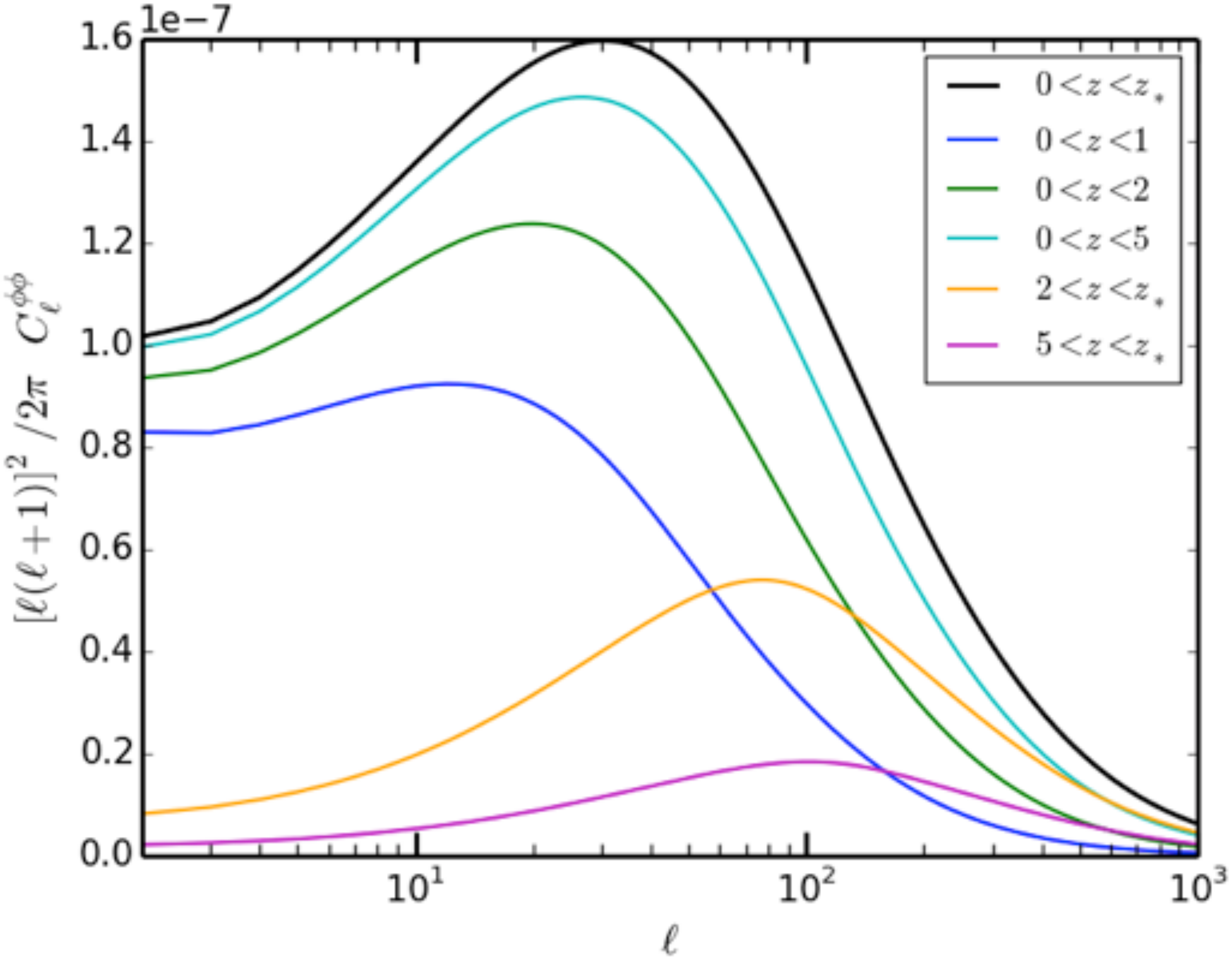

Ratio

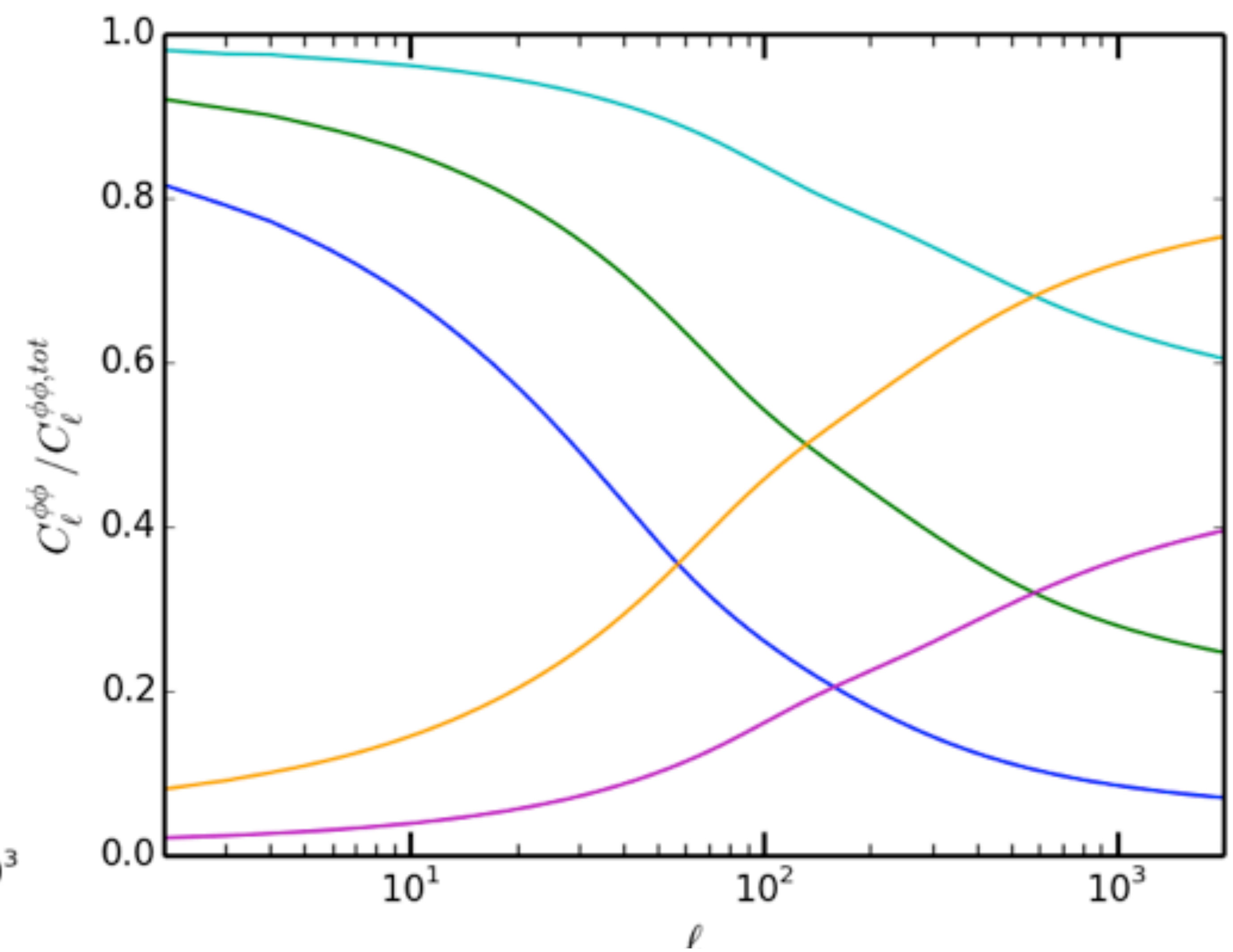

The CMB lensing kernel is wide. Almost all redshift contribute

CMB lensing

$$\Theta[\hat{\mathbf{n}}] = \tilde{\Theta}[\hat{\mathbf{n}} + \nabla\phi(\hat{\mathbf{n}})] \approx \tilde{\Theta}[\hat{\mathbf{n}}] + \nabla\phi[\hat{\mathbf{n}}]\ \nabla\tilde{\Theta}[\hat{\mathbf{n}}] + \cdots$$

Deflections are about 2 arcmin

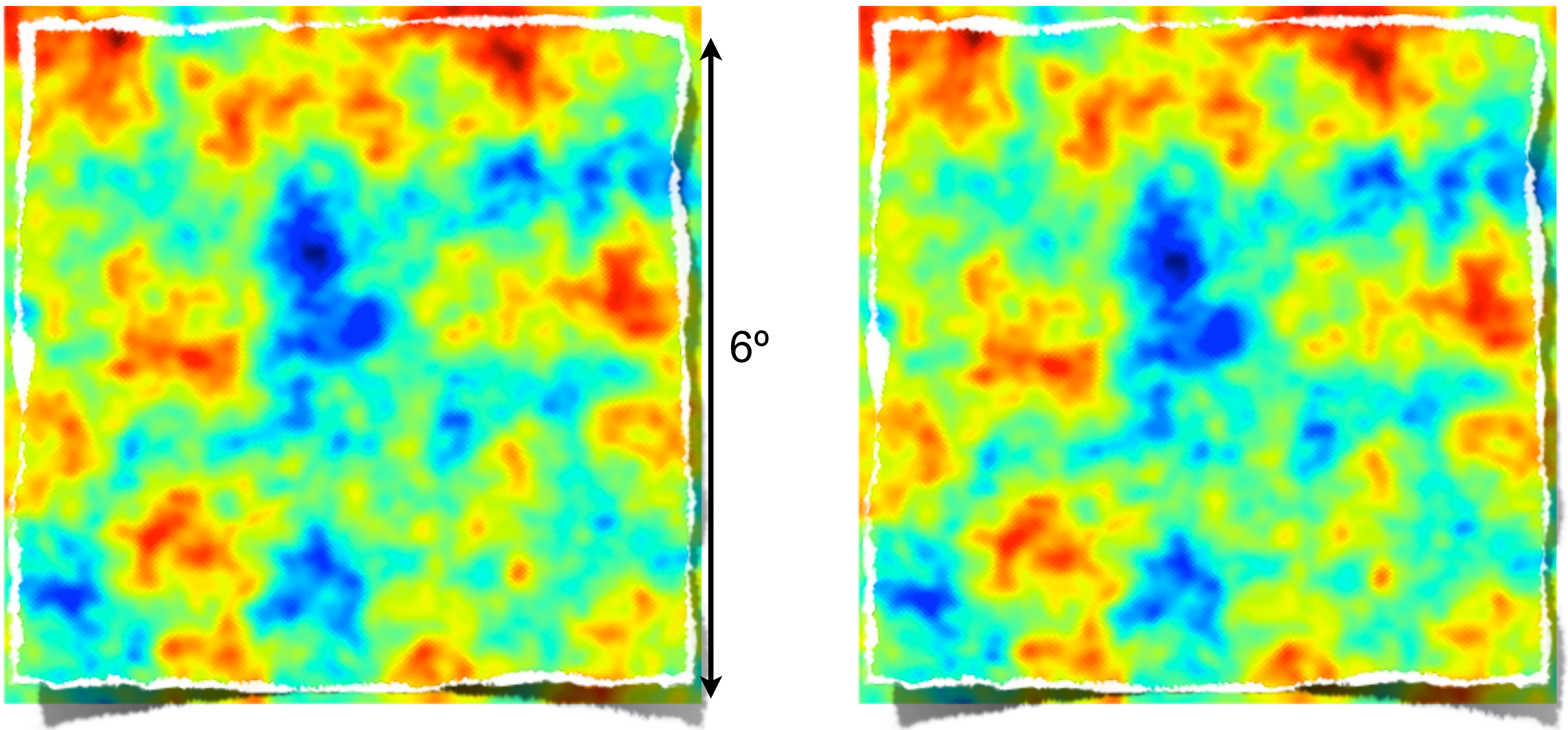

Unlensed

Lensed

CMB lensing

$$\Theta[\hat{\mathbf{n}}] = \tilde{\Theta}[\hat{\mathbf{n}} + \nabla\phi(\hat{\mathbf{n}})] \approx \tilde{\Theta}[\hat{\mathbf{n}}] + \nabla\phi[\hat{\mathbf{n}}]\ \nabla\tilde{\Theta}[\hat{\mathbf{n}}] + \cdots$$

Deflections are about 2 arcmin

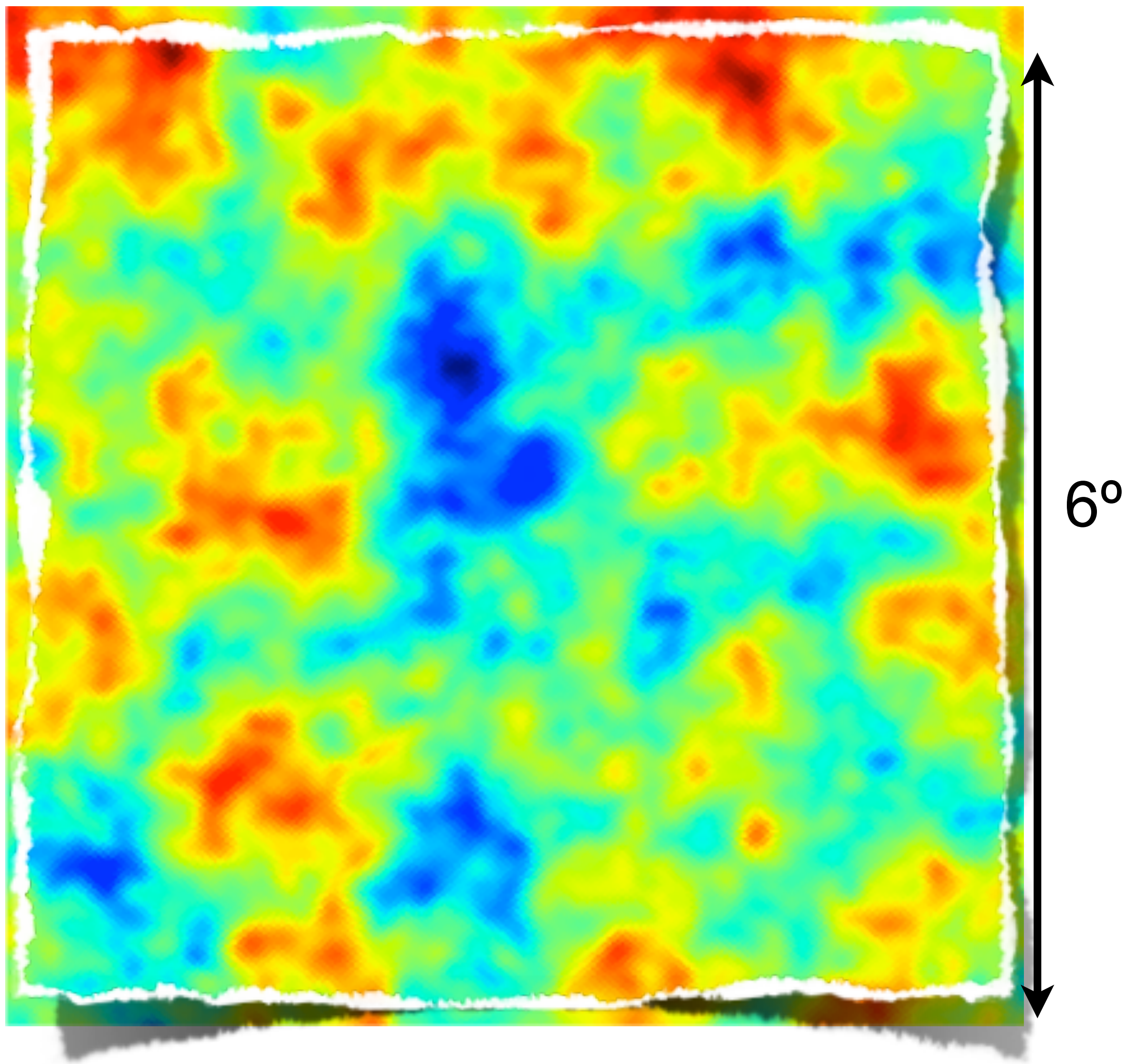

Unlensed

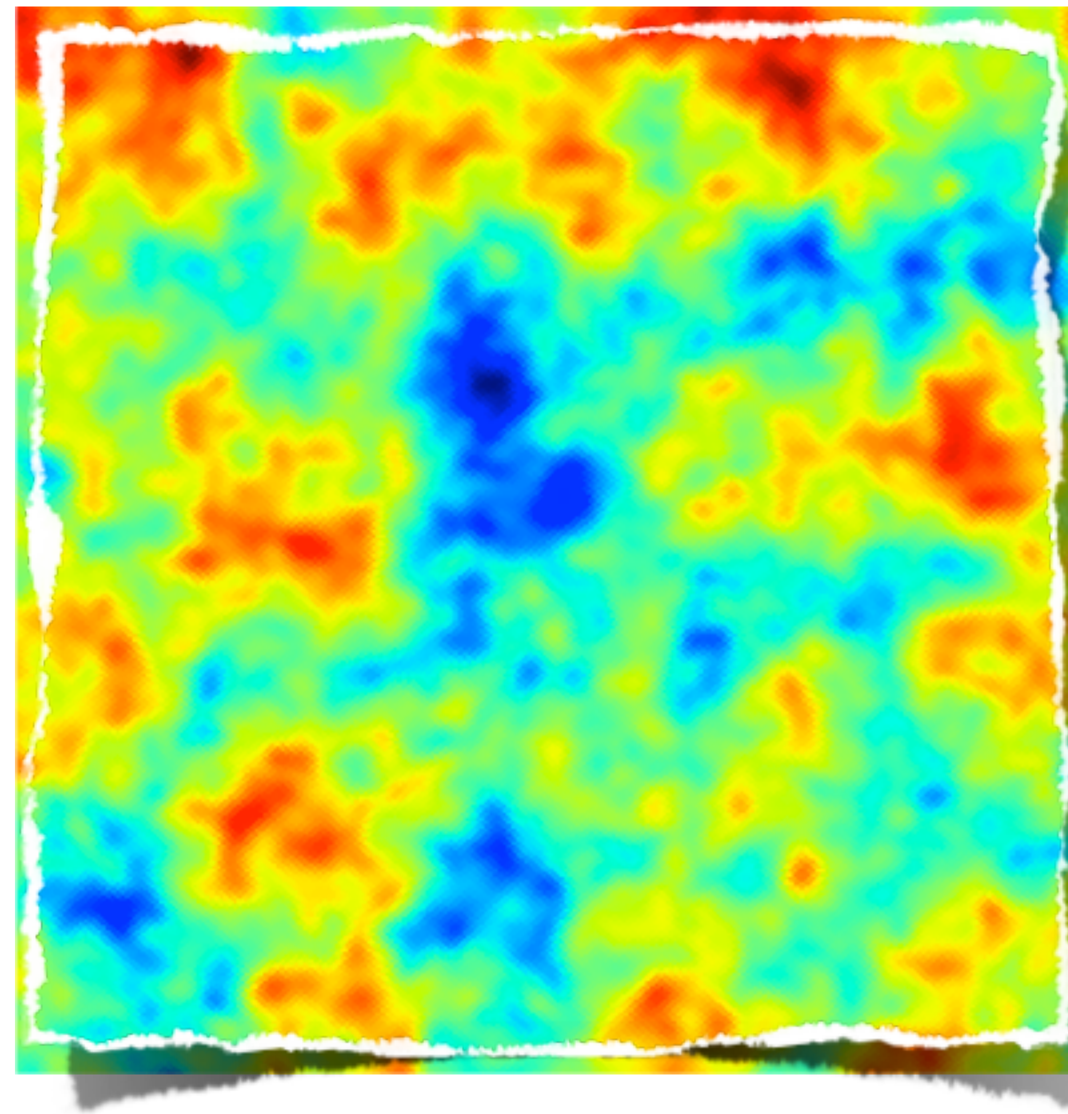

Unlensed

CMB lensing

$$\Theta[\hat{\mathbf{n}}] = \tilde{\Theta}[\hat{\mathbf{n}} + \nabla\phi(\hat{\mathbf{n}})] \approx \tilde{\Theta}[\hat{\mathbf{n}}] + \nabla\phi[\hat{\mathbf{n}}]\ \nabla\tilde{\Theta}[\hat{\mathbf{n}}] + \cdots$$

Deflections are about 2 arcmin

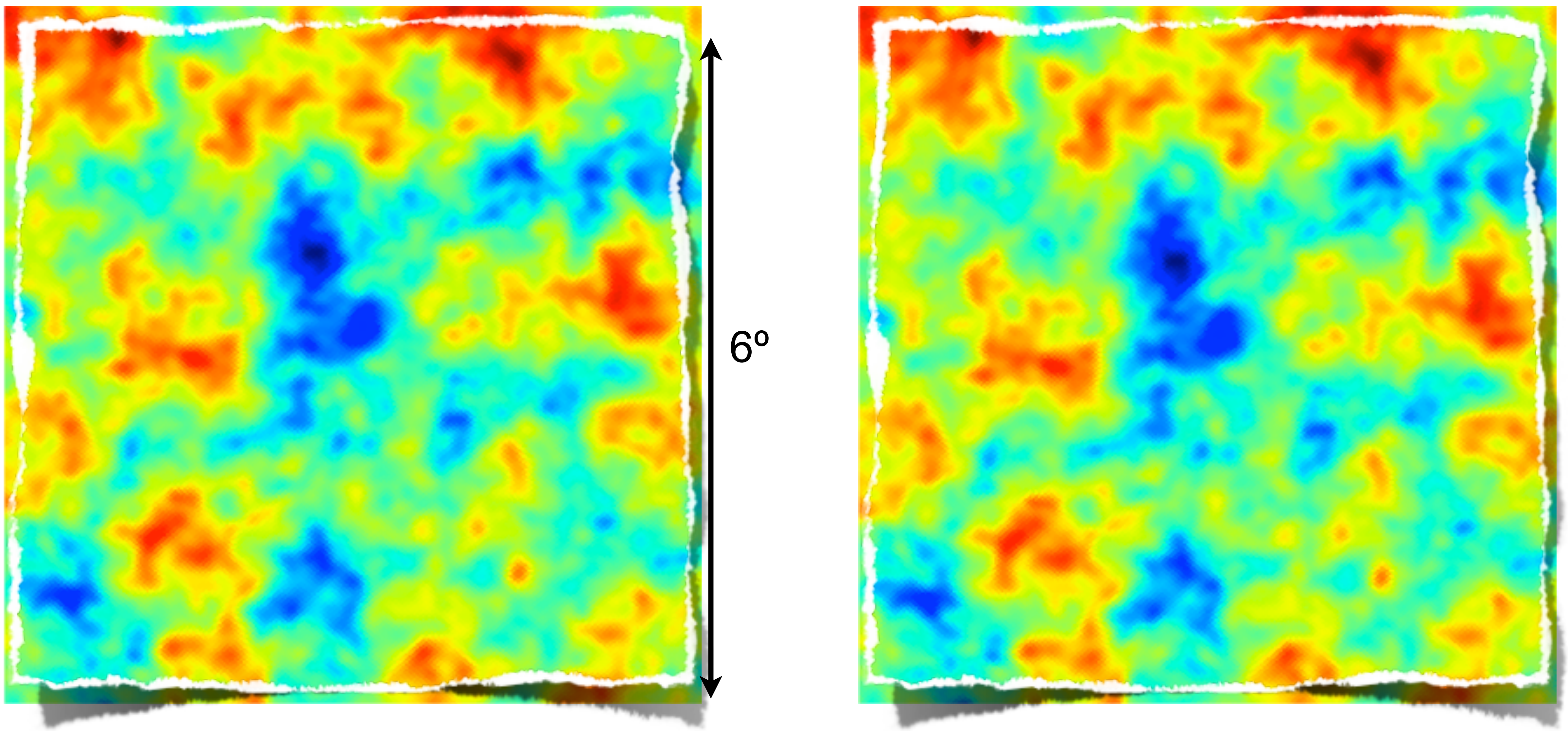

Unlensed

Lensed

CMB lensing

$$\Theta[\hat{\mathbf{n}}] = \tilde{\Theta}[\hat{\mathbf{n}} + \nabla\phi(\hat{\mathbf{n}})] \approx \tilde{\Theta}[\hat{\mathbf{n}}] + \nabla\phi[\hat{\mathbf{n}}]\ \nabla\tilde{\Theta}[\hat{\mathbf{n}}] + \cdots$$

Deflections are about 2 arcmin

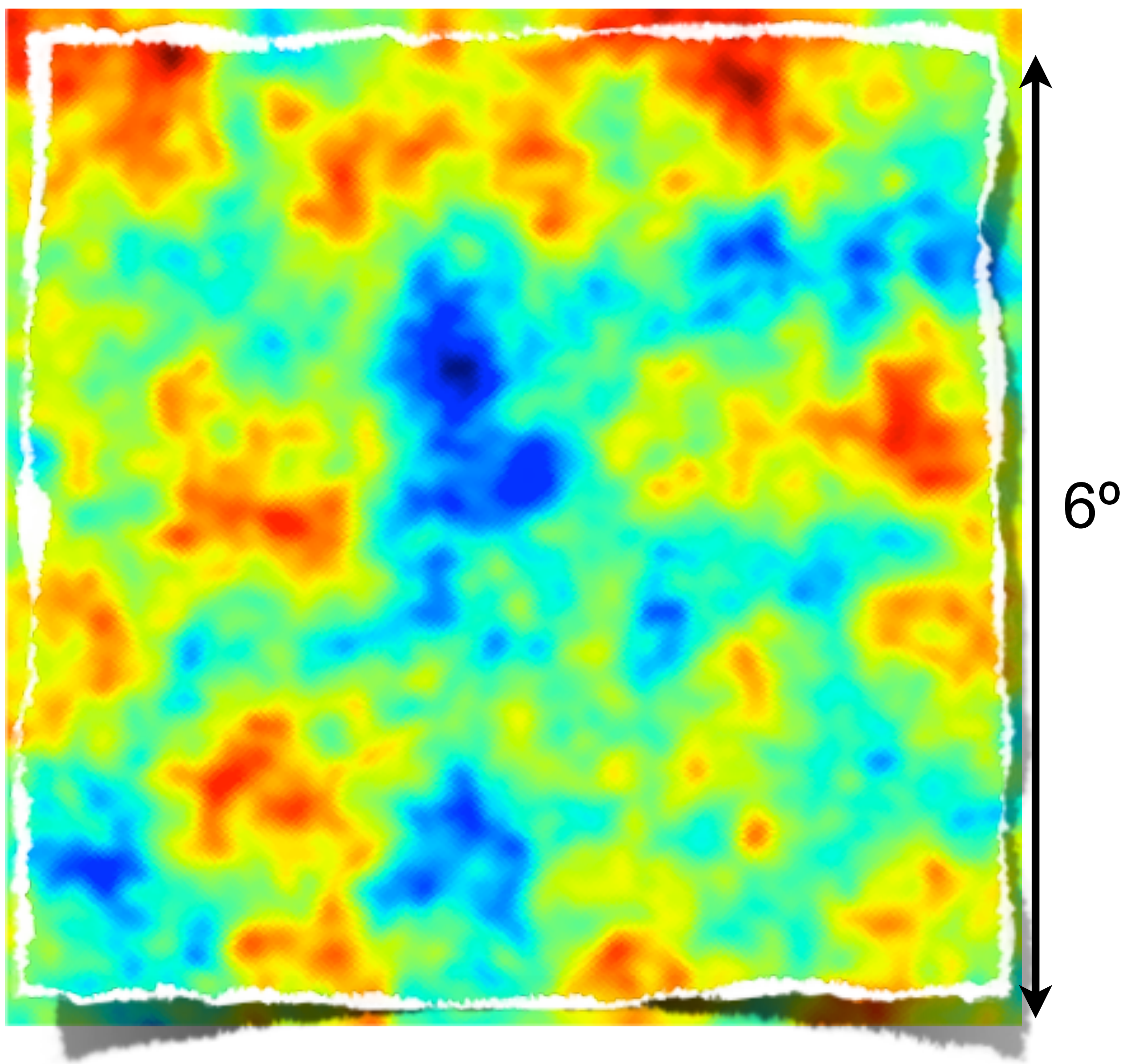

Unlensed

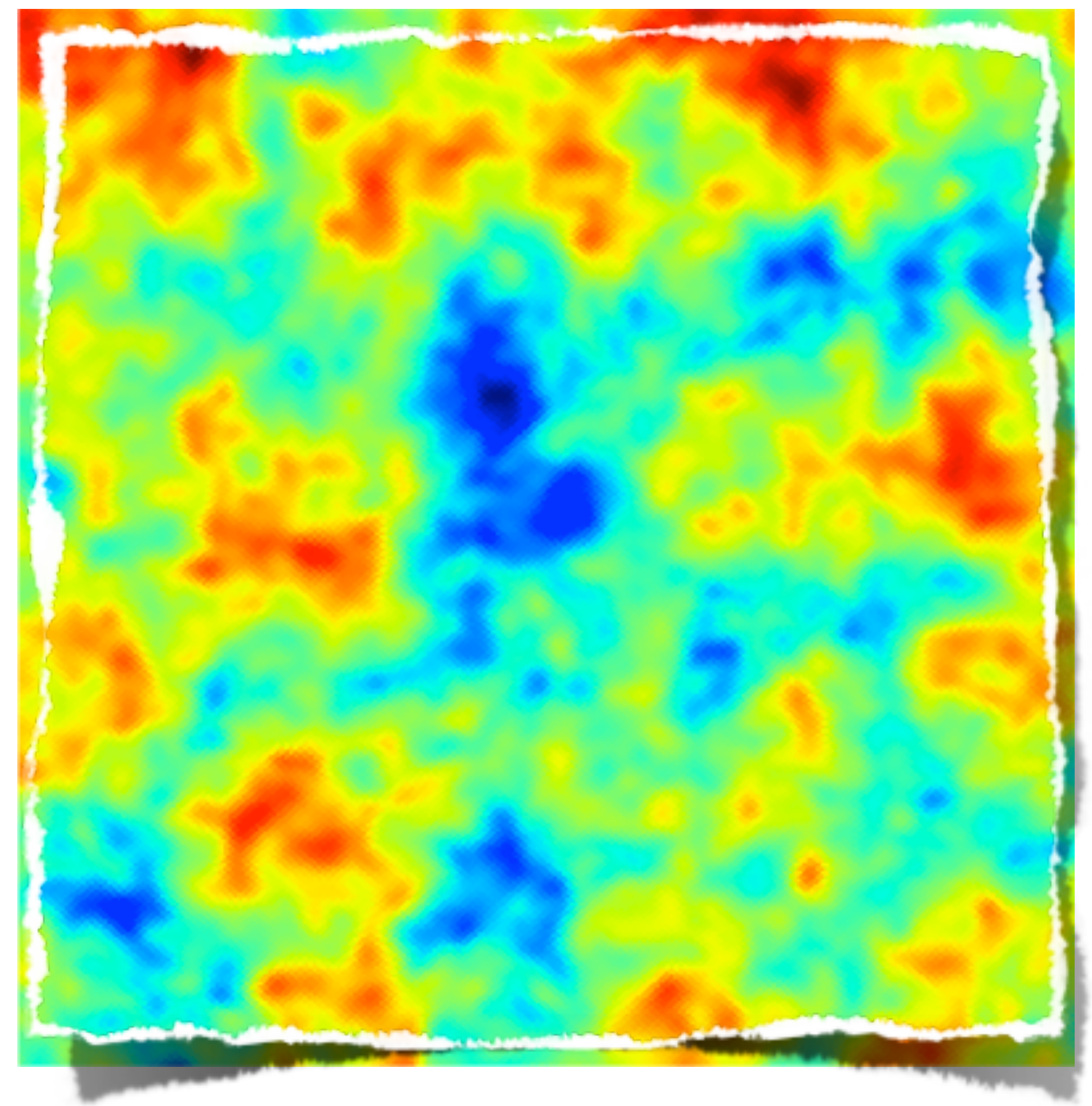

Lensed

Deflections are correlated on the degree scale

CMB lensing

$$\Theta[\hat{\mathbf{n}}] = \tilde{\Theta}[\hat{\mathbf{n}} + \nabla\phi(\hat{\mathbf{n}})] \approx \tilde{\Theta}[\hat{\mathbf{n}}] + \nabla\phi[\hat{\mathbf{n}}]\ \nabla\tilde{\Theta}[\hat{\mathbf{n}}] + \cdots$$

Deflections are about 2 arcmin

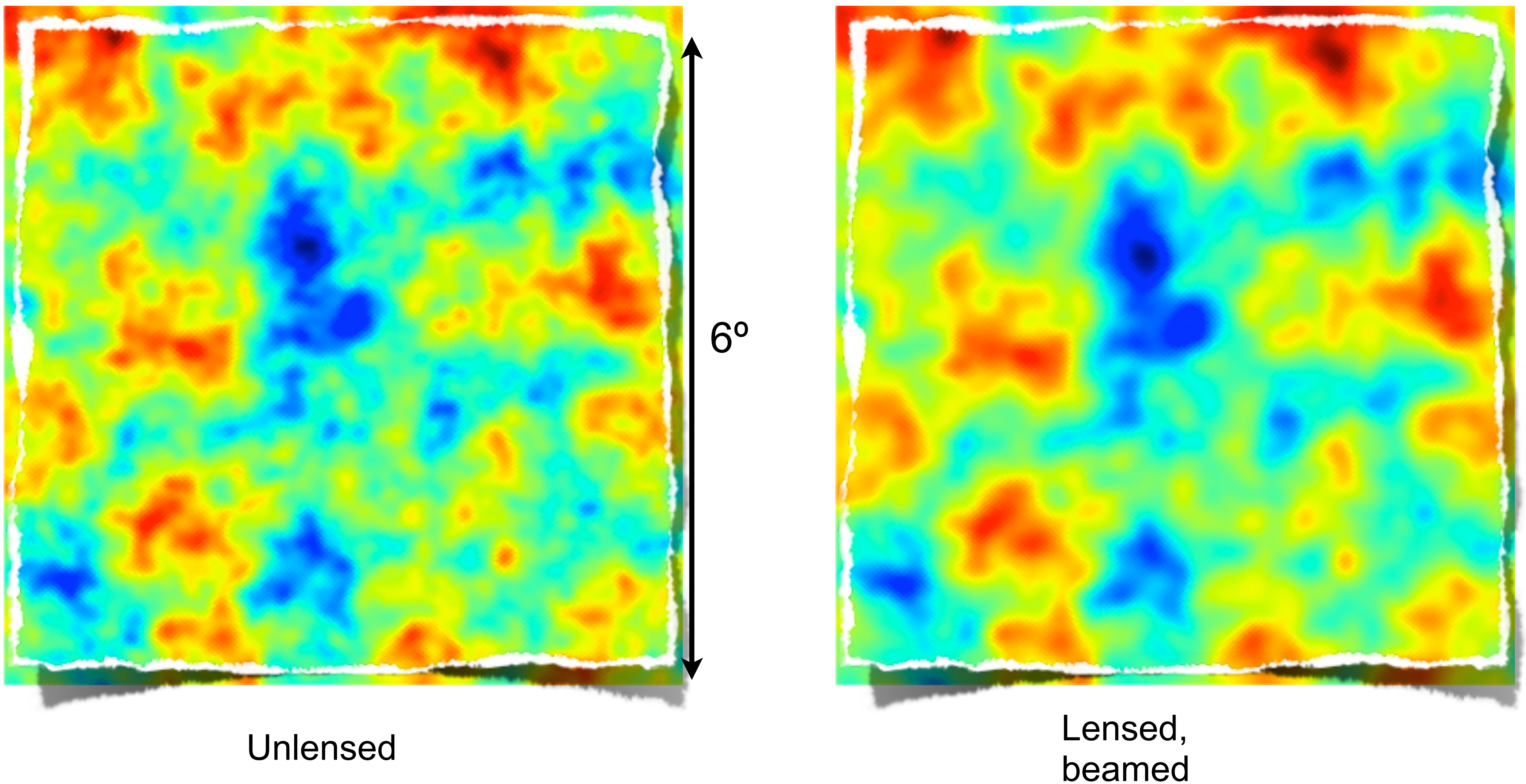

Deflections are correlated on the degree scale

CMB lensing

$$\Theta[\hat{\mathbf{n}}] = \tilde{\Theta}[\hat{\mathbf{n}} + \nabla\phi(\hat{\mathbf{n}})] \approx \tilde{\Theta}[\hat{\mathbf{n}}] + \nabla\phi[\hat{\mathbf{n}}]\,\nabla\tilde{\Theta}[\hat{\mathbf{n}}] + \cdots$$

Deflections are about 2 arcmin

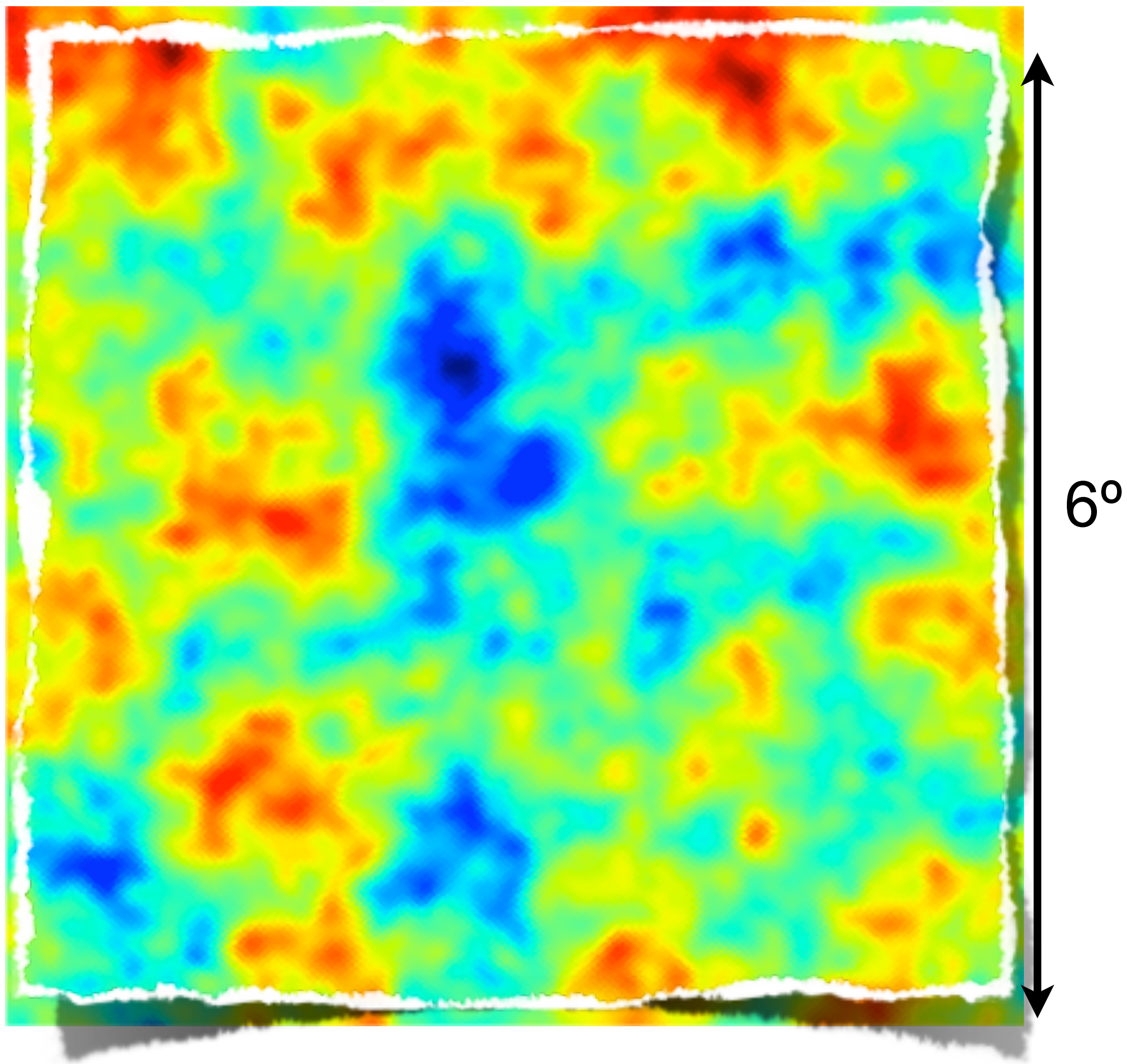

Unlensed

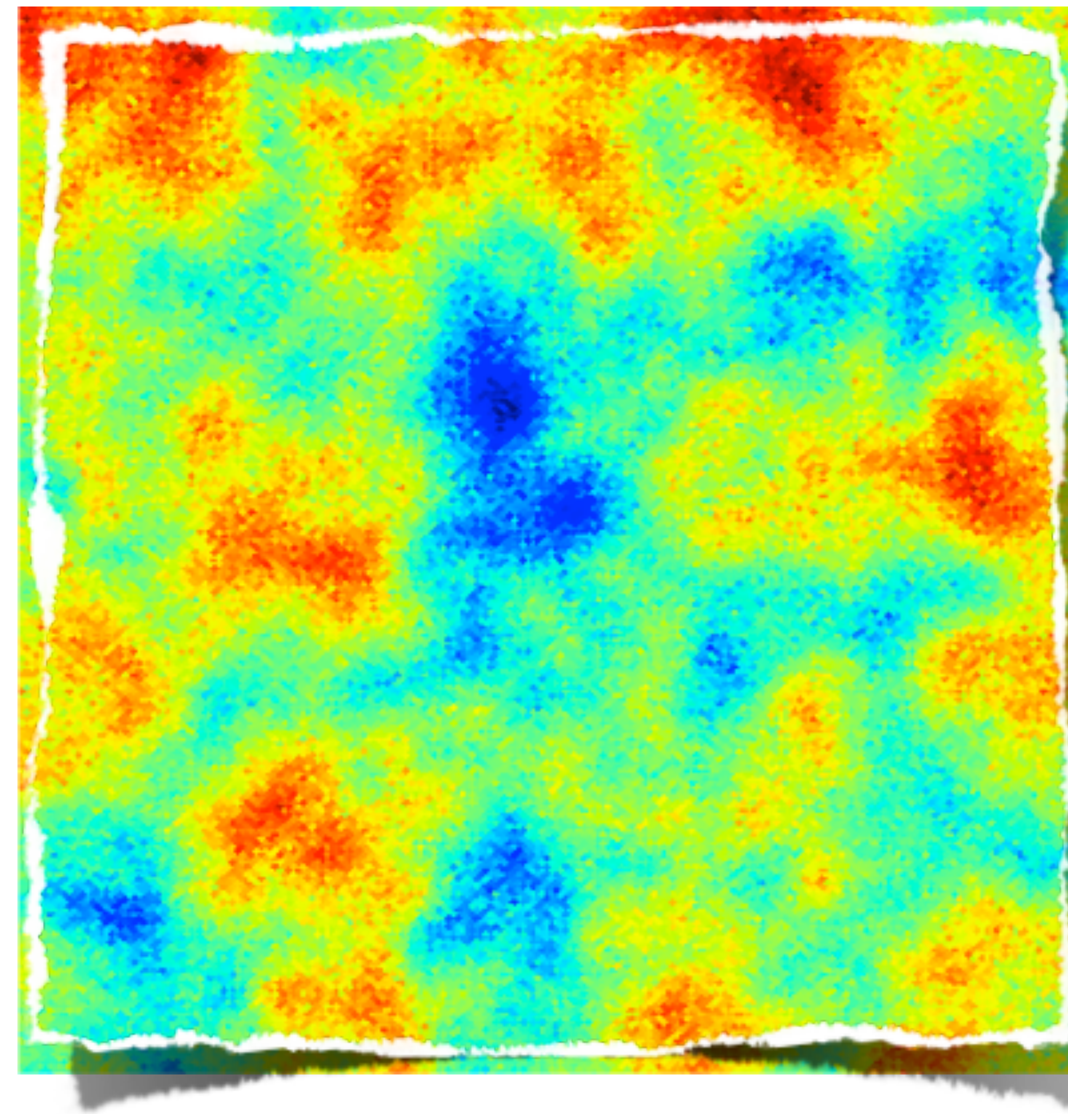

Lensed,
beamed, noised

Deflections are correlated on the degree scale

Impact on CMB

- CMB lensing induces temperature-gradient correlations

$$\Theta[\hat{\mathbf{n}}] = \tilde{\Theta}[\hat{\mathbf{n}} + \nabla\phi(\hat{\mathbf{n}})] \approx \tilde{\Theta}[\hat{\mathbf{n}}] + \nabla\phi[\hat{\mathbf{n}}]\, \nabla\tilde{\Theta}[\hat{\mathbf{n}}] + \cdots$$

$$\tilde{C}_l^{\Theta\Theta} = [1 - l(l+1)R]C_l^{\Theta\Theta} + \sum_{l_1, l_2} C_{l_1}^{\phi\phi} C_{l_2} \frac{(F_{l l_1 l_2})^2}{2l+1},$$

Lensed power spectra using the harmonic approach

Hu, 2000

$$\tilde{C}_l^{EE} = [1 - (l^2 + l - 4)R]C_l^{EE} + \frac{1}{2}\sum_{l_1, l_2} C_{l_1}^{\phi\phi} \frac{({}_2F_{l l_1 l_2})^2}{2l+1}$$
$$\times [C_{l_2}^{EE} + C_{l_2}^{BB} + (-1)^L (C_{l_2}^{EE} - C_{l_2}^{BB})],$$

$$\tilde{C}_l^{BB} = [1 - (l^2 + l - 4)R]C_l^{BB} + \frac{1}{2}\sum_{l_1, l_2} C_{l_1}^{\phi\phi} \frac{({}_2F_{l l_1 l_2})^2}{2l+1}$$
$$\times [C_{l_2}^{EE} + C_{l_2}^{BB} - (-1)^L (C_{l_2}^{EE} - C_{l_2}^{BB})],$$

Inacurrate a small scale (it is better to use the lensed correlation functions) but gives simpler expressions

Lewis & Challinor, 2005

Impact on anisotropies power spectra

$$C_\ell \sim (1-\alpha_\ell)\tilde{C}_\ell + \sum_{\ell_1 \ell_2} C_{\ell_1}^{\phi\phi} \tilde{C}_{\ell_2} F_{\ell \ell_1 \ell_2}$$

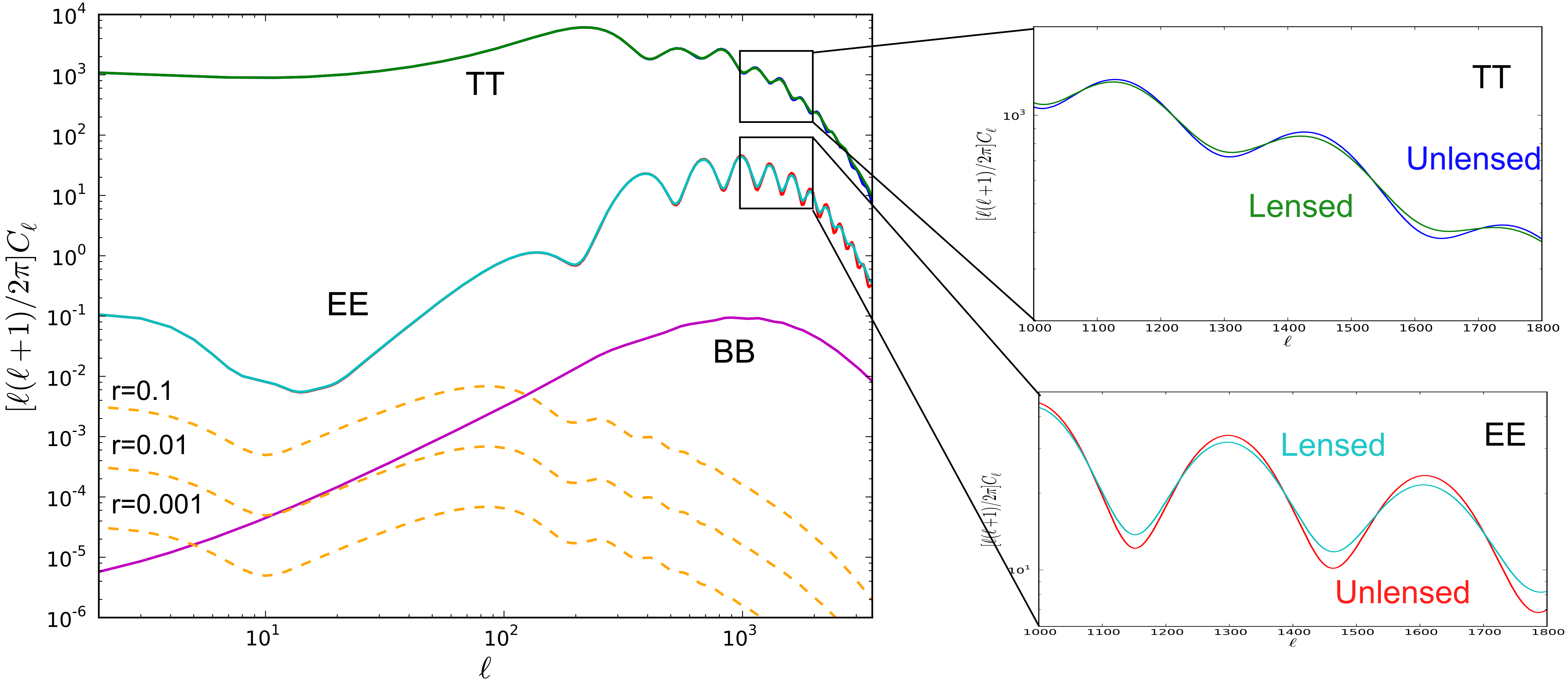

1) Lensing can also be detected in TT
~10 sigma with Planck2013

Impact on anisotropies power spectra

$$C_\ell \sim (1-\alpha_\ell)\tilde{C}_\ell + \sum_{\ell_1 \ell_2} C^{\phi\phi}_{\ell_1} \tilde{C}_{\ell_2} F_{\ell \ell_1 \ell_2}$$

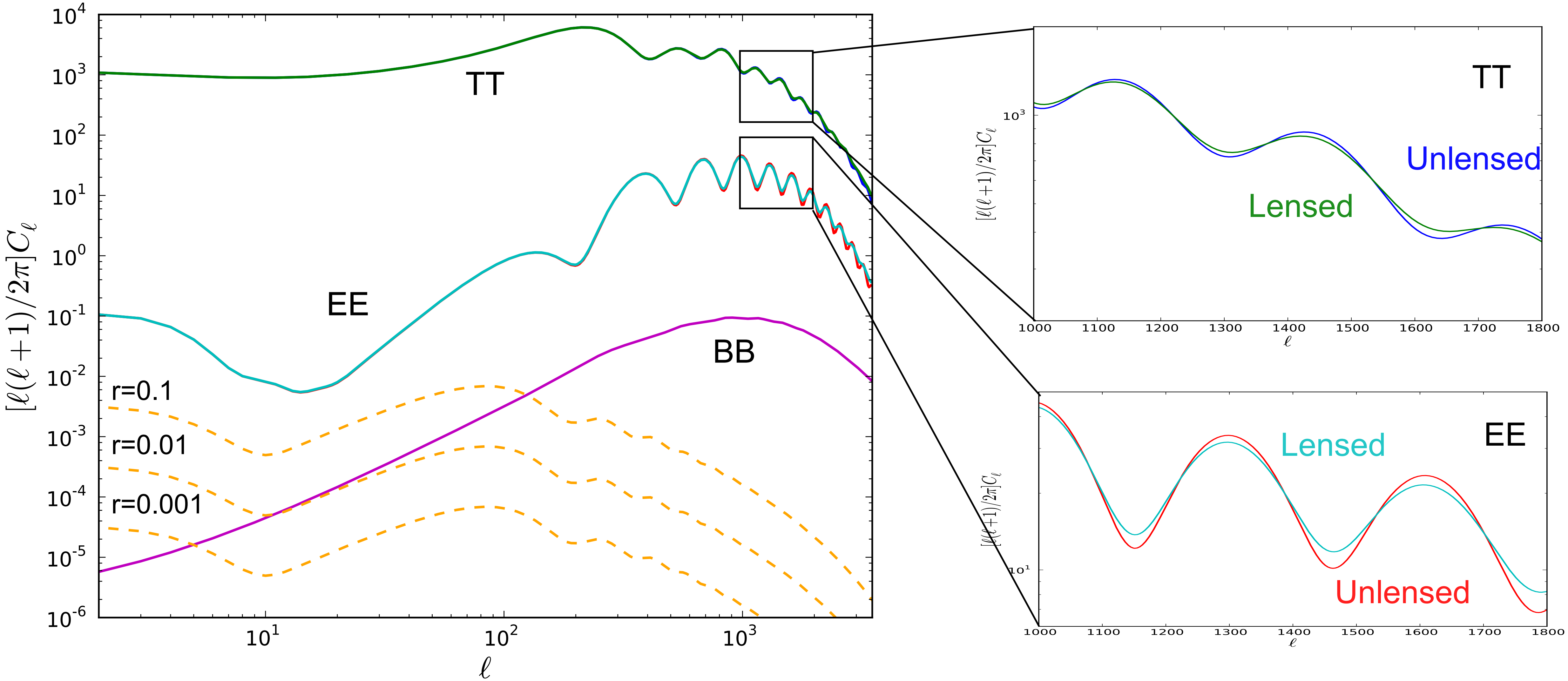

2) Multipoles become correlated.
Lensing induced non-Gaussian covariance

Effect on power spectra covariance

- Covariance induced by CMB lensing

$$\mathrm{cov}(\mathrm{C}^{\mathrm{XY}}_{\ell_1}, \mathrm{C}^{\mathrm{WZ}}_{\ell_2}) = \mathrm{cov}^{\mathrm{G}}(\mathrm{C}^{\mathrm{XY}}_{\ell_1}, \mathrm{C}^{\mathrm{WZ}}_{\ell_2}) + \mathrm{cov}^{\mathrm{NG}}(\mathrm{C}^{\mathrm{XY}}_{\ell_1}, \mathrm{C}^{\mathrm{WZ}}_{\ell_2})$$

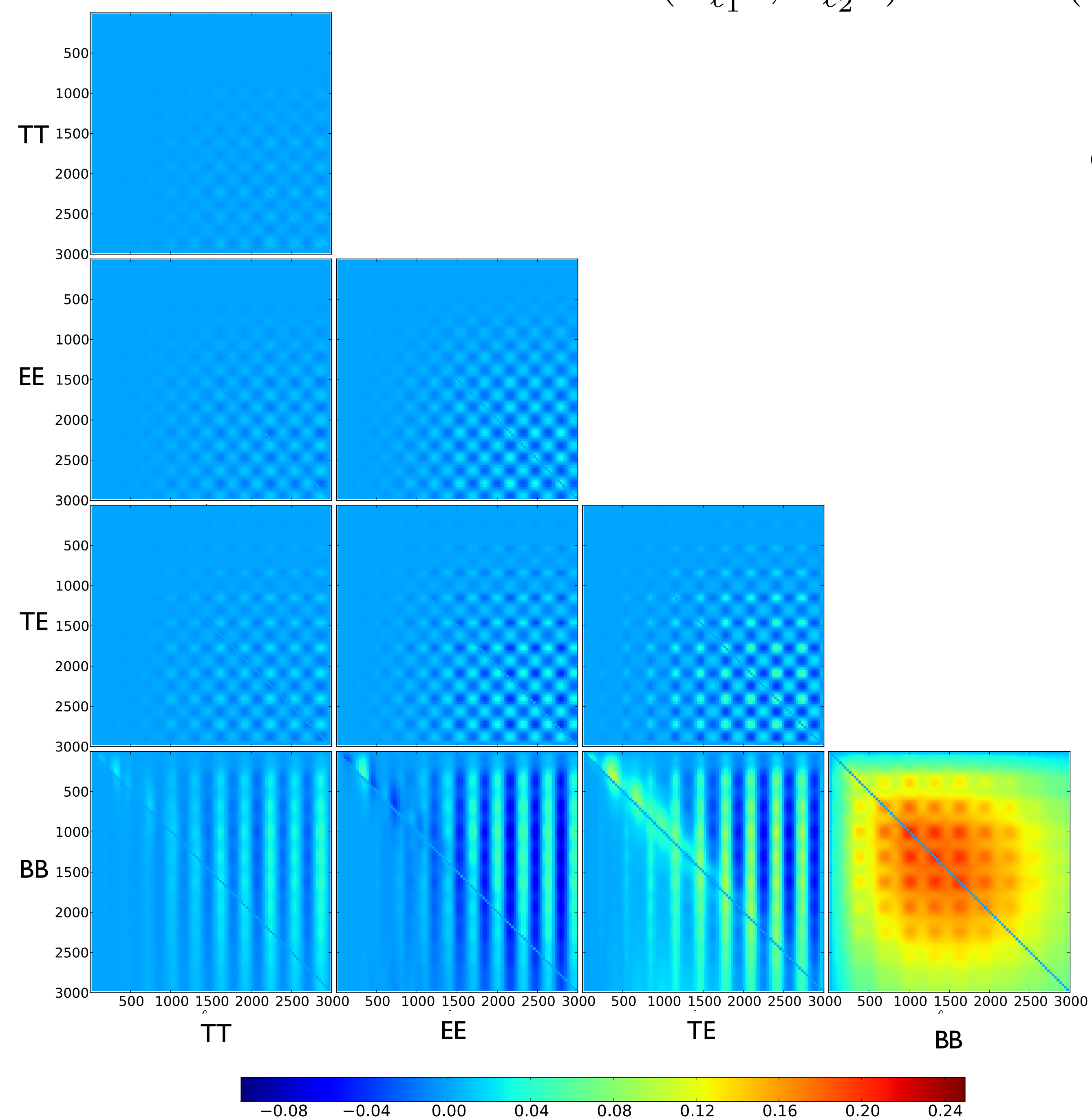

$$\mathrm{Cov}^{XY,WZ}_{\ell_1\ell_2} = \frac{1}{2\ell_1+1}[C^{XW}_{\ell_1}C^{YZ}_{\ell_1} + C^{XZ}_{\ell_1}C^{YW}_{\ell_1}]\delta_{\ell_1,\ell_2} + \sum_{\ell}\left[\frac{\partial C^{XY}_{\ell_1}}{\partial C^{\phi\phi}_{\ell}}\mathrm{Cov}^{\phi\phi,\phi\phi}_{\ell\ell}\frac{\partial C^{WZ}_{\ell_2}}{\partial C^{\phi\phi}_{\ell}}\right]$$

$$\mathrm{Cov}^{BB,BB}_{\ell_1\ell_2} = \frac{2}{2\ell_1+1}\left(C^{BB}_{\ell_1}\right)^2\delta_{\ell_1,\ell_2} + \sum_{\ell}\left(\frac{\partial C^{BB}_{\ell_1}}{\partial C^{\tilde{E}\tilde{E}}_{\ell}}\mathrm{Cov}^{\tilde{E}\tilde{E},\tilde{E}\tilde{E}}_{\ell\ell}\frac{\partial C^{BB}_{\ell_2}}{\partial C^{\tilde{E}\tilde{E}}_{\ell}}\right) + \sum_{\ell}\left(\frac{\partial C^{BB}_{\ell_1}}{\partial C^{\phi\phi}_{\ell}}\mathrm{Cov}^{\phi\phi,\phi\phi}_{\ell\ell}\frac{\partial C^{BB}_{\ell_2}}{\partial C^{\phi\phi}_{\ell}}\right)$$

ABL, Smith & Hu (PRD, 2012)

- safely negligible for Planck
- significant for post-Planck experiments

Impact on CMB

- CMB lensing induces temperature-gradient correlations

$$\Theta[\hat{\mathbf{n}}] = \tilde{\Theta}[\hat{\mathbf{n}} + \nabla\phi(\hat{\mathbf{n}})] \approx \tilde{\Theta}[\hat{\mathbf{n}}] + \nabla\phi[\hat{\mathbf{n}}]\ \nabla\tilde{\Theta}[\hat{\mathbf{n}}] + \cdots$$

Impact on CMB

- CMB lensing induces temperature-gradient correlations

$$\Theta[\hat{\mathbf{n}}] = \tilde{\Theta}[\hat{\mathbf{n}} + \nabla\phi(\hat{\mathbf{n}})] \approx \tilde{\Theta}[\hat{\mathbf{n}}] + \nabla\phi[\hat{\mathbf{n}}]\ \nabla\tilde{\Theta}[\hat{\mathbf{n}}] + \cdots$$

- CMB lensing induces statistical anisotropies

$$\langle T_{\ell_1 m_1} T^*_{\ell_2 m_2} \rangle = C_{\ell_1}\delta_{\ell_1\ell_2}\delta_{m_1 m_2} + \sum_{LM} \sum_{\ell_1 m_1, \ell_2 m_2} (-1)^M \begin{pmatrix} \ell_1 & \ell_2 & L \\ m_1 & m_2 & -M \end{pmatrix} W^{\phi}_{\ell_1\ell_2 L}\phi_{LM}$$

CMB covariance at fixed lensing potential

lensed power spectrum

off-diagonal term sources by lensing

$$W^{\phi}_{\ell_1\ell_2 L} = -\sqrt{\frac{(2\ell_1+1)(2\ell_2+1)(2L+1)}{4\pi}}\sqrt{L(L+1)\ell_1(\ell_1+1)} \times C^{TT}_{\ell_1}\left(\frac{1+(-1)^{\ell_1+\ell_2+L}}{2}\right)\begin{pmatrix} \ell_1 & \ell_2 & L \\ 1 & 0 & -1 \end{pmatrix} + (\ell_1 \leftrightarrow \ell_2). \quad (6)$$

Lensing reconstruction

- Quadratic estimator on the full sky

$$\bar{x}_{LM} = \frac{1}{2} \sum_{\ell_1 m_1, \ell_2 m_2} (-1)^M \begin{pmatrix} \ell_1 & \ell_2 & L \\ m_1 & m_2 & -M \end{pmatrix} W^x_{\ell_1 \ell_2 L} \bar{T}^{(1)}_{\ell_1 m_1} \bar{T}^{(2)}_{\ell_2 m_2}.$$

Okamoto & Hu, 2003

Lensing reconstruction

- Quadratic estimator on the full sky

$$\bar{x}_{LM} = \frac{1}{2} \sum_{\ell_1 m_1, \ell_2 m_2} (-1)^M \begin{pmatrix} \ell_1 & \ell_2 & L \\ m_1 & m_2 & -M \end{pmatrix} W^x_{\ell_1 \ell_2 L} \boxed{\bar{T}^{(1)}_{\ell_1 m_1} \bar{T}^{(2)}_{\ell_2 m_2}.}$$

Okamoto & Hu, 2003

Filtered temperature. Multiple choices.

Typically: T_1 is inverse-variance filtered, and T_2 is Wiener filtered

Estimator is unbiased (in the absence of real-life issues), but noisy

CMB lensing reconstruction

$$\mathrm{var}(\hat{\phi}) \sim \langle \hat{\phi}\hat{\phi}^* \rangle \sim \langle \mathrm{TTTT} \rangle \sim \mathrm{C}_\ell^{\phi\phi} + \mathrm{N}_\ell^0$$

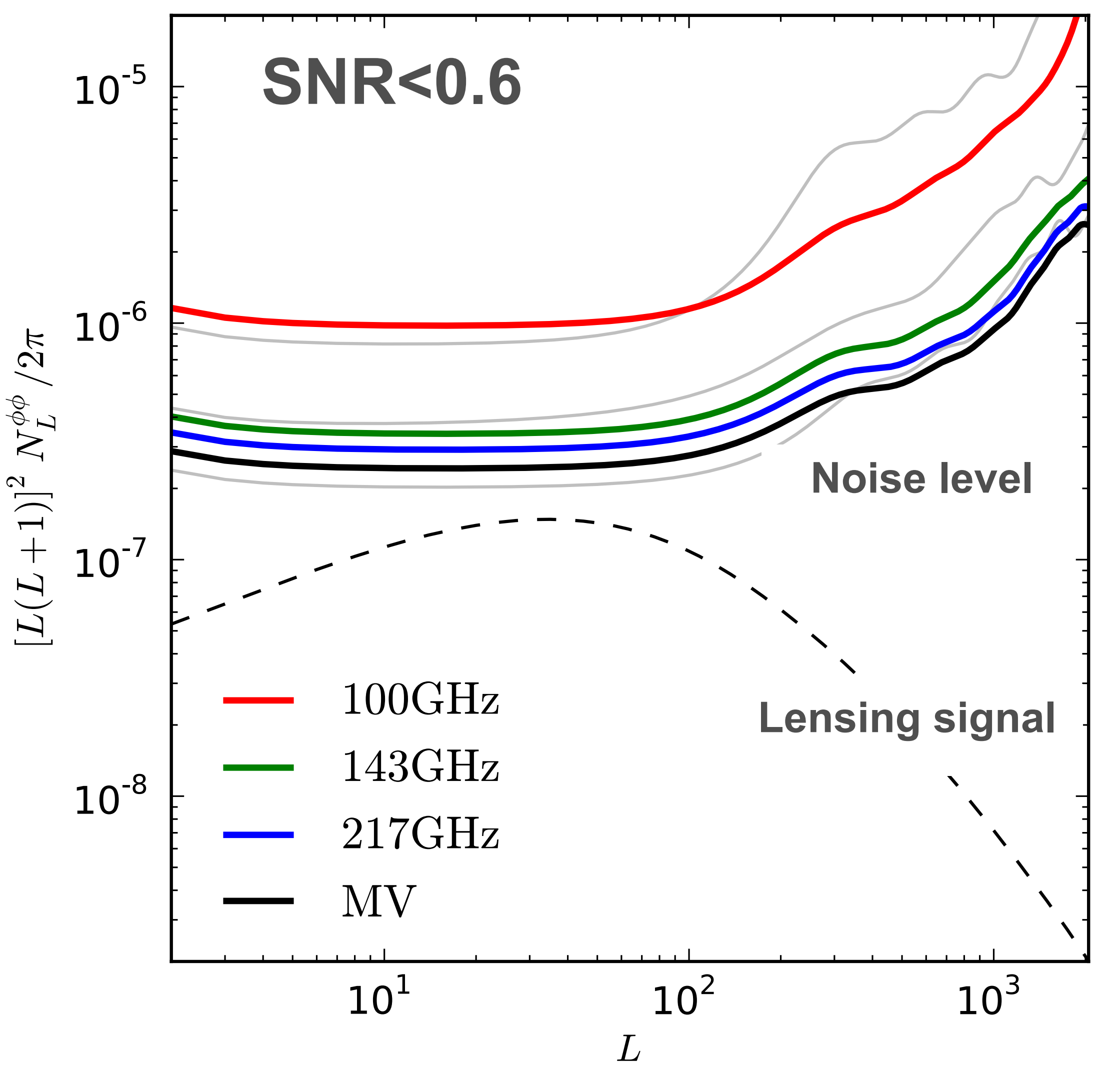

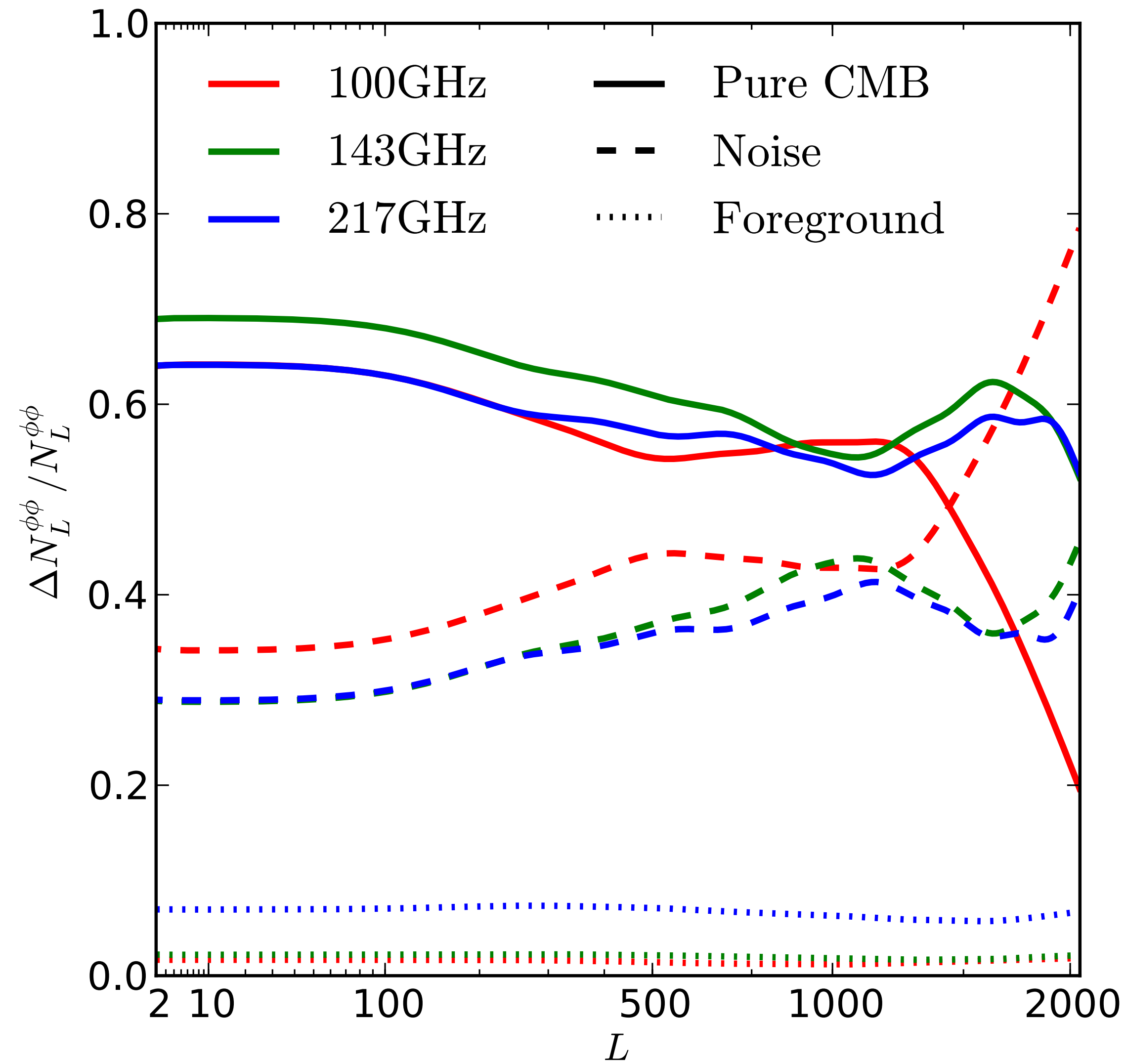

CMB lensing reconstruction

- Other sources of statistical anisotropies

Galactic + PS mask

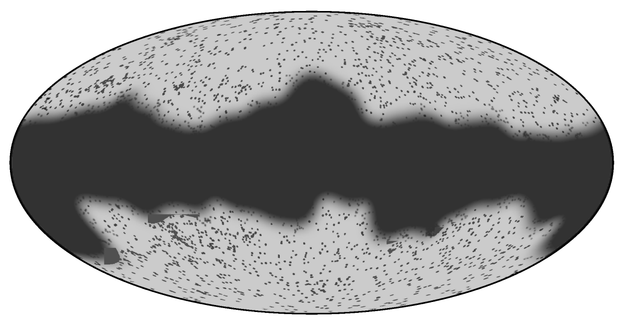

Inh. noise

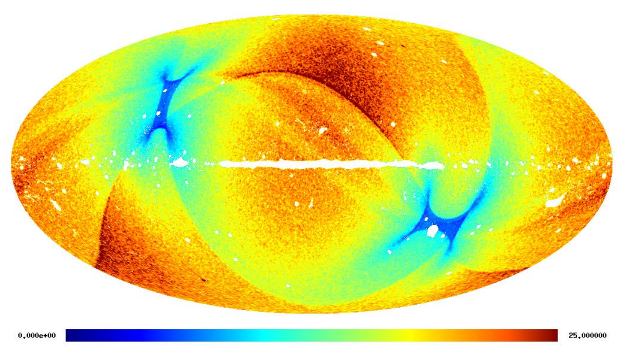

Beam ellipticity

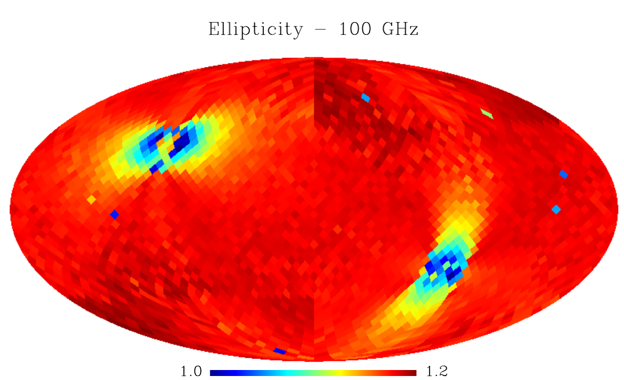

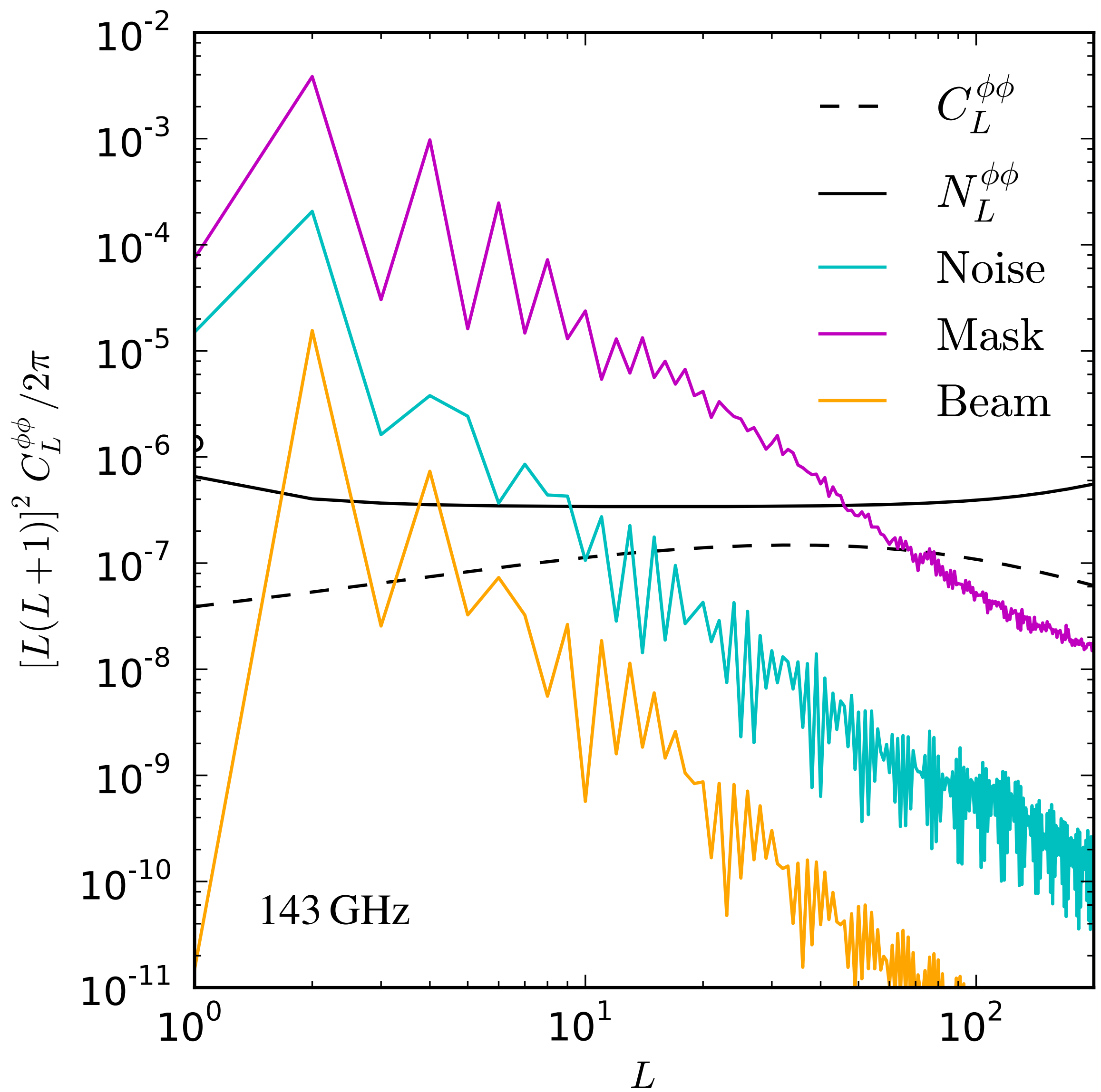

CMB lensing reconstruction

$$\hat{\phi}^x_{LM} = \frac{1}{\mathcal{R}^{x\phi}_L}\left(\bar{x}_{LM} - \bar{x}^{MF}_{LM}\right).$$

$$\bar{x}_{LM} = \frac{1}{2}\sum_{\ell_1 m_1, \ell_2 m_2} (-1)^M \begin{pmatrix} \ell_1 & \ell_2 & L \\ m_1 & m_2 & \end{pmatrix} W^x \bar{T}^{(1)} \bar{T}^{(2)} \qquad \bar{x}^{MF}_{LM} = \frac{1}{} \sum (-1)^M \begin{pmatrix} \ell_1 & \ell_2 & L \\ m_1 & m_2 & -M \end{pmatrix} W^x_{\ell_1 \ell_2 L} \langle \bar{T}^{(1)}_{\ell_1 m_1} \bar{T}^{(2)}_{\ell_2 m_2} \rangle$$

$$\bar{\phi}_{\ell m} = \left[(C^{-1}T)\nabla(SC^{-1}T)\right]_{\ell m}$$

$$\bar{T}_{\ell m} = [S+N]^{-1} T_{\ell m} \approx [C^{TT}_\ell + C^{NN}_\ell]^{-1} T_{\ell m} = F_\ell T_{\ell m} \qquad \mathcal{R}_L = \frac{}{(2L+1)} \sum_{\ell_1 \ell_2} \frac{1}{2} W^x_{\ell_1 \ell_2 L} W^\phi_{\ell_1 \ell_2 L} F^{(1)}_{\ell_1} F^{(2)}_{\ell_2}.$$

- Take two temperature maps and inverse-variance filter them

- Multiply one by the temperature power spectrum and differentiate it

- Multiply it with the first filtered map

- Do the same on a set of realistic simulations

- Take the difference and normalize to get unbiased estimator

CMB lensing reconstruction

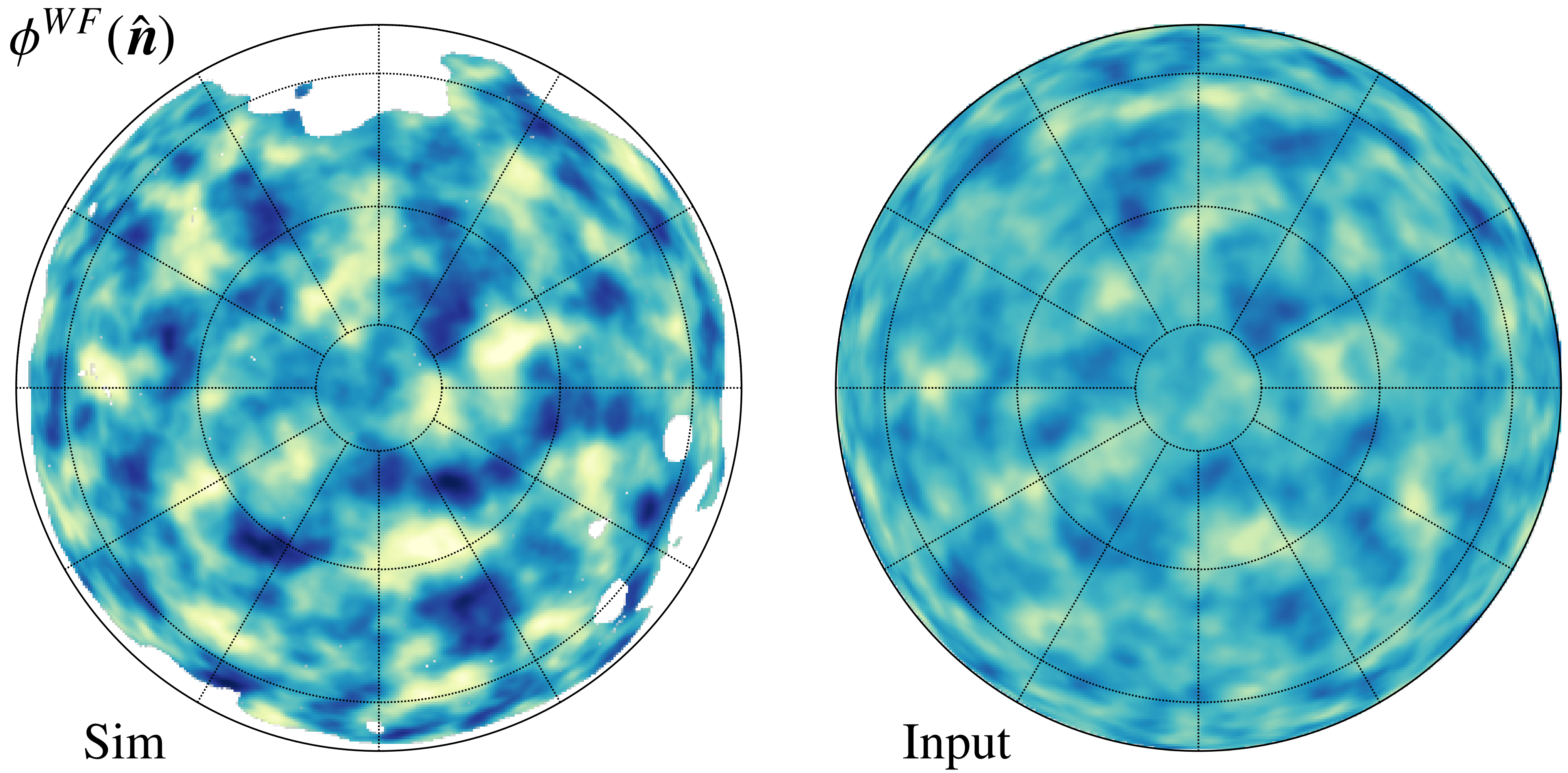

Reconstruction on a realistic Planck simulation

Power spectrum estimator

$$\hat{C}^{\phi\phi}_{L,x} = \boxed{\frac{f^{-1}_{\mathrm{sky},2}}{2L+1}\sum_M |\widetilde{\phi}^x_{LM}|^2} - \Delta C^{\phi\phi}_L\Big|_{\mathrm{N0}} - \Delta C^{\phi\phi}_L\Big|_{\mathrm{N1}} - \Delta C^{\phi\phi}_L\Big|_{\mathrm{PS}} - \Delta C^{\phi\phi}_L\Big|_{\mathrm{MC}},$$

Pseudo-Cl of an apodized version of the reconstructed lensing potential

Power spectrum estimator

$$\hat{C}^{\phi\phi}_{L,x} = \frac{f^{-1}_{\mathrm{sky},2}}{2L+1} \sum_M |\widetilde{\phi}^x_{LM}|^2 - \boxed{\Delta C^{\phi\phi}_L\big|_{\mathrm{N0}}} - \Delta C^{\phi\phi}_L\big|_{\mathrm{N1}} - \Delta C^{\phi\phi}_L\big|_{\mathrm{PS}} - \Delta C^{\phi\phi}_L\big|_{\mathrm{MC}},$$

Pseudo-Cl of an apodized version of the reconstructed lensing potential

Gaussian noise. Disconnected part of the CMB trispectrum. Computed by simulations

Power spectrum estimator

$$\hat{C}^{\phi\phi}_{L,x} = \frac{f^{-1}_{\mathrm{sky},2}}{2L+1} \sum_M |\widetilde{\phi}^x_{LM}|^2 - \Delta C^{\phi\phi}_L\Big|_{\mathrm{N0}} - \boxed{\Delta C^{\phi\phi}_L\Big|_{\mathrm{N1}}} - \Delta C^{\phi\phi}_L\Big|_{\mathrm{PS}} - \Delta C^{\phi\phi}_L\Big|_{\mathrm{MC}},$$

Pseudo-Cl of an apodized version of the reconstructed lensing potential

Gaussian noise. Disconnected part of the CMB trispectrum. Computed by simulations

High-order term. Depends on the lensing spectrum. Computed with fiducial spectrum.

Power spectrum estimator

$$\hat{C}^{\phi\phi}_{L,x} = \frac{f^{-1}_{\mathrm{sky},2}}{2L+1} \sum_{M} |\widetilde{\phi}^{x}_{LM}|^2 - \Delta C^{\phi\phi}_{L}\big|_{\mathrm{N0}} - \Delta C^{\phi\phi}_{L}\big|_{\mathrm{N1}} - \boxed{\Delta C^{\phi\phi}_{L}\big|_{\mathrm{PS}}} - \Delta C^{\phi\phi}_{L}\big|_{\mathrm{MC}},$$

Pseudo-Cl of an apodized version of the reconstructed lensing potential

Gaussian noise. Disconnected part of the CMB trispectrum. Computed by simulations

High-order term. Depends on the lensing spectrum. Computed with fiducial spectrum.

Contribution from unresolved point sources. Measured on data

Power spectrum estimator

$$\hat{C}^{\phi\phi}_{L,x} = \frac{f^{-1}_{\mathrm{sky},2}}{2L+1} \sum_M |\widetilde{\phi}^x_{LM}|^2 - \Delta C^{\phi\phi}_L\Big|_{\mathrm{N0}} - \Delta C^{\phi\phi}_L\Big|_{\mathrm{N1}} - \Delta C^{\phi\phi}_L\Big|_{\mathrm{PS}} - \boxed{\Delta C^{\phi\phi}_L\Big|_{\mathrm{MC}}},$$

Pseudo-Cl of an apodized version of the reconstructed lensing potential

Gaussian noise. Disconnected part of the CMB trispectrum. Computed by simulations

High-order term. Depends on the lensing spectrum. Computed with fiducial spectrum.

Contribution from unresolved point sources. Measured on data

Additional uncertainties dealt with by Monte-Carlo.

Best reconstruction

- Minimun-variance combination of 143GHz & 217 GHz

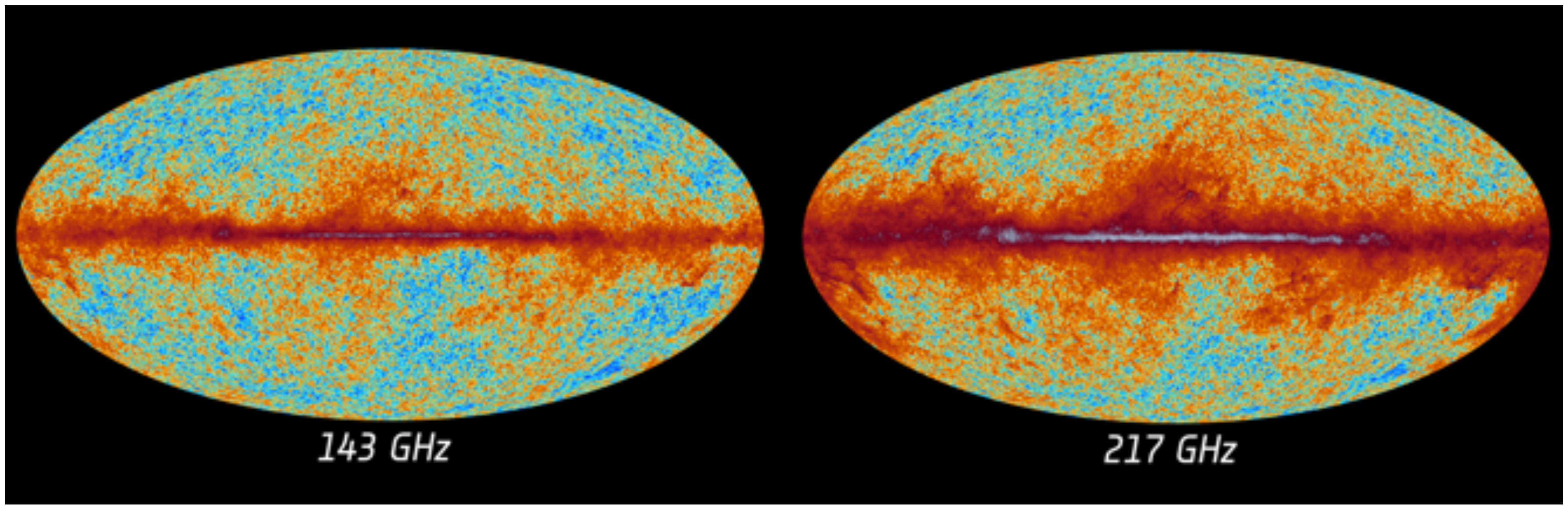

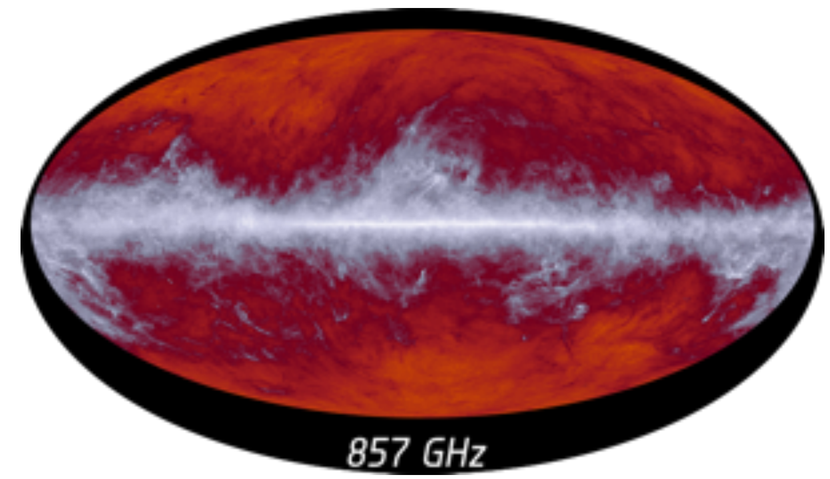

- 857 GHz map used as a template for dust cleaning
- 30 % Galactic mask +CO+ point sources
- 5º apodization (for lensing power spectrum estimation)

Best reconstruction

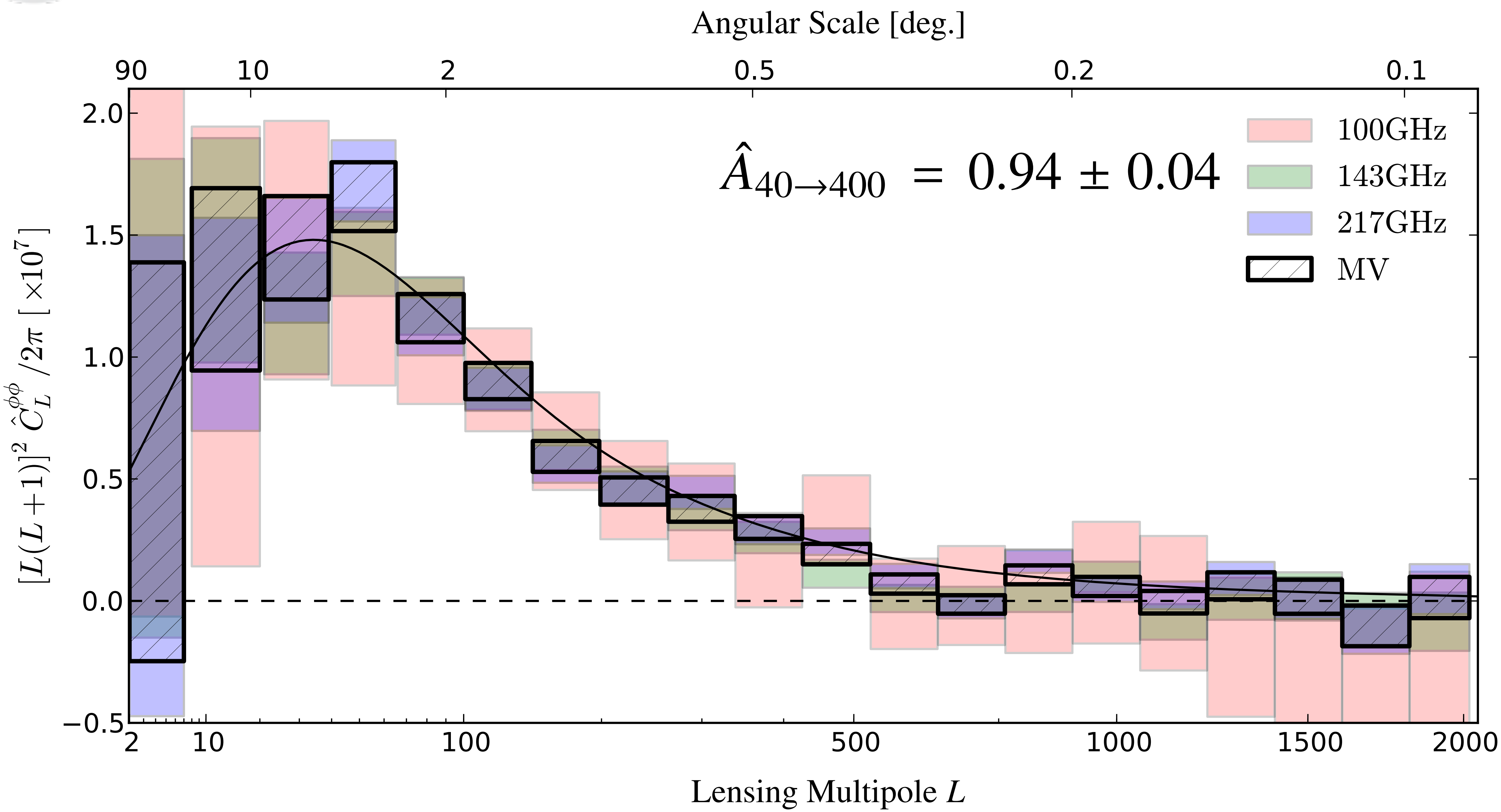

Comparison to other surveys

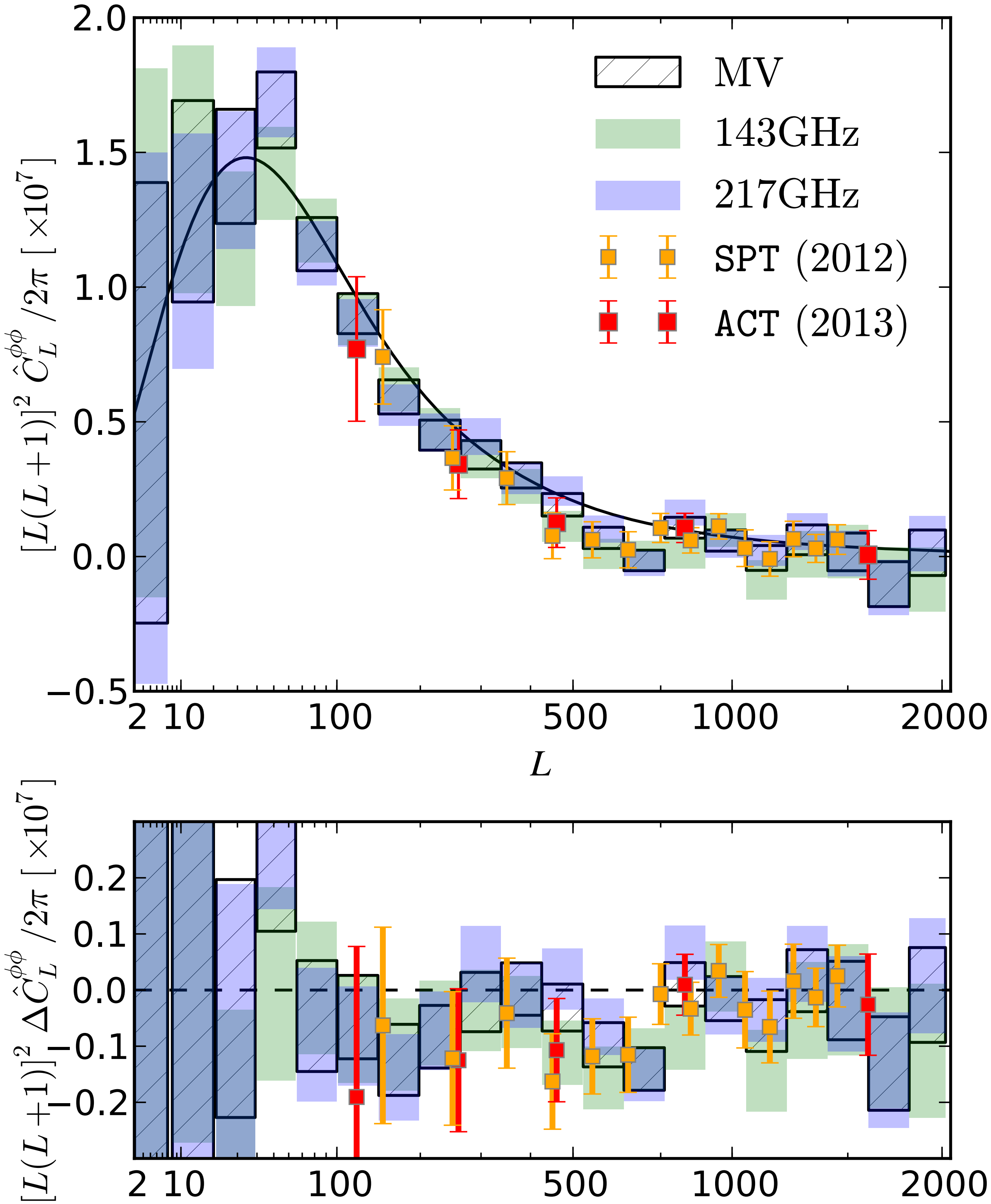

Tests

Testing foreground contamination

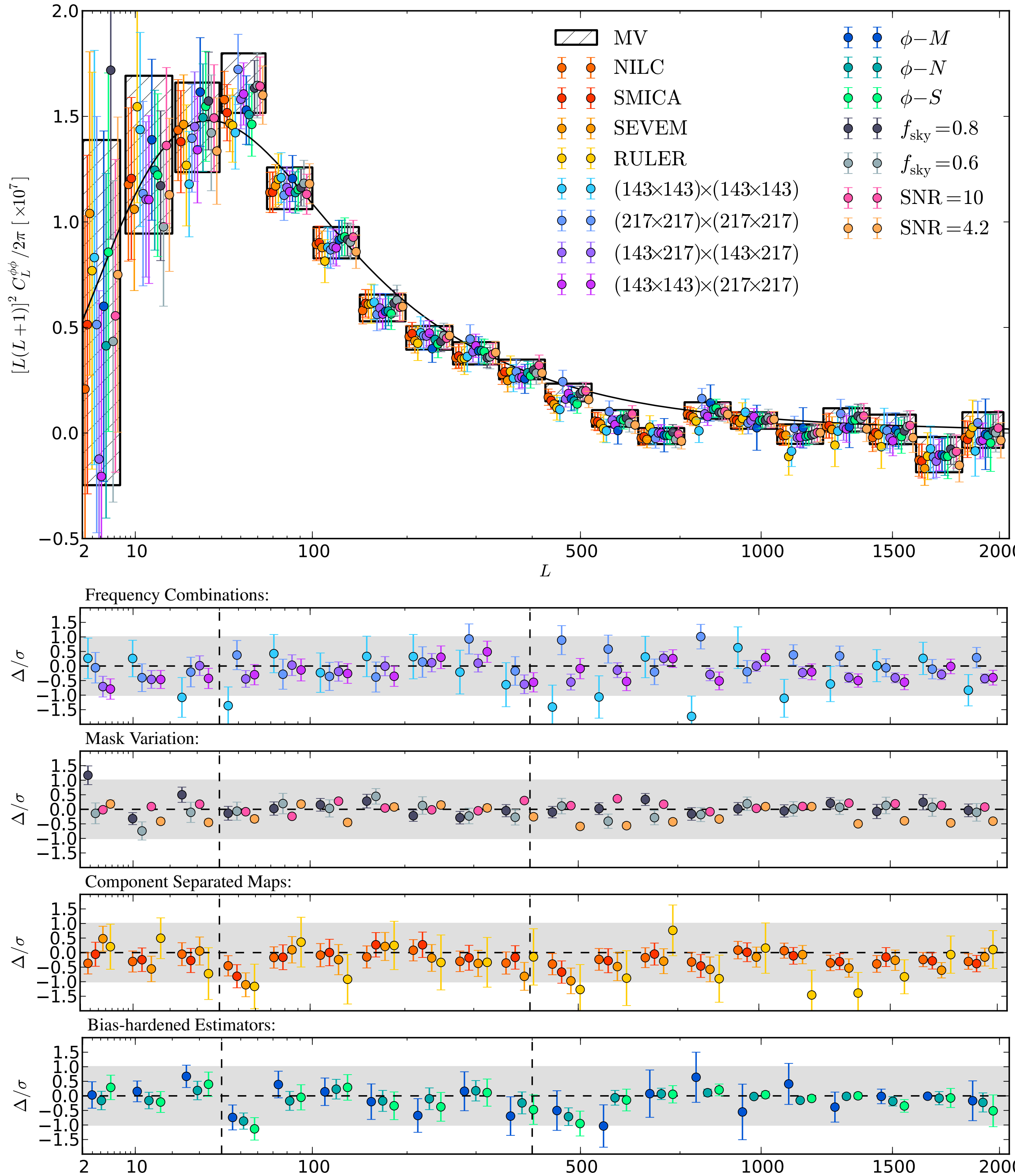

Testing the filter & implementation

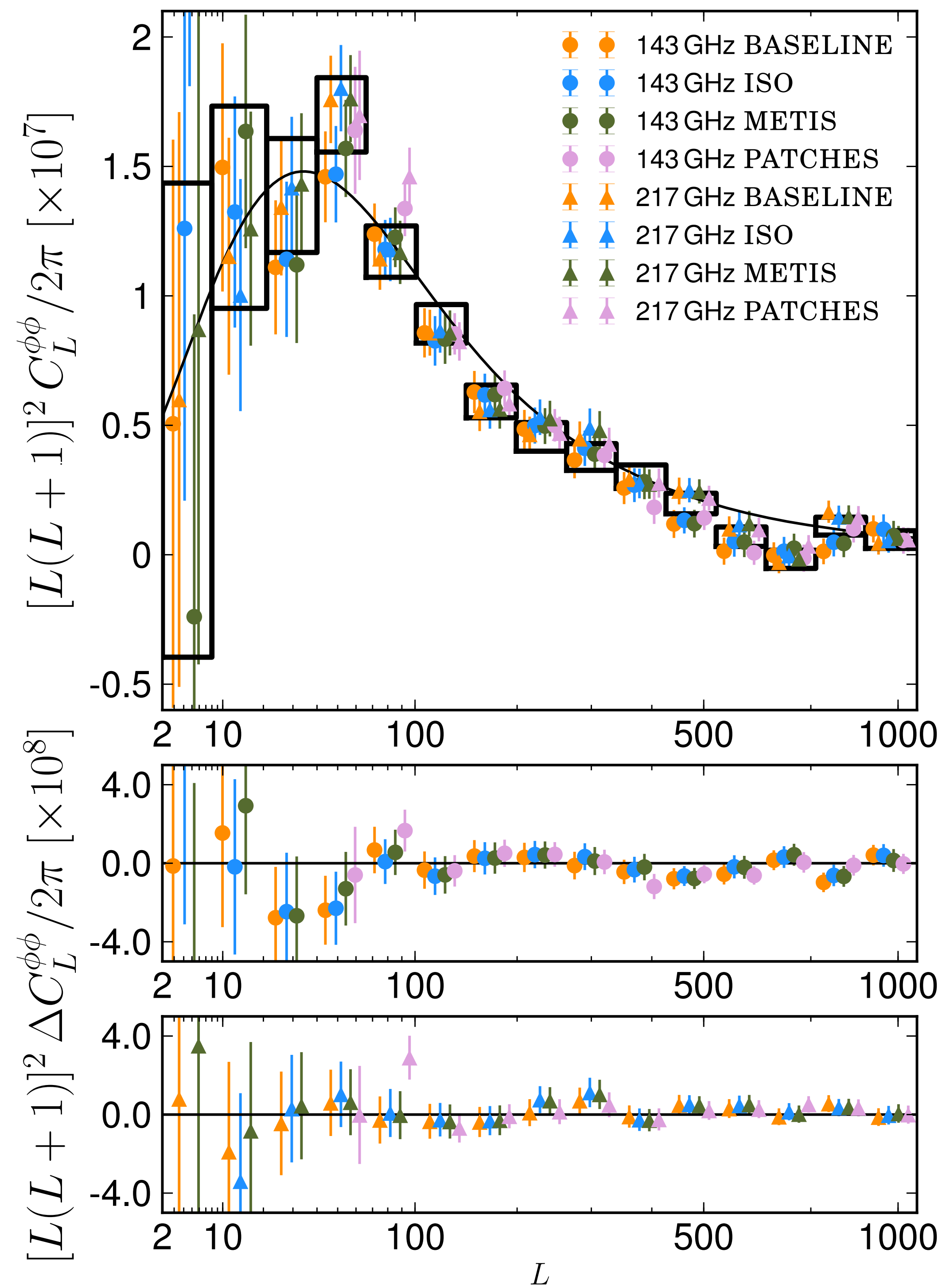

Cosmology

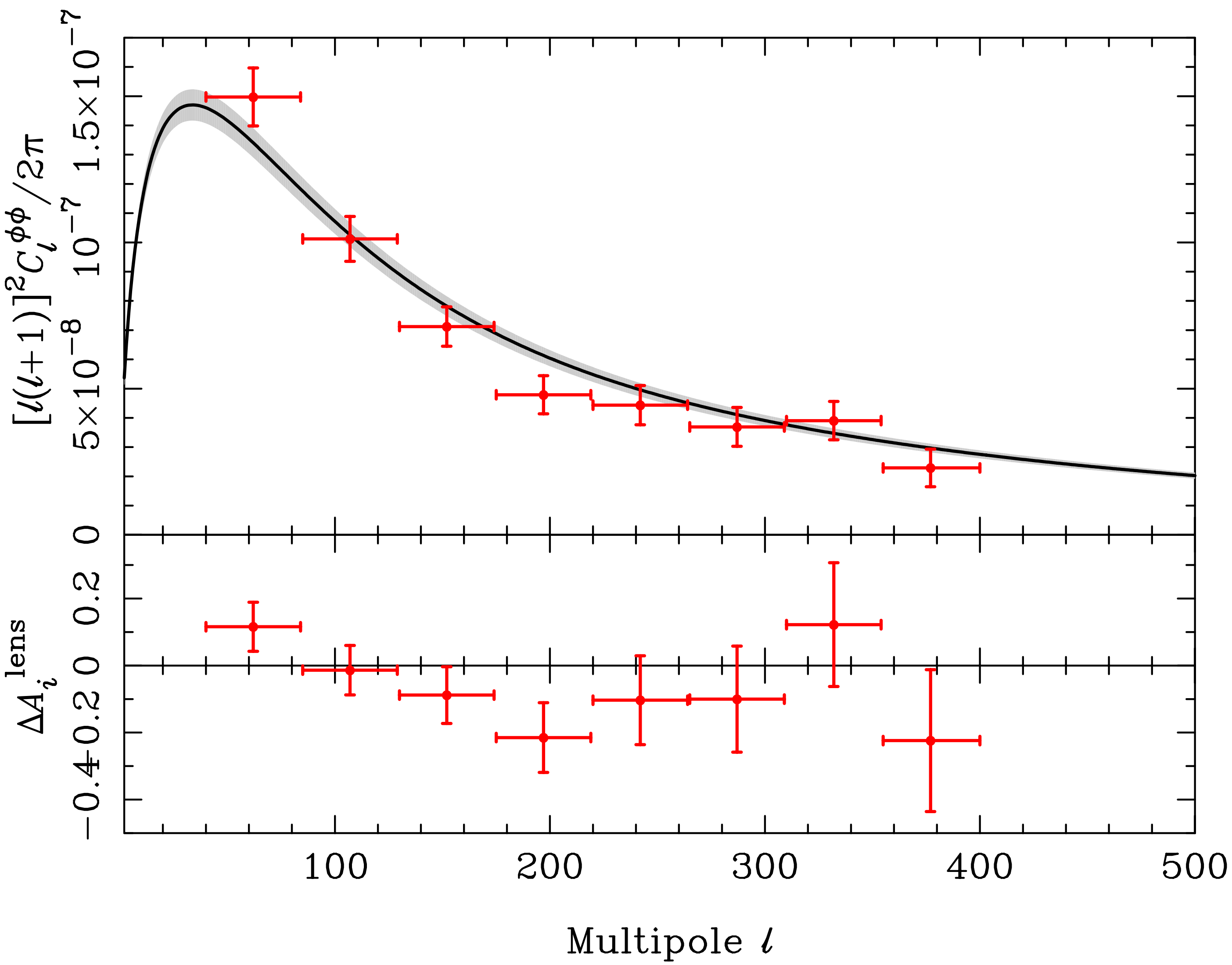

$[\ell(\ell+1)]^2 C_\ell^{\phi\phi}/2\pi$
$\Delta A_i^{\rm lens}$
Multipole ℓ

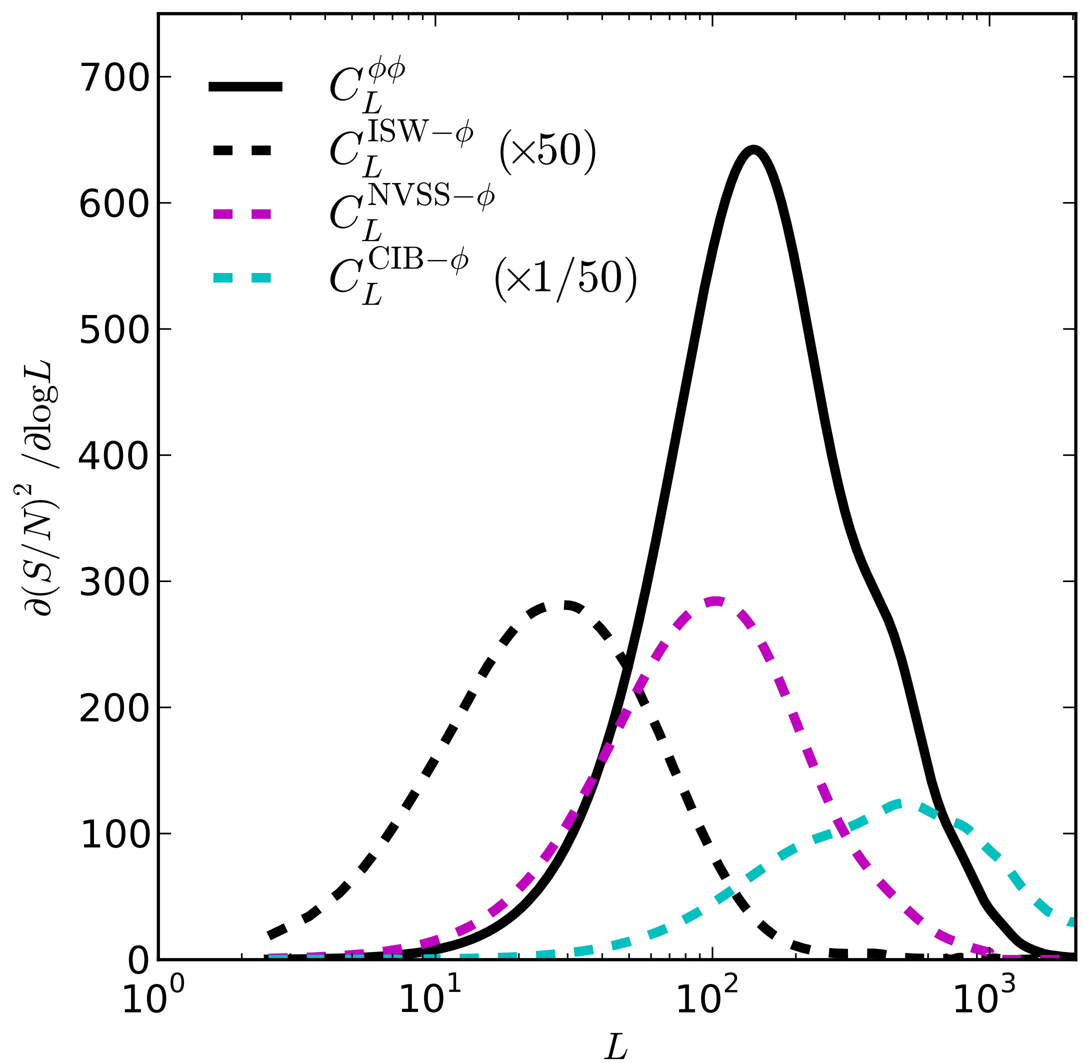

$C_L^{\phi\phi}$
$C_L^{\rm ISW-\phi}$ (×50)
$C_L^{\rm NVSS-\phi}$
$C_L^{\rm CIB-\phi}$ (×1/50)
$\partial (S/N)^2/\partial \log L$
L

Cosmology

- «Lensing breaks diameter degeneracy»

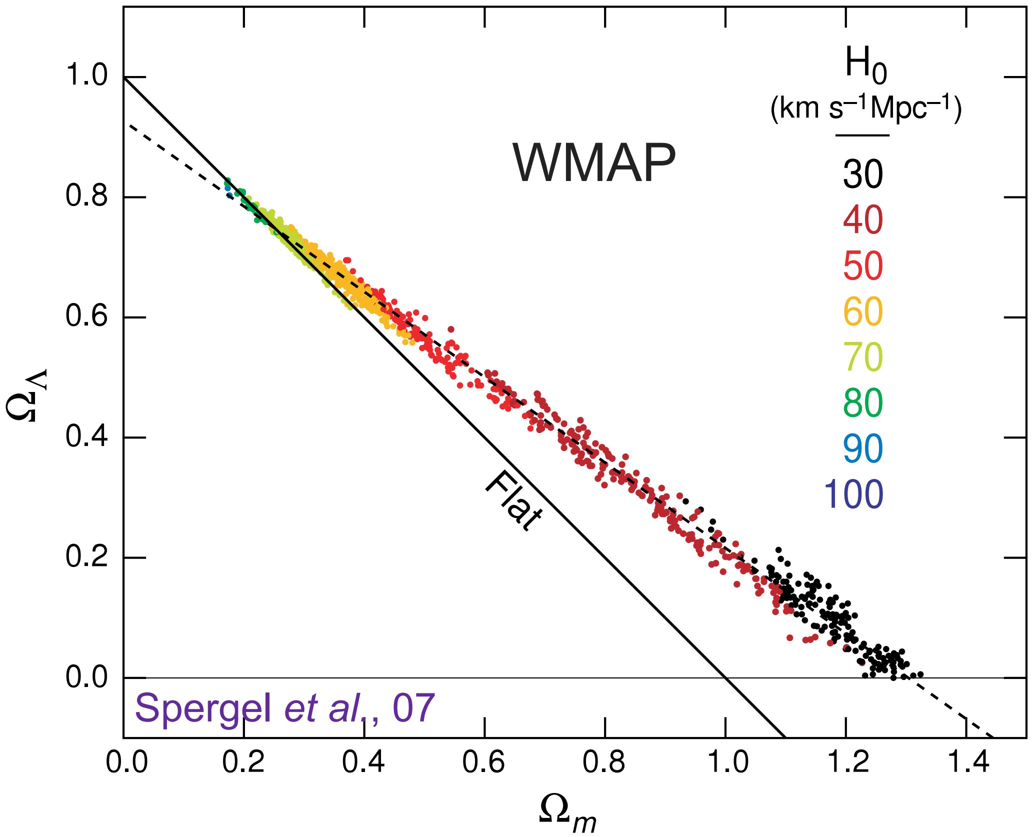

Cosmology

- «Lensing breaks diameter degeneracy»

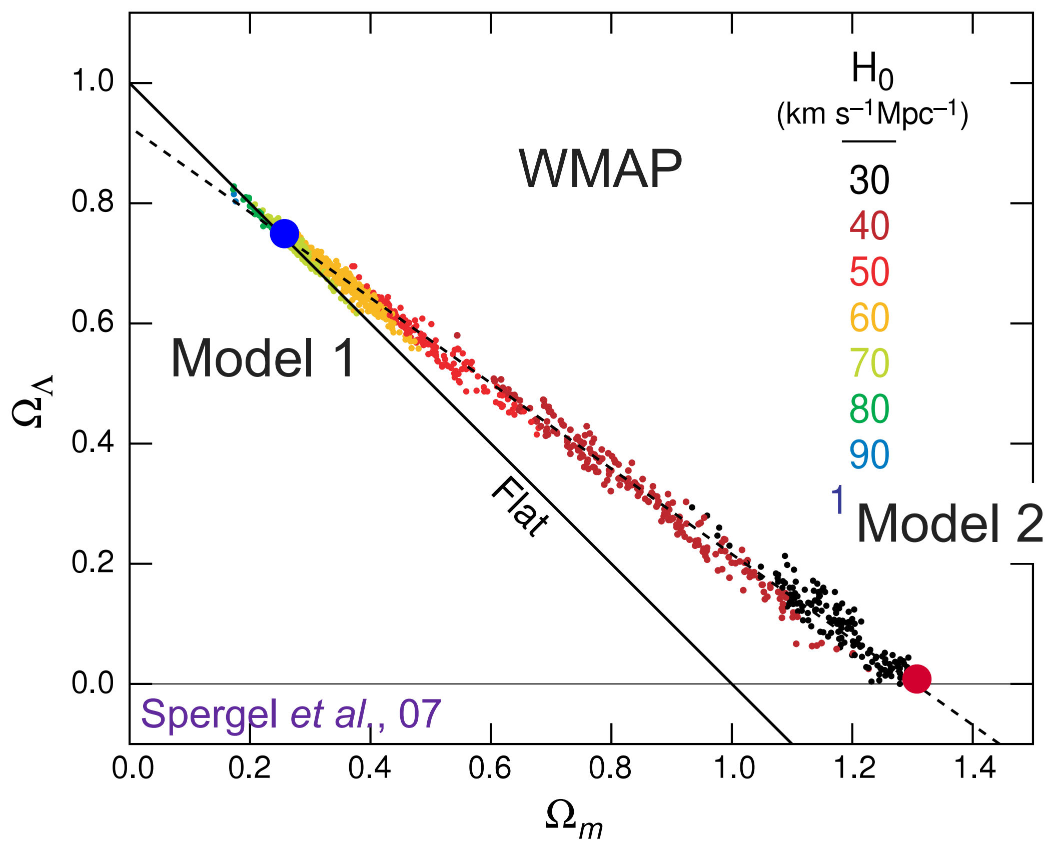

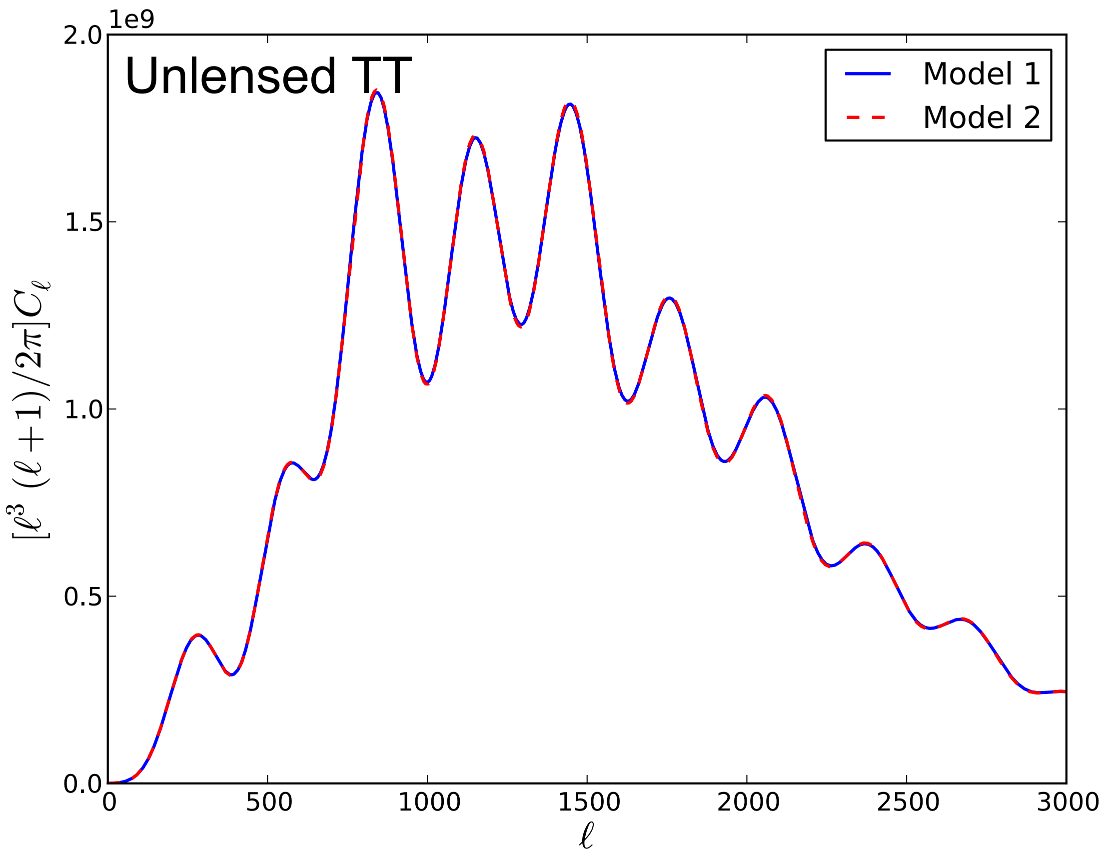

Cosmology

- «Lensing breaks diameter degeneracy»

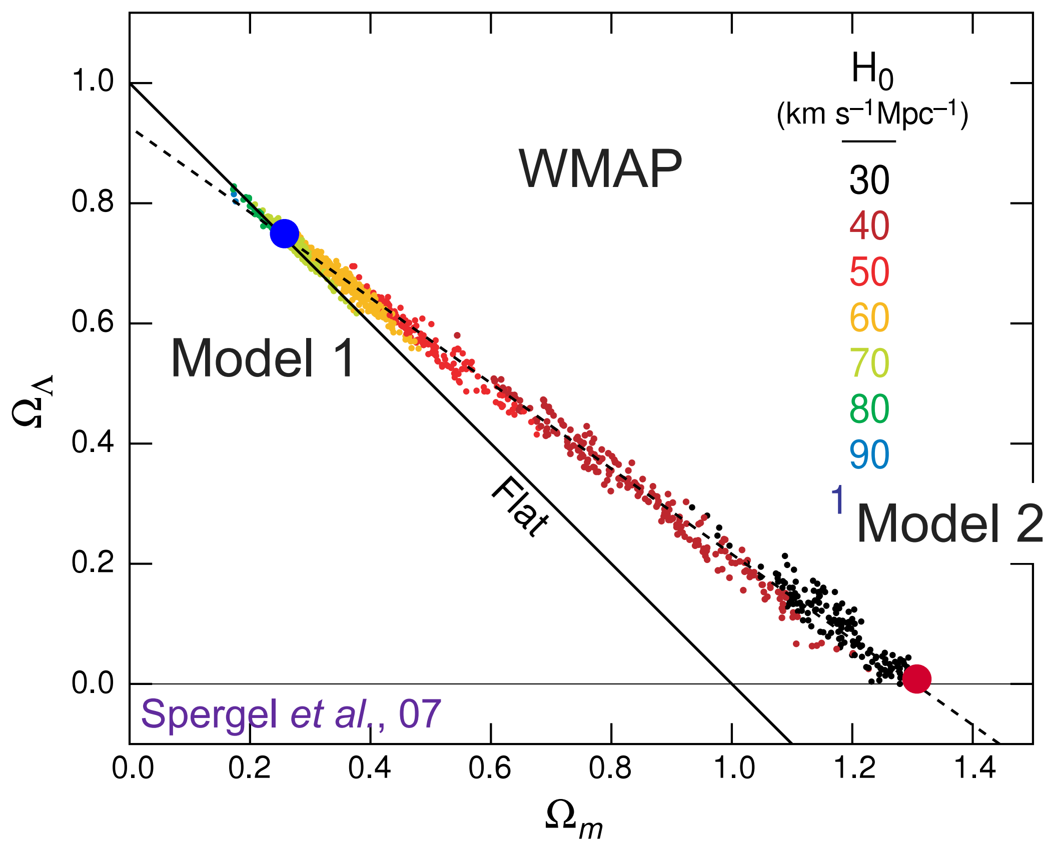

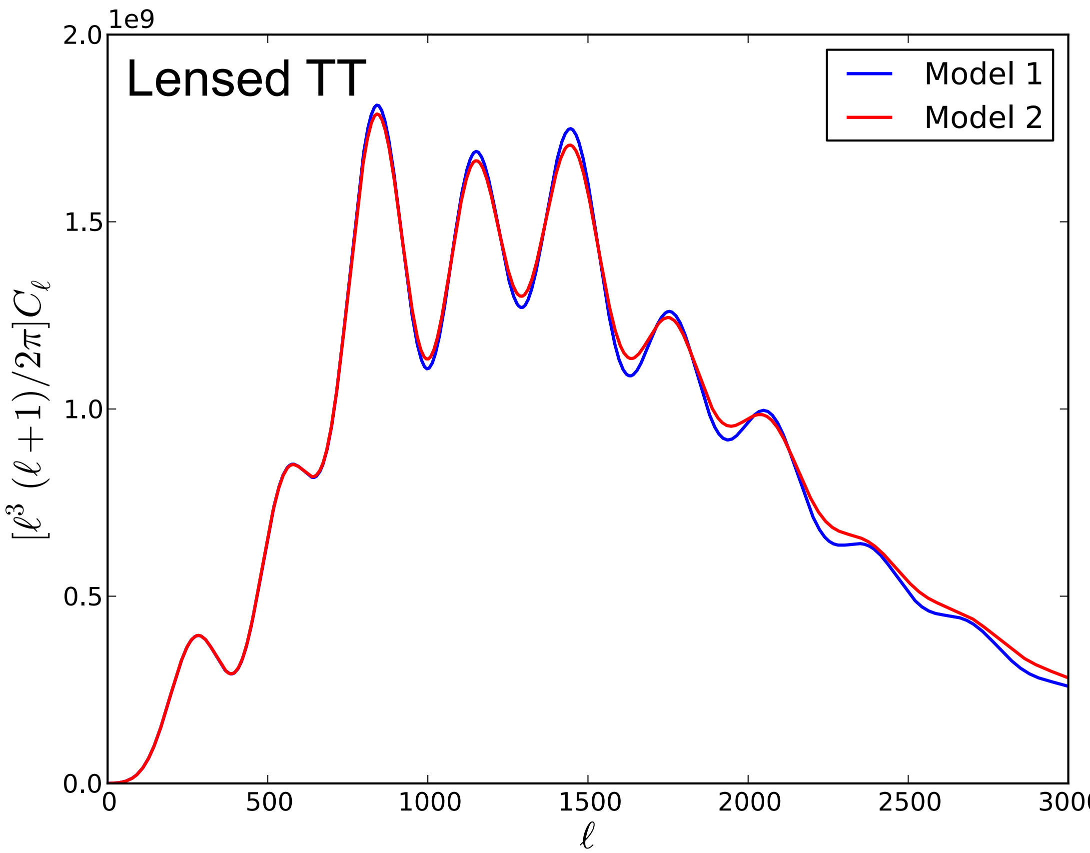

Cosmology

- «Lensing breaks diameter degeneracy»

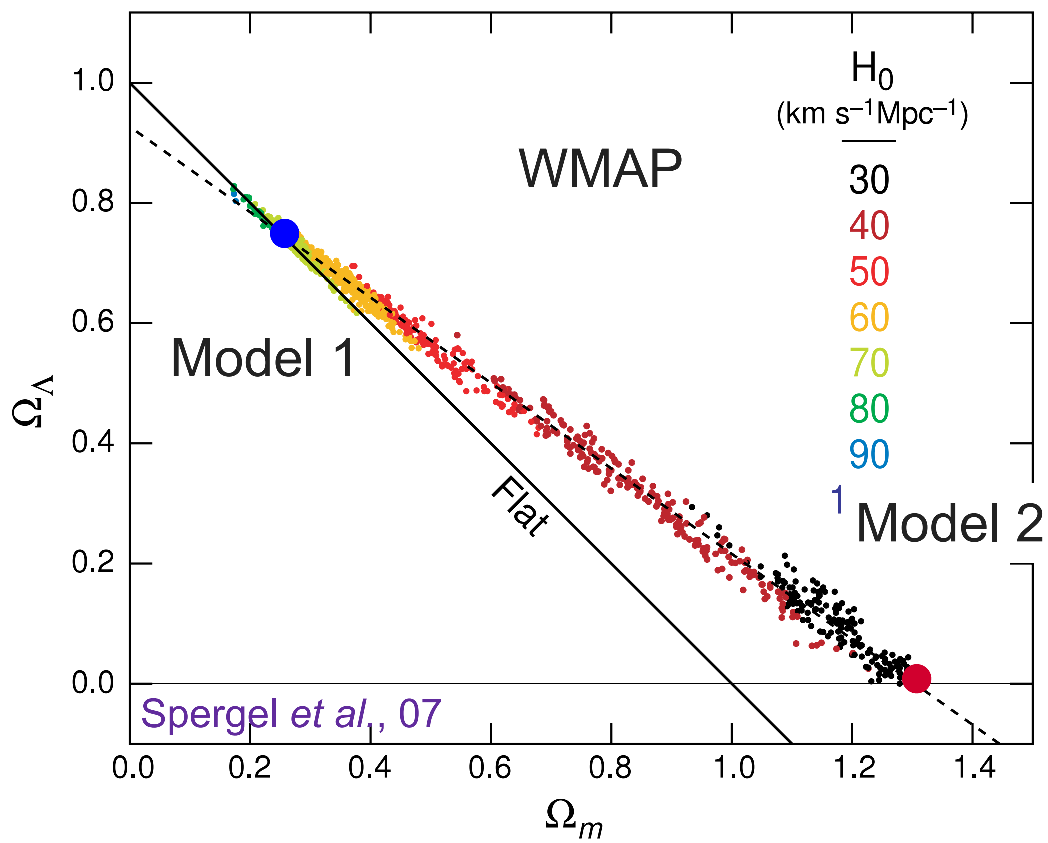

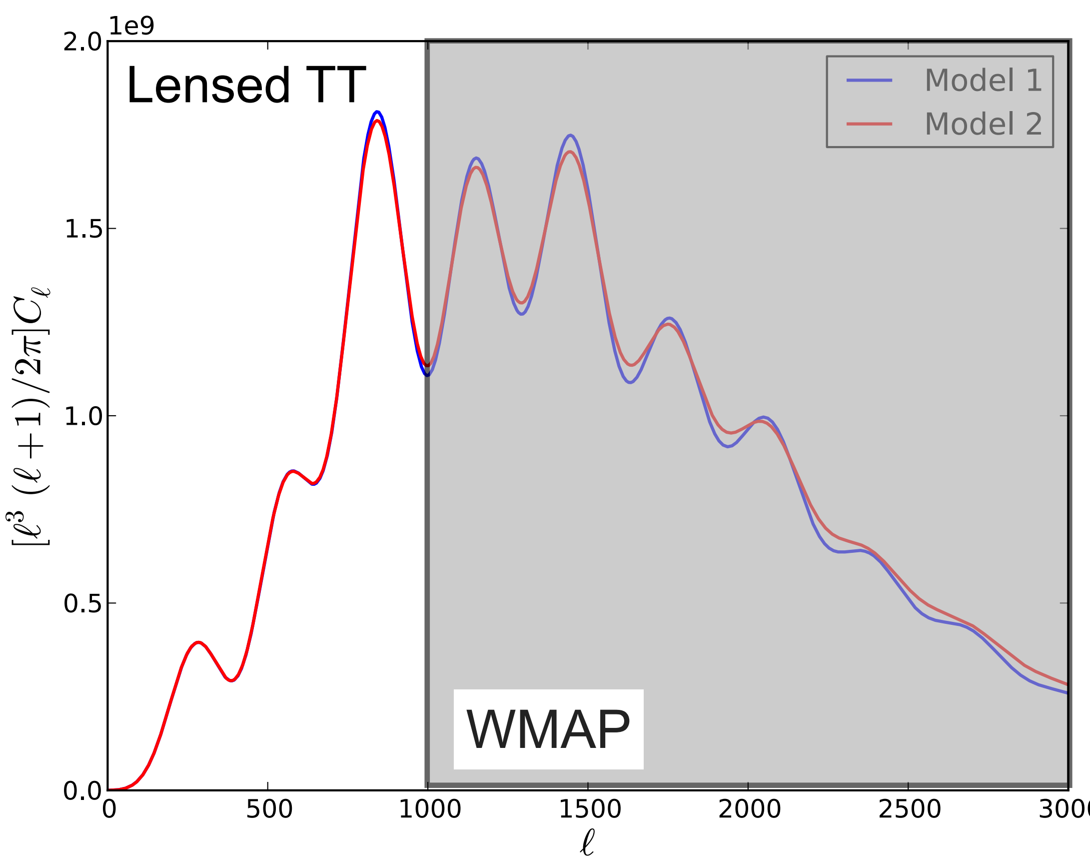

Cosmology

- «Lensing breaks diameter degeneracy»

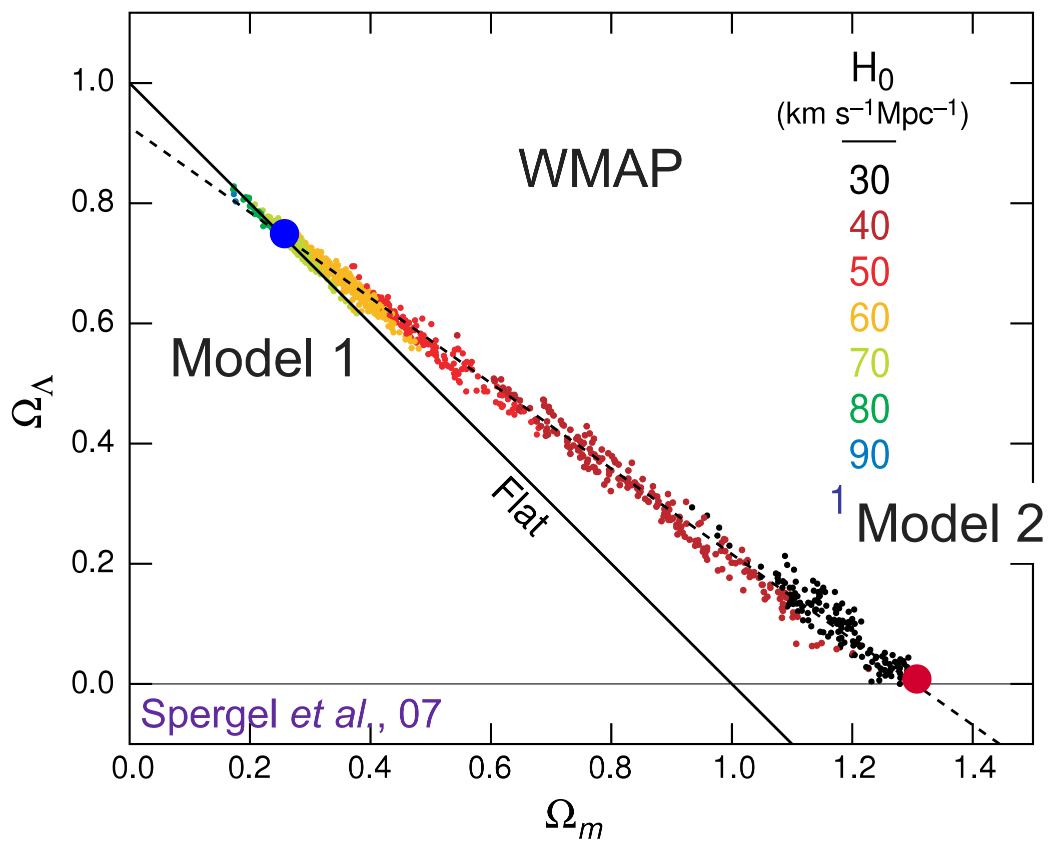

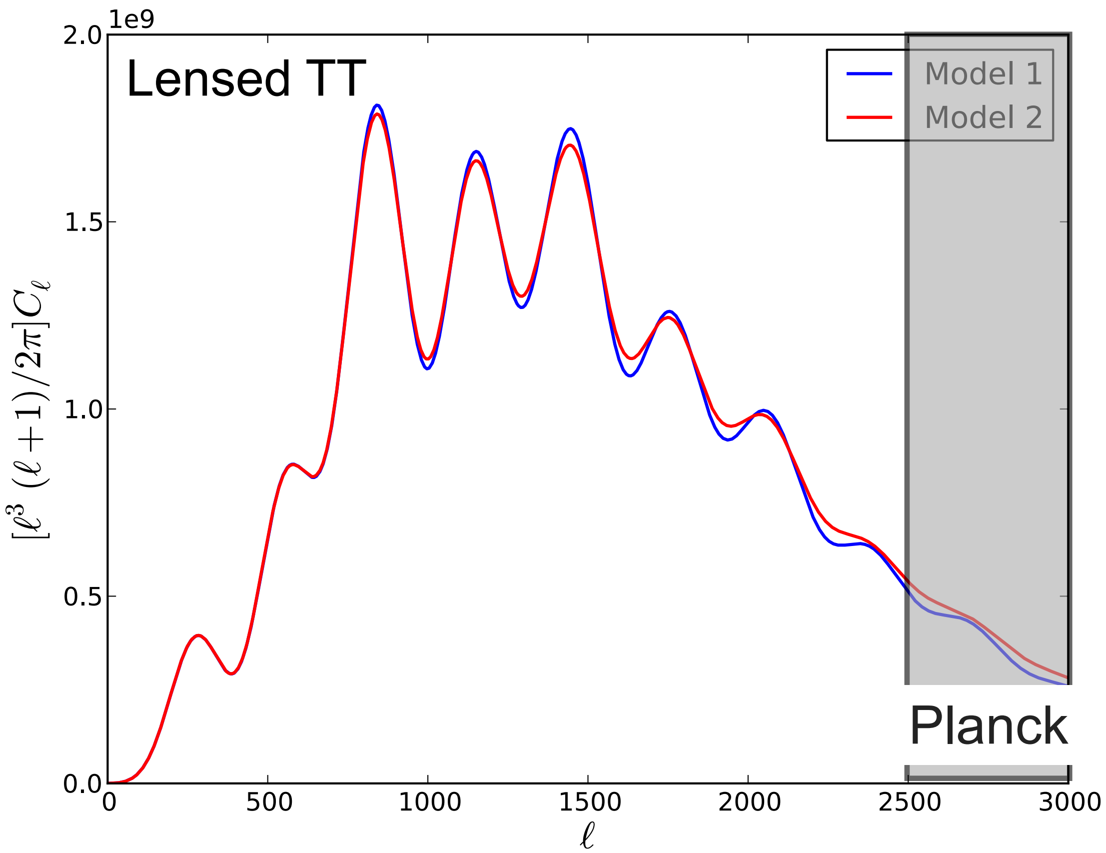

Cosmology

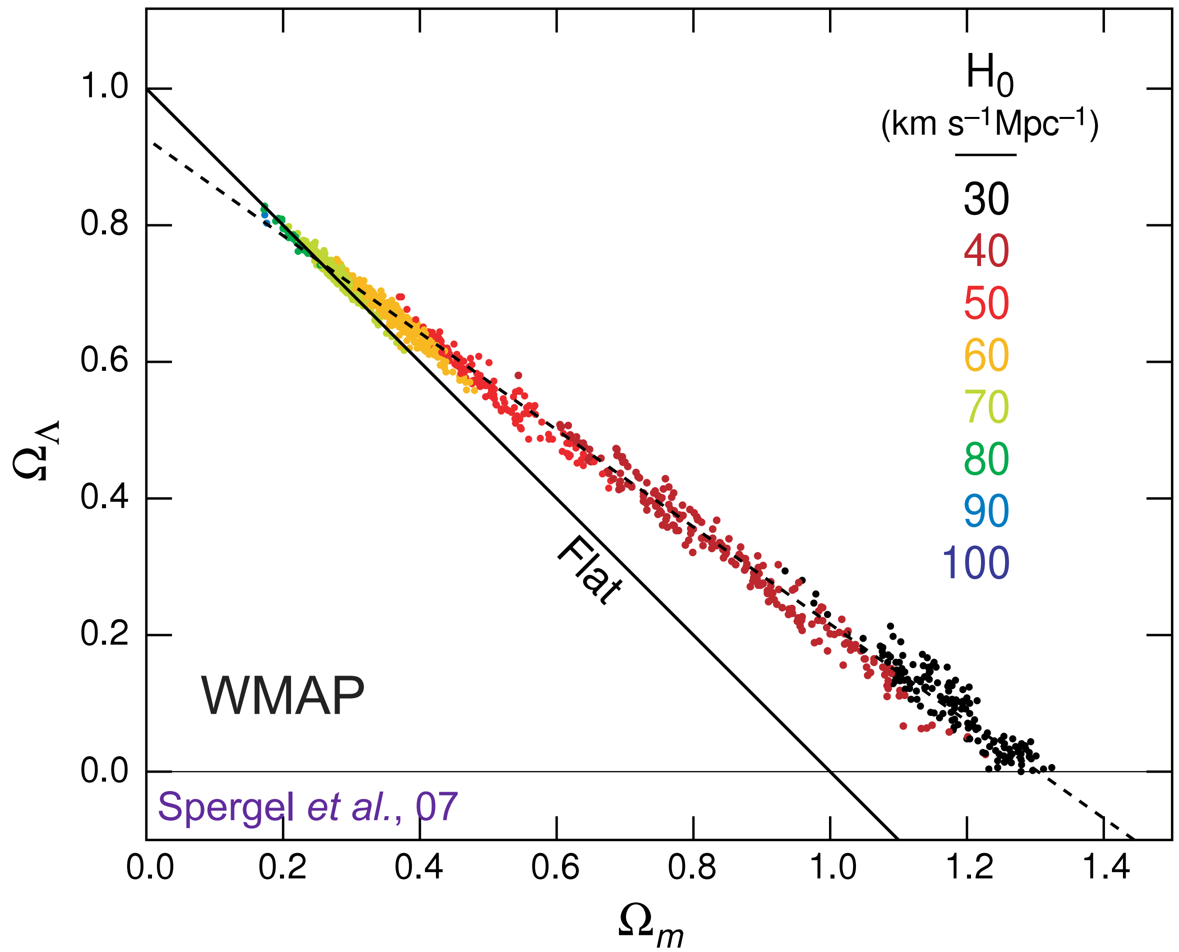

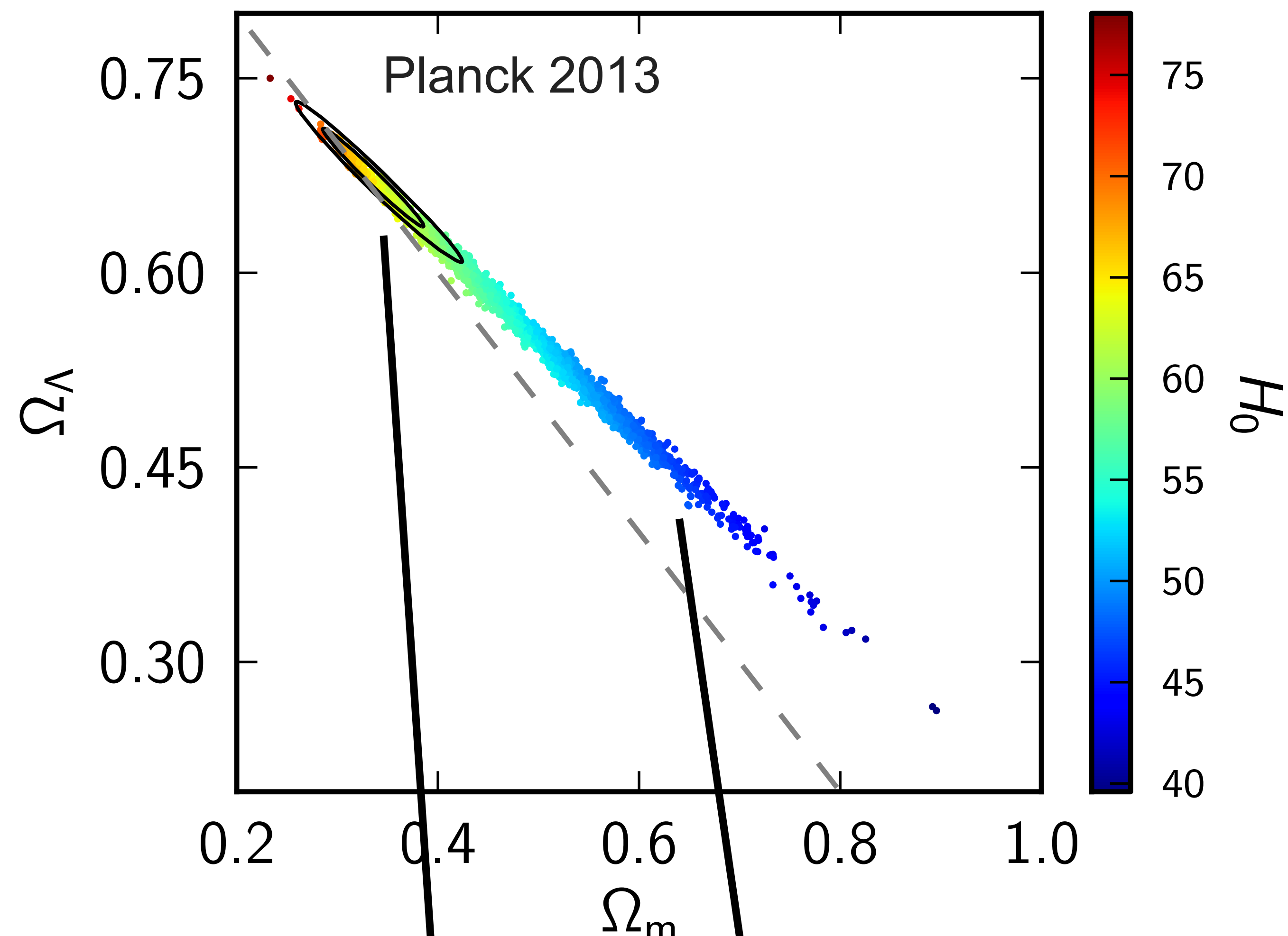

Using only the temperature power spectrum

Adding CMB lensing reconstruction

Cosmology

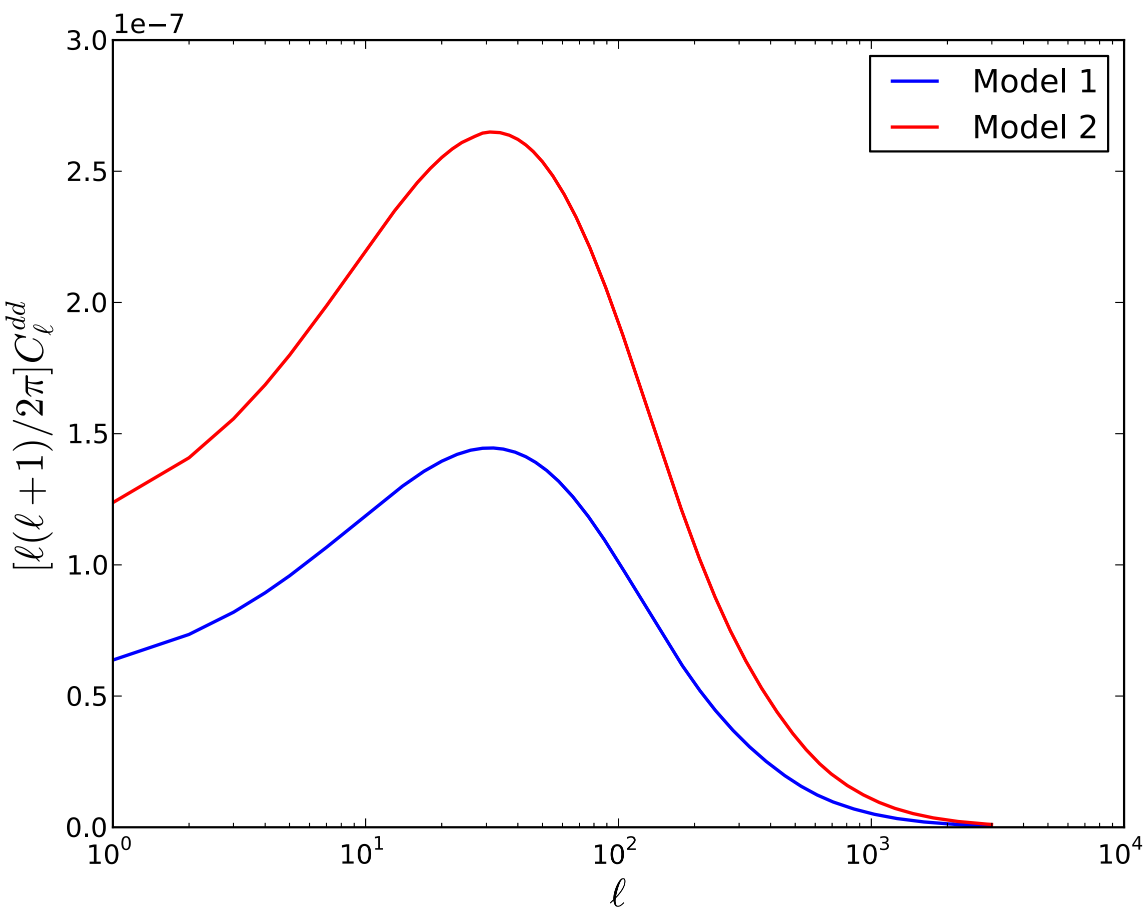

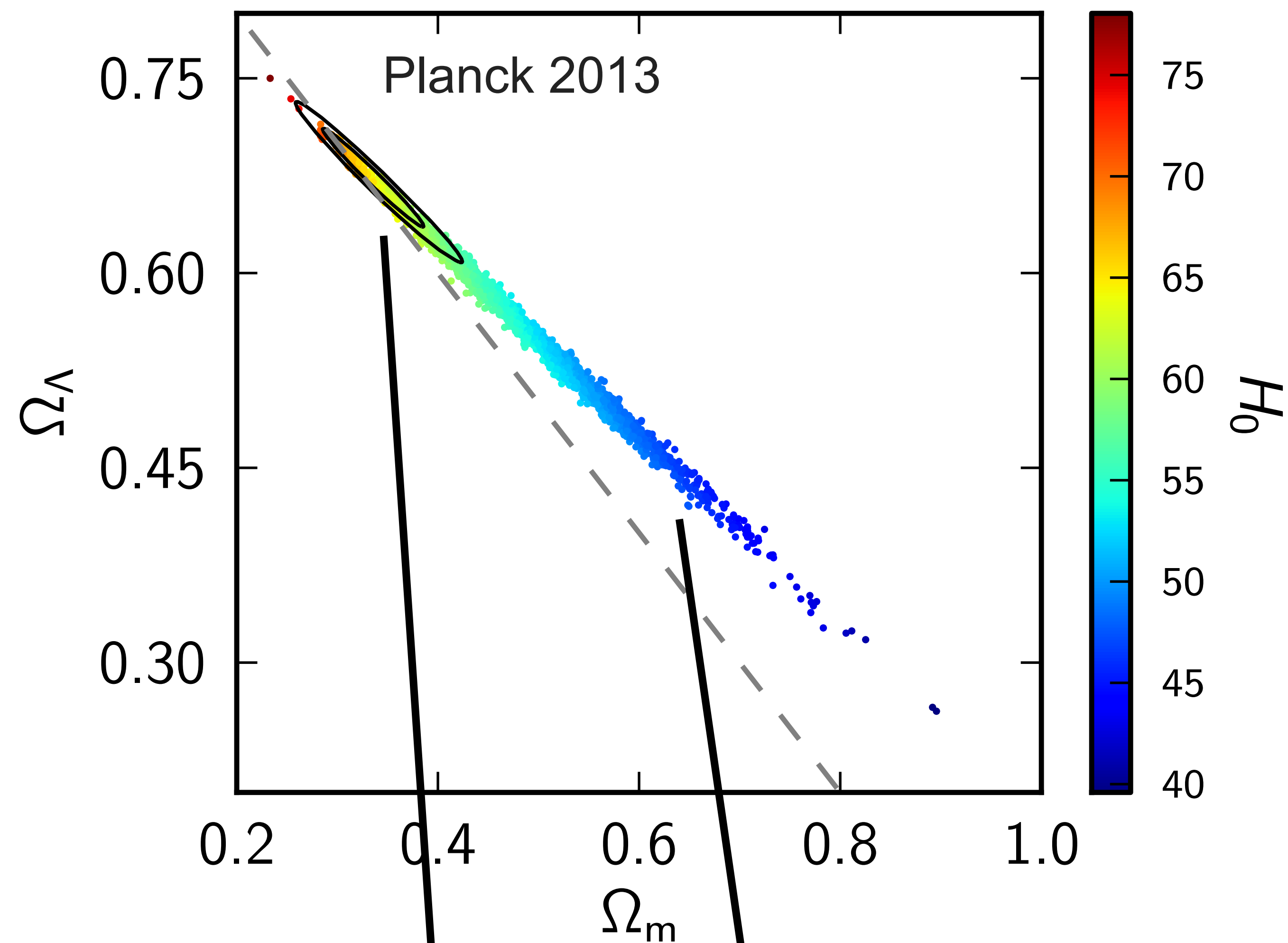

The lensing potential provides additional sensitivity to cosmological parameters

Using only the temperature power spectrum

Adding CMB lensing reconstruction

Cosmology

- CMB lensing breaks the angular diameter degeneracy

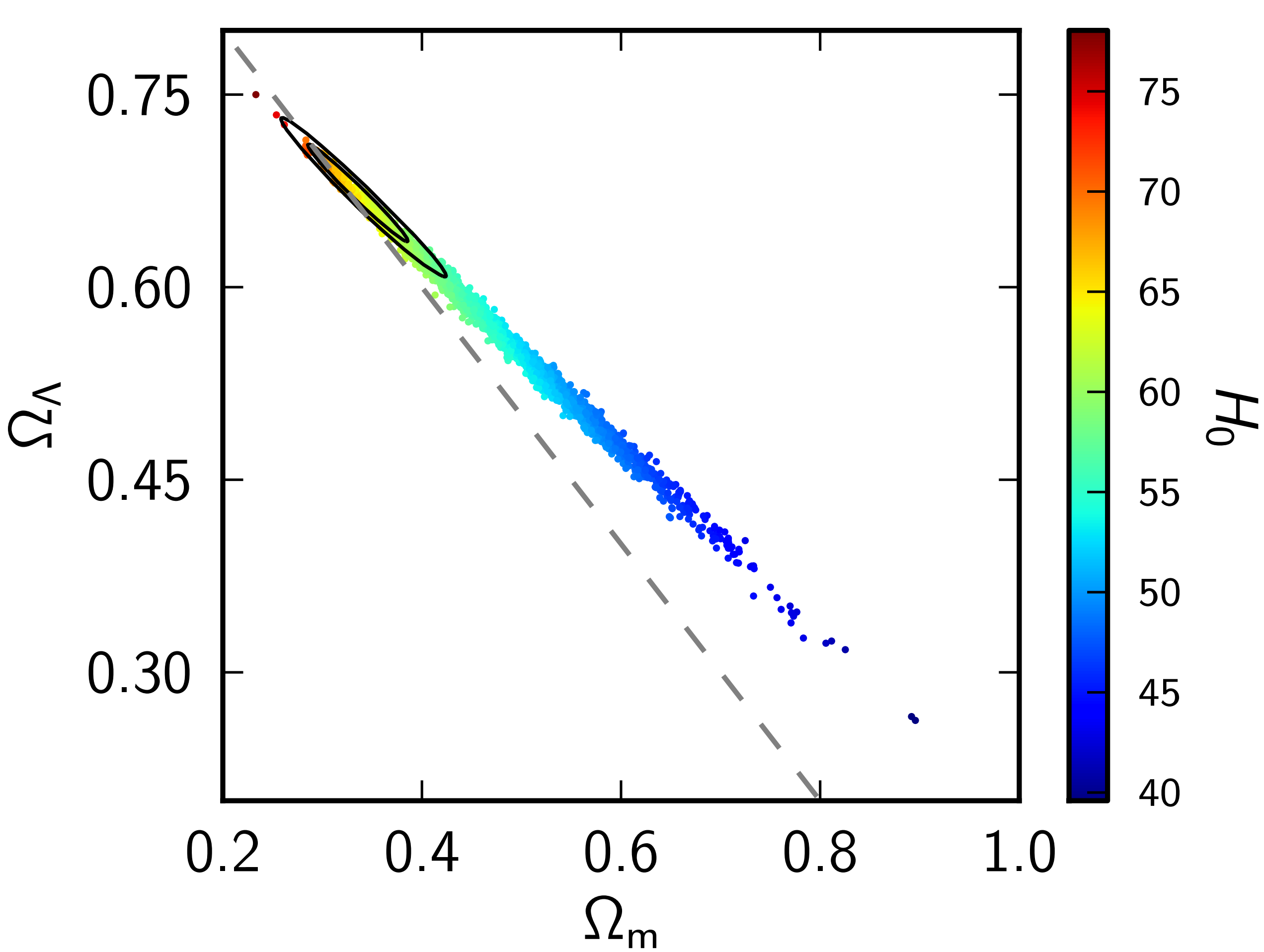

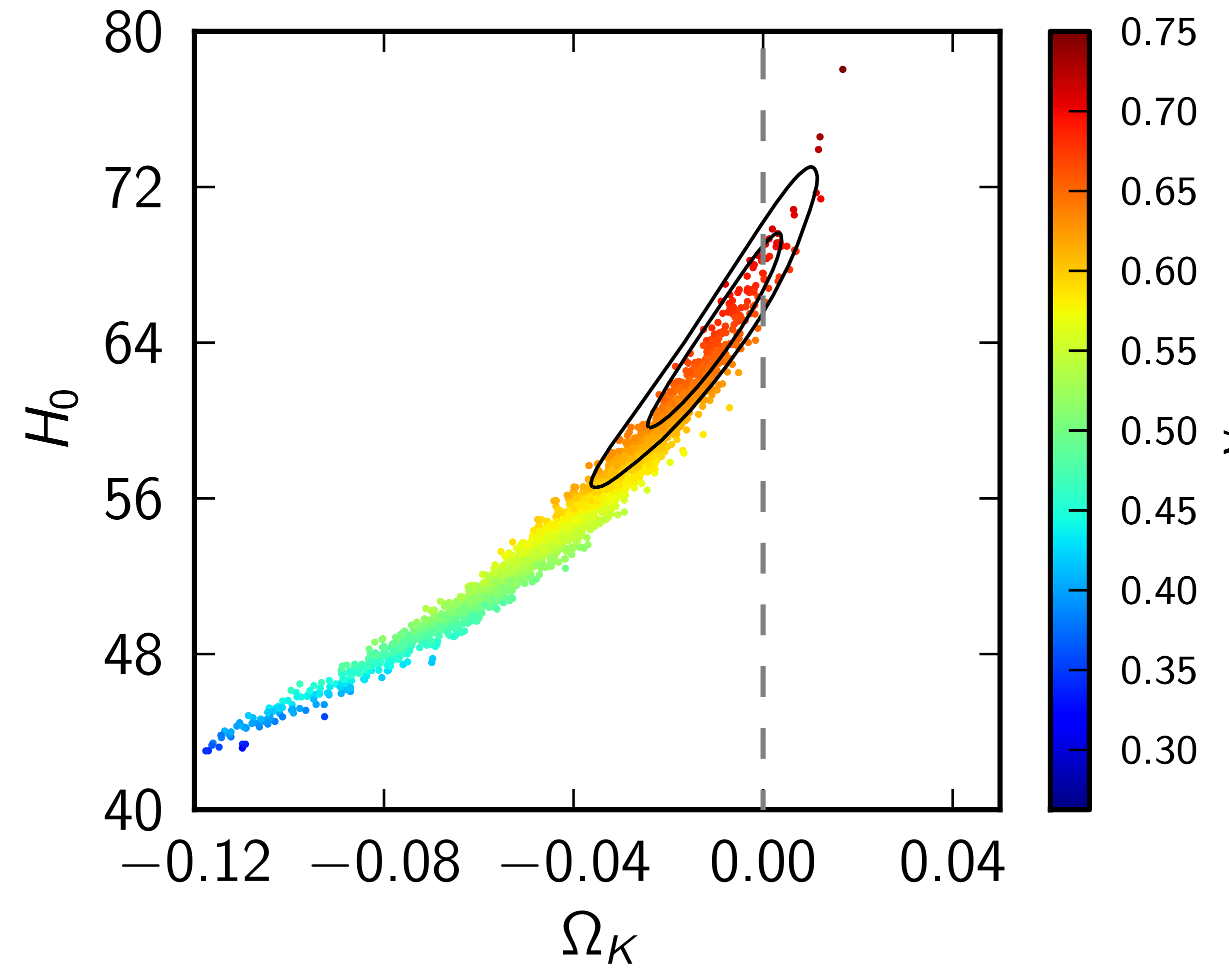

$$\Omega_\Lambda = 0.57^{+0.073}_{-0.055} \quad (68\%;\ \textit{Planck}\text{+WP+highL})$$
$$\Omega_\Lambda = 0.67^{+0.027}_{-0.023} \quad (68\%;\ \textit{Planck}\text{+lensing+WP+highL}).$$

$$100\Omega_K = -4.2^{+4.3}_{-4.8} \quad (95\%;\ \textit{Planck}\text{+WP+highL});$$
$$100\Omega_K = -1.0^{+1.8}_{-1.9} \quad (95\%;\ \textit{Planck}\text{+lensing} + \text{WP+highL}).$$

Cosmology

- Reionization

Optical depth - Amplitude degeneracy $A_s e^{-2\tau}$

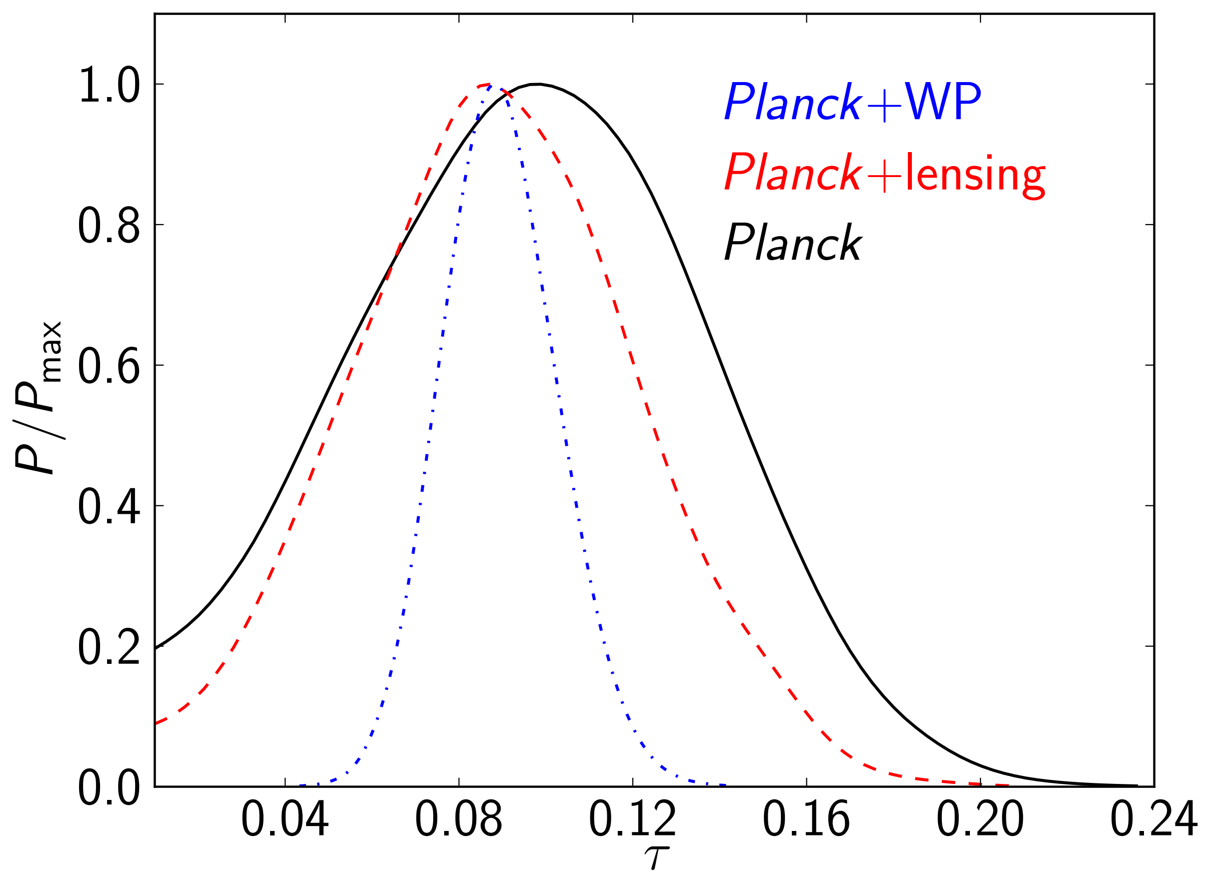

$$\tau = 0.097 \pm 0.038 \quad (68\%; \textit{Planck})$$
$$\tau = 0.089 \pm 0.032 \quad (68\%; \textit{Planck}\text{+lensing}).$$

Cosmology

Sum of neutrinos masses

- Mild tension : constraint weaker than expected!
- Temperature power spectra: more lensing = smaller mass
- Reconstruction: less lensing = larger mass

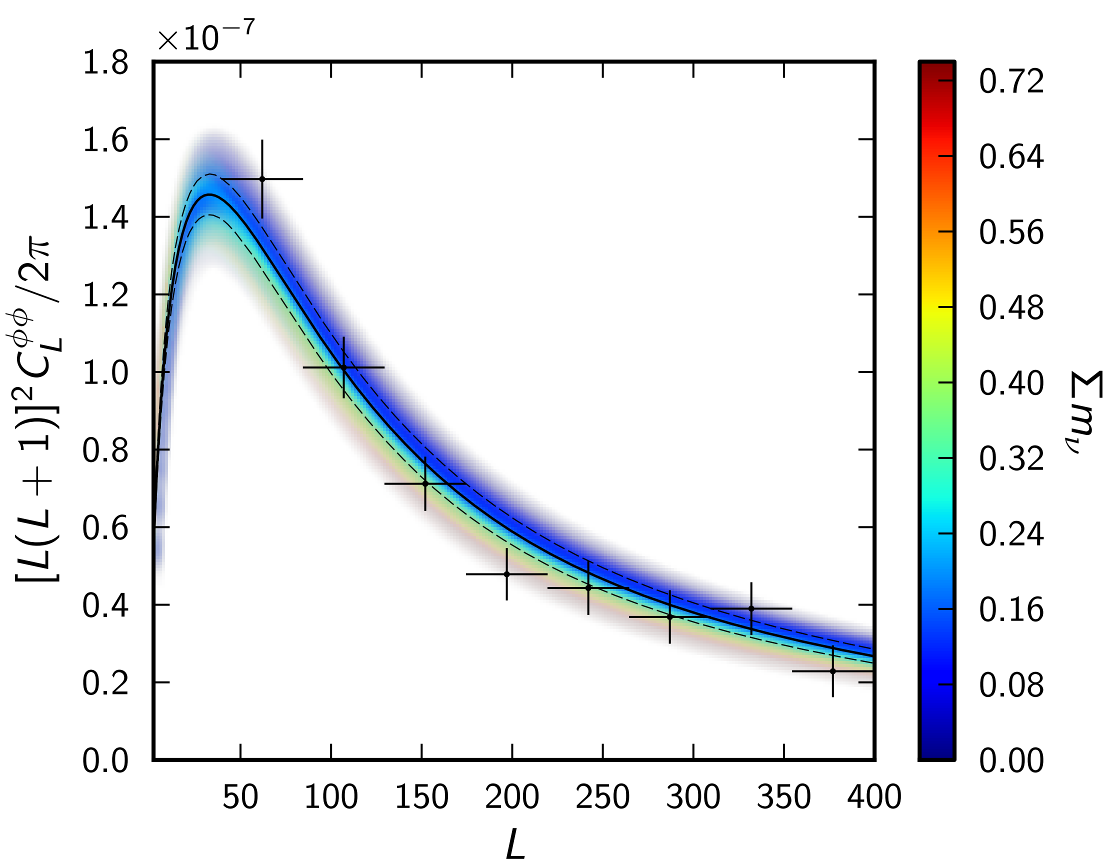

$$\sum m_\nu < 0.66\,\mathrm{eV}, \quad (95\%;\ \textit{Planck}\mathrm{+WP+highL}),$$
$$\sum m_\nu < 0.85\,\mathrm{eV}, \quad (95\%;\ \textit{Planck}\mathrm{+lensing+WP+highL}),$$

How to use the Planck lensing map

- **On the Plank Legacy Archive: COM_CompMap_Lensing_2048_R1.10.fits**
  - Un-normalized lensing potential $\bar{\phi}$, mask
  - «Normalisation window» $R_\ell^{\phi\phi}$, lensing noise $N_\ell^{\phi\phi}$

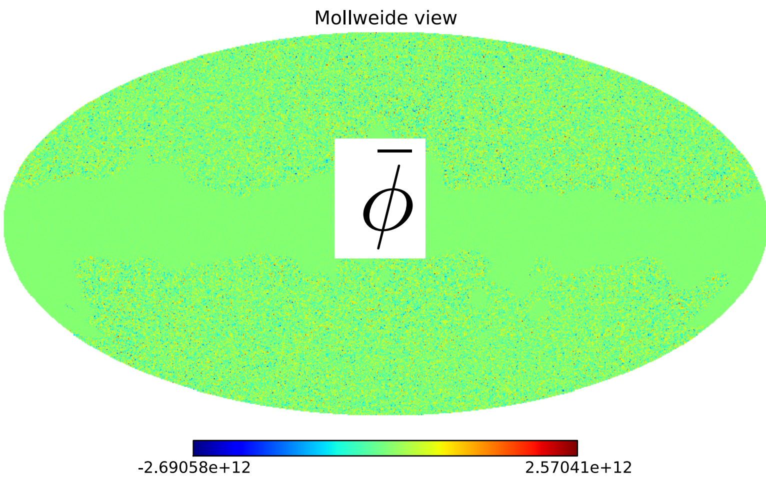

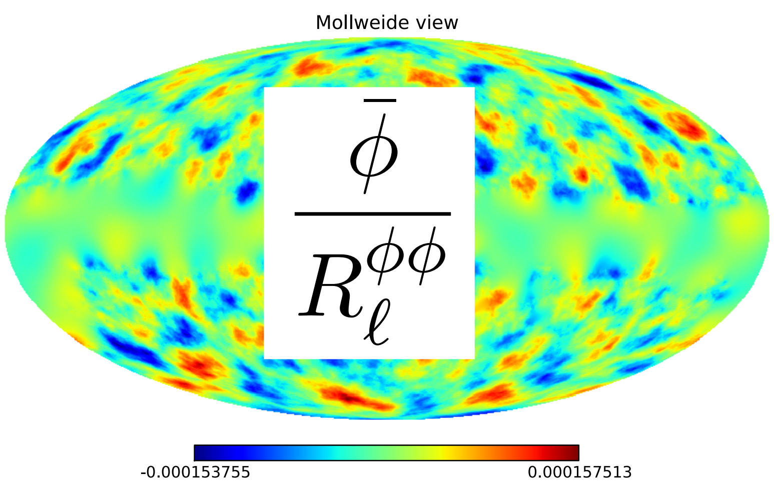

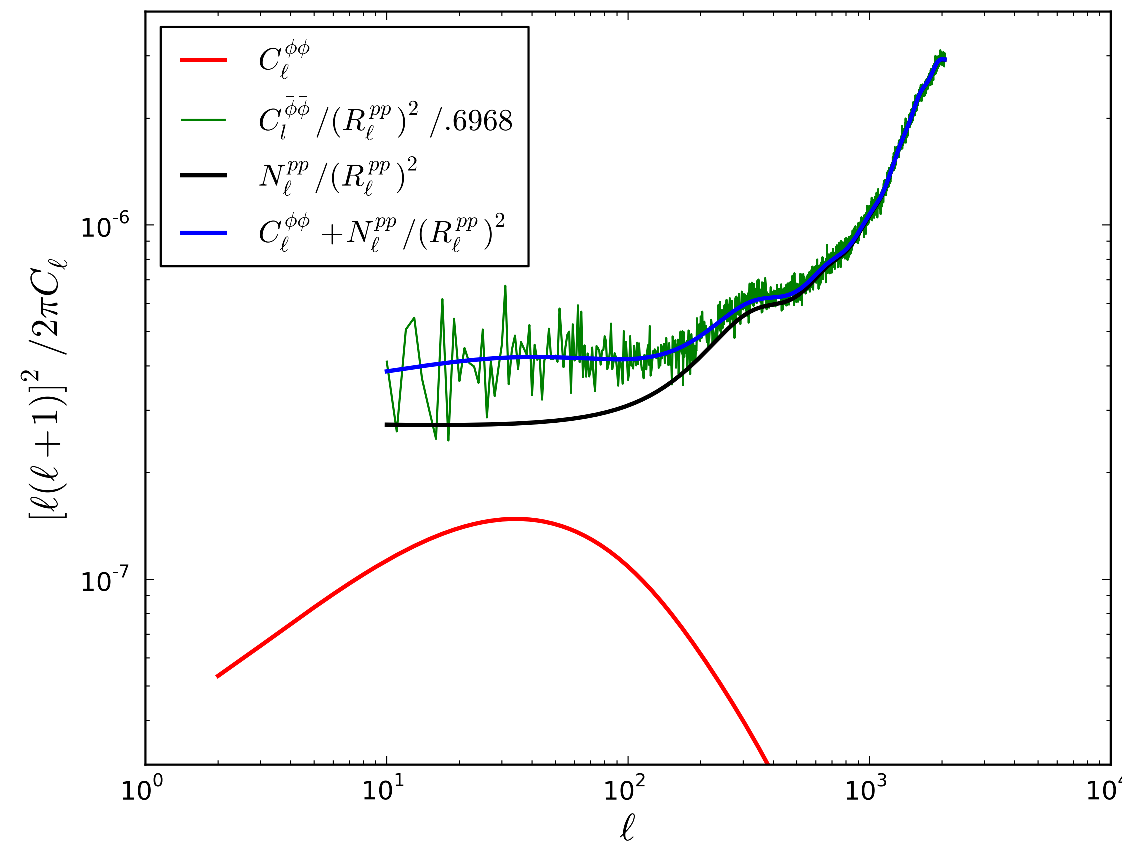

CMB lensing landscape in the coming years

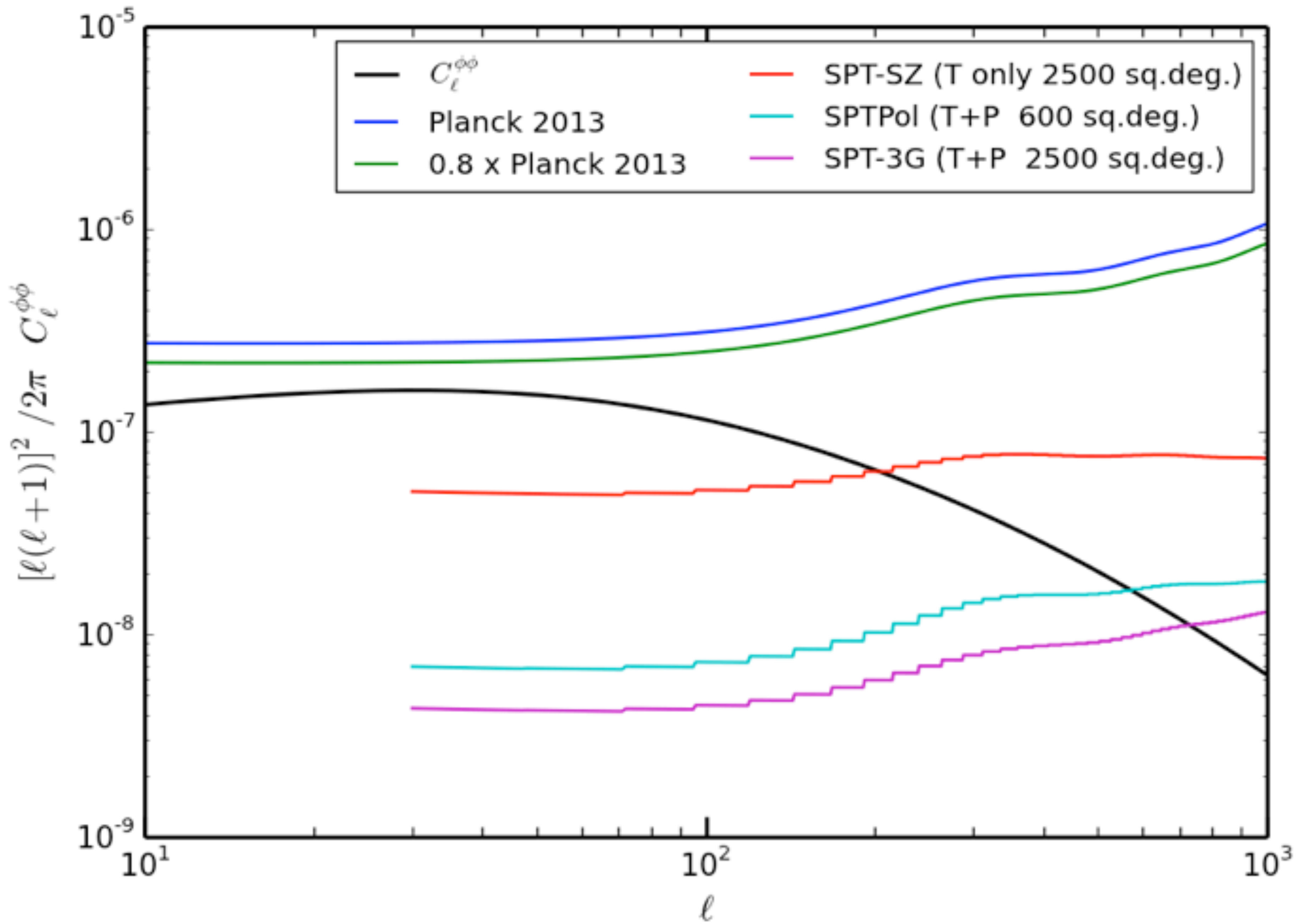

2013

2014

Present (not fully public)

soon, data is here

2016?

SPT noise levels kindly provided by G. Simard & G. Holder (McGill Univ.)

+ ACT, ACTpol, Advanced ACT: similar timescale and properties as SPT surveys
+ Possible post-planck CMB mission ESA-M4, USA CMB-S4

Lensing potential

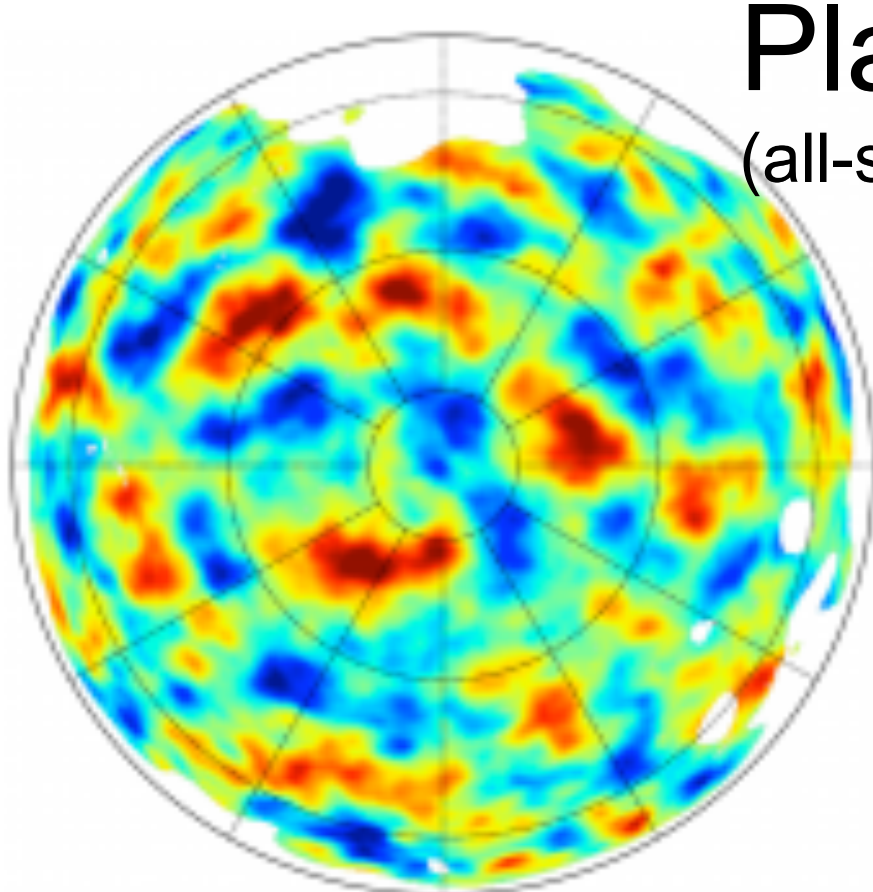

Planck

(all-sky more noise)

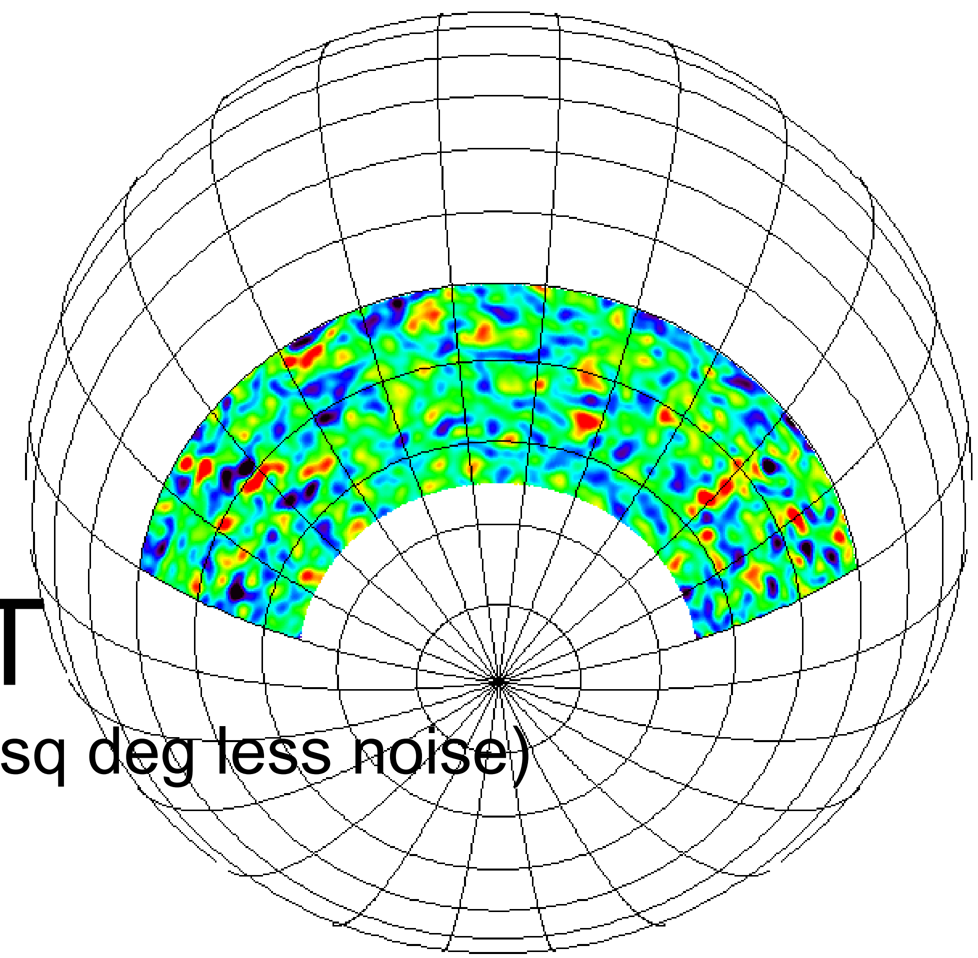

SPT

(2500 sq deg less noise)

SPT from Holder talk 2013

Conclusion (I) - Perspectives

Weak lensing is sensitive to all the matter present between the source and the observer

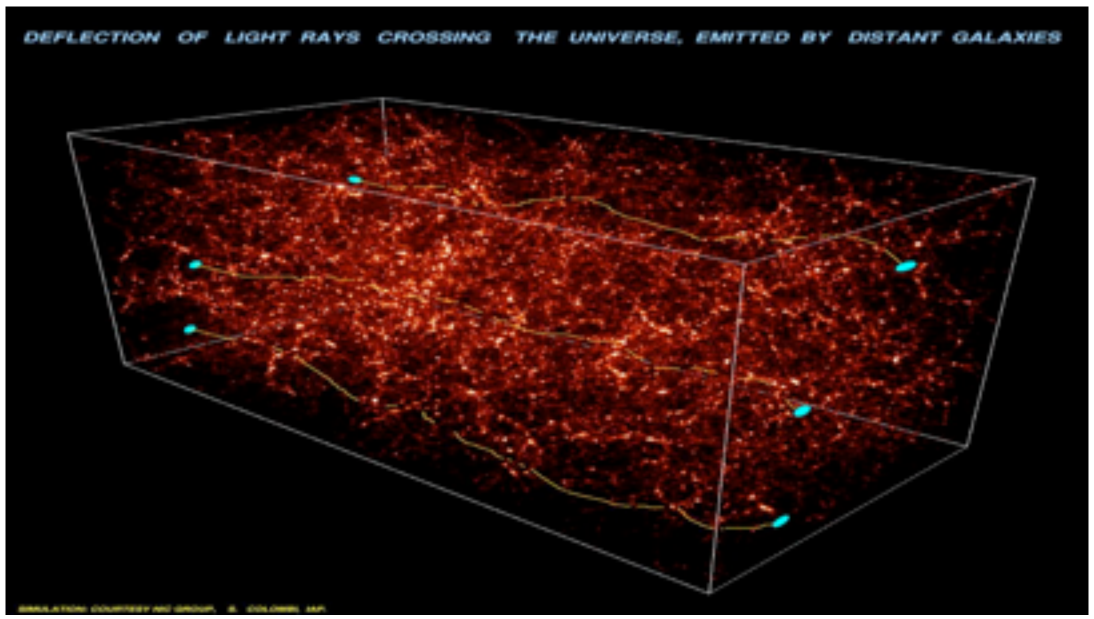

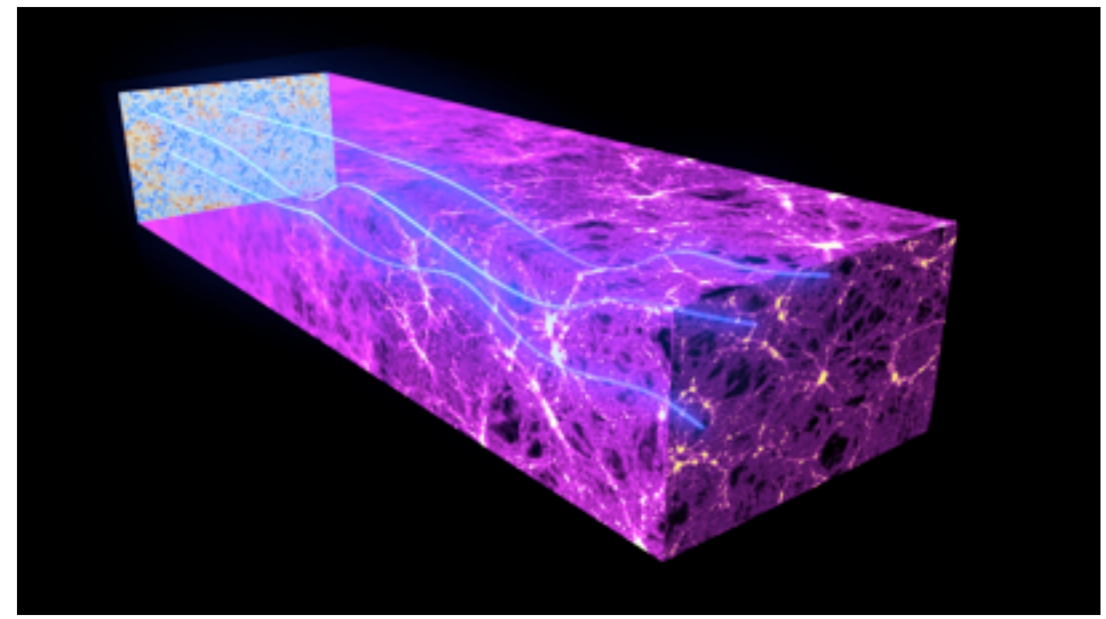

If we have access to the source redshift, we can reconstruct mass at different epoch: tomography

This will be possible with DES, Euclid and LSST

Can only reconstruct the projected mass. But is sensitive to higher redshift than photometric surveys

Conclusion (II) - Perspectives

$$C_\ell^{XY} = \int_0^{\chi_*} d\chi \frac{w^X(\chi) w^Y(\chi)}{f_K^2(\chi)} P(\ell/\chi, \chi)$$

Observing the projected matter power spectrum on the sky, through various tracers:

CMB lensing
$$w^l(\chi) = \frac{3\Omega_m H_0^2}{c^2 l^2} \frac{\chi_* - \chi}{\chi_*} \frac{\chi}{a},$$

Galaxy population
$$w^g(\chi) = \frac{1}{\int d\chi \frac{dN}{d\chi}} b \frac{dN}{d\chi},$$

Weak lensing
$$w^s(\chi) = \frac{1}{\int d\chi \frac{dN}{d\chi}} \frac{3H_0^2 \Omega_m}{2c^2} \frac{\chi}{a} \int_\chi^{\chi_*} d\chi' \frac{dN}{d\chi'} \frac{\chi' - \chi}{\chi'},$$

Conclusion (II) - Perspectives

$$C_\ell^{XY} = \int_0^{\chi_*} d\chi \frac{w^X(\chi) w^Y(\chi)}{f_K^2(\chi)} P(\ell/\chi, \chi)$$

Observing the projected matter power spectrum on the sky, through various tracers:

CMB lensing
$$w^l(\chi) = \frac{3\Omega_m H_0^2}{c^2 l^2} \frac{\chi_* - \chi}{\chi_*} \frac{\chi}{a},$$

Galaxy population
$$w^g(\chi) = \frac{1}{\int d\chi \frac{dN}{d\chi}} b \frac{dN}{d\chi},$$

Weak lensing
$$w^s(\chi) = \frac{1}{\int d\chi \frac{dN}{d\chi}} \frac{3H_0^2 \Omega_m}{2c^2} \frac{\chi}{a} \int_\chi^{\chi_*} d\chi \frac{dN}{d\chi'} \frac{\chi' - \chi}{\chi'},$$

galaxy bias
Source distribution

Combining these probes will improve the constraints on parameters by breaking degeneracies or helping control of nuisance parameters/systematics.
This leads to Éric’s talk on cross-correlations

References

General reviews on CMB lensing

A. Lewis & A. Challinor, *Weak gravitational lensing of the CMB,* Phys. Rep., 429 (2006) 1-65. astro-ph/0601594

Lensing reconstruction

Okamoto& Hu, 2003
Hirata & Seljak, 2004

Planck 2013 Lensing result